On-site energy generation for a decarbonized Irish manufacturing industry

---

A thesis submitted to the
Department of Mechanical & Manufacturing Engineering
Trinity College Dublin, the University of Dublin
in partial fulfilment of the requirements for the degree of

Doctor of Philosophy

by

Alessia Sgobba

Supervisor:
Dr. Craig Meskell

November 8, 2020

Declaration of Authorship

I, Alessia Sgobba, declare that this thesis titled "On-site energy generation for a decarbonized Irish manufacturing industry" has not been submitted as an exercise for a degree at this or any other university and it is entirely my own work.

I agree to deposit this thesis in the University's open access institutional repository or allow the library to do so on my behalf, subject to Irish Copyright Legislation and Trinity College Library conditions of use and acknowledgement.

Signed: 

To my family

To all the women in STEM

"Don't let anyone rob you of your imagination, your creativity, or your curiosity.
It's your place in the world; it's your life.
Go on and do all you can with it, and make it the life you want to live."

Dr. Mae Jemison

Abstract

The objective of the thesis is to explore whether it is technically, economically and environmentally feasible for an Irish manufacturing facility to become an energy prosumer, by producing energy on-site, and decrease the environmental impact of its electric and thermal energy demand as the energy sector is progressively decarbonized. A new model has been developed and implemented in Matlab in this thesis. It allows to simulate the techno-economic and environmental feasibility of on-site energy generation for a manufacturing facility through an integrated Variable Renewable Energy (VRE) system and a Combined Heat and Power (CHP) system. The model is built as a robust and flexible tool that can be used for any facility worldwide by updating inputs such as geographical location, solar and wind availability and hourly energy demand. The implemented model allows also to evaluate the feasibility of on-site energy generation in possible future scenarios by conducting a sensitivity analysis of parameters that may change in the future, such as discount rate, commodities price and grid carbon intensity.

An existing Irish manufacturing facility has been used as a real case study to provide realistic data as input to the analysis, capturing real requirements and constraints that characterize this type of end-user. The first option investigated to decarbonize the electric load of the facility is an on-site VRE system composed of solar PV and wind turbines. The modelled VRE system results technically viable but not economically feasible in isolation: its Pay Back Time is too high (PBT >25 years) to be attractive for a manufacturing facility and it would remain unattractive even with substantial subsidies and a reduction in the capital cost of VRE technologies. The second option investigated, both to economically support the on-site VRE system and to decarbonize the thermal energy load of the facility, is to add an on-site CHP system. The integrated system results to be both technically and economically feasible with a PBT close to 6 years. However, the environmental benefits of reducing carbon emissions by producing energy for self consumption on-site are limited in time: if the project was to be commissioned in 2020, the cumulative emissions savings would become negative in 2040 as the electric grid is progressively decarbonized, creating a potential misalignment between decarbonizing policies and the manufacturing facility's economic strategy. Another issue arises with the installation of the on-site system: the almost constant electric load of the manufacturing facility becomes more variable and difficult to predict due to the intermittency of renewable sources. Despite its inherent operating flexibility, the CHP system does not significantly reduce the occurrence of high fluctuations in the residual electric load that the grid has to cover.

It is concluded that a techno-economic opportunity does exist for on-site energy cogeneration in the Irish manufacturing industry, however the environmental benefits are limited in time. The effects on the electric grid of a switch from a predictable and constant load to a more variable one should be considered as the penetration of distributed generation increases.

Publications and Conferences

Journal publications

- A. Sgobba, C. Meskell, *Combined Heat and Power: not a feasible solution for Irish manufacturing industry with a decarbonized grid*, Journal of Cleaner Production, Vol. 278, 2021.
- A. Sgobba, C. Meskell, *On-site renewable electricity production and self consumption for manufacturing industry in Ireland: Sensitivity to techno-economic conditions*, Journal of Cleaner Production, Vol. 207, pp 894-907, 2019.

Conference papers

- A. Sgobba, C. Meskell, G. Manzolini, *On-site energy generation in the manufacturing industry: effects on the variability of the net electricity demand*, CIRED 2020 Berlin Workshop, Berlin, Germany, 2020.
- A. Sgobba, C. Meskell, *On-site integration of renewable and Combined Heat and Power generation for Irish manufacturing industry in a decarbonized energy system: A case study*, The Economics of Environmental Policy and Innovation, Ottawa, Canada, 2019.
- A. Sgobba, C. Meskell, *Assessment of on-site solar and wind energy at a manufacturing facility in Ireland*, 16th Wind Integration Workshop, Berlin, Germany, 2017.

Posters and other presentations

- A. Sgobba, C. Meskell, *On-site energy generation in the Irish manufacturing industry: effect on the net demand*, poster presented at the symposium "Investing in our energy future", University College Dublin, Dublin, Ireland, 2019.
- A. Sgobba, C. Meskell, *On-site integration of renewable and Combined Heat and Power generation for Irish manufacturing industry in a decarbonized energy system: A case study*, article presented at the workshop "The Economics of Environmental Policy and Innovation", University of Ottawa, Ottawa, Canada, 2019.

- A. Sgobba, C. Meskell, *Assessment of on-site cogeneration at a manufacturing facility in Ireland*, poster presented at the symposium "Unlocking the Potential of Energy Users in the Energy Transition", University College Dublin, Dublin, Ireland, 2018.
- A. Sgobba, C. Meskell, *Assessment of on site solar and wind energy at a manufacturing facility in Ireland*, poster presented at the symposium "Rethinking our Energy Future: Collaboration and Integration", University College Dublin, Dublin, Ireland, 2017.
- A. Sgobba, C. Meskell, *Assessment of on-site solar and wind energy at a manufacturing facility in Ireland*, poster presented at the 16th Wind Integration Workshop, Berlin, Germany, 2017.

Acknowledgements

I would like to express my deep and sincere gratitude to my supervisor Dr. Craig Meskell, for his precious guidance, patience and support throughout this work. He has given me the great opportunity of pursuing a Ph.D. and the tools to always carry on. He has inspired me to give my best, to challenge myself and to always try to raise the bar. I can see the impact his guidance has had not only on my professional but also on my personal growth.

My gratitude goes to all my colleagues in the Department of Mechanical and Manufacturing Engineering, and to all the academic and technical staff in the Parsons Building.

My sincere thanks go to Sara, dearest colleague and friend that has always been by my side in the difficult and happy moments. She shared her expertise and knowledge, giving me always useful advice and support.

Finally, a special thanks goes to Marco and my family. Marco, thanks for all the sacrifices you made during this challenging time, for being always by my side even if from far away. Thanks for all the flights you took at unspeakable hours, for repeatedly reading all the documents I have written in these four years and giving me the best advices on powerpoint presentations. Thanks for always cheering me on through this challenging experience. My deepest gratitude to my family, that has supported me in all the toughest decisions and has shown me how hard work and persistence are key to reach your goal. Irene, Pietro, Nico, Alby, Ada and Umberto you are the most precious people I could hope to have in my life.

The research leading to the results presented in this thesis was conducted with the financial support of Science Foundation Ireland under the SFI Strategic Partnership Programme Grant Number SFI/15/SPP/E3125. The opinions, findings and conclusions or recommendations expressed in this material are those of the author and do not necessarily reflect the views of the Science Foundation Ireland.

The author would like to thank Dr. Lisa Ryan, Dr. Conor Sweeney, Dr. Francesco Casella and Mr. Dan Donovan for their valuable comments on this work.

Contents

List of Figures

List of Tables

Nomenclature

Acronyms

A-CAES	Adiabatic Compressed Air Energy Storage
BA	BAlancing market
BESS	Battery Energy Storage System
BRP	Balancing Responsible Party
BSP	Balancing Service Provider
CAES	Compressed Air Energy Storage
CCGT	Combined Cycle Gas Turbine
CCS	Carbon Capture and Storage
CHP	Combined Heat and Power
CPV	Concentrating PhotoVoltaic
CT	Carbon Tax
DA	Day Ahead spot market
DC	Direct Current
DER	Distributed Energy Resource
DR	Demand Response
DSM	Demand Side Management
ESI	Energy System Integration
ESS	Energy Storage System
FES	Flywheel Energy Storage
GHG	GreenHouse Gases
GT	Gas Turbine
HAWT	Horizontal Axis Wind Turbine
HOMER	Hybrid Optimization of Multiple Electric Renewables
HRSG	Heat Recovery Steam Generator
ID	IntraDay market
KDE	Kernel Density Estimation
LA	Lead Acid
LCOE	Levelized Cost Of Energy
LHV	Lower Heating Value
Li-ion	Lithium-ion battery
MBE	Mean Bias Error

MERRA-2	Modern-Era Retrospective analysis for Research Applications, ver. 2
NASA	National Aeronautic and Space Administration
NG	Natural Gas
NPV	Net Present Value
NREL	National Renewable Energy Laboratory
O&M	Operation and Maintainance
OECD	Organisation for Economic Cooperation and Development
P2G	Power-to-Gas
PBT	Pay Back Time
PDF	Probability Density Function
PHS	Pumped Hydro Storage
PV	PhotoVoltaic
RCP	Representative Concentration Pathways
RES	Renewable Energy Source
RMSE	Root Mean Square Error
ROI	Return On Investment
SAM	System Advisory Model
SB	Secondary Boiler
SC	Super Capacitor
SCADA	Supervisory Control And Data Acquisition
SMES	Superconductive Magnetic Energy Storage
TES	Thermal Energy Storage
TSO	Transmission System Operator
T&D	Transmission and Distribution
UPS	Uninterruptable Power Supply
VAWT	Vertical Axis Wind Turbine
VOLL	Value Of Lost Load
VRE	Variable Renewable Energy

Physical Quantities

α	Corrected solar azimuth angle [°]
α_s	Solar azimuth angle [°]
α_w	Hellman exponent [-]
β	Pitch angle of the PV panel [°]
β_{opt}	Optimum pitch angle of the PV panel [°]
γ	Orientation of the panel [°]
Δh_{eva}	Latent heat of evaporation [kJ/kg]
δ	Declination of the sun [°]
η_{el}	Electrical efficiency [-]
η_{HRSG}	Heat Recovery Steam Generator thermal efficiency [-]
η_{inv}	Inverter efficiency [-]

η_{mec}	Mechanical efficiency [-]
η_{PV}	Efficiency of the photovoltaic modules [-]
θ	Angle between the sun irradiance and the normal to the panel [°]
θ_z	Solar zenith angle [°]
λ	Weibull distribution scale parameter [-]
ρ	Density of air $[kg/m^3]$
${\sigma_h}^*$	Normalized variability of the net demand [-]
$\bar{\sigma}_h^*$	Normalized mean variability of the net demand [-]
ϕ	Latitude of the location [°]
ψ	Longitude of the location [°]
ψ_s	Longitude of the standard meridian [°]
ω	Hour angle [°]
A_{PV}	Area of the photovoltaic system $[m^2]$
A_{swept}	Wind turbine rotor swept area $[m^2]$
C_p	Power coefficient [-]
c_w	Specific heat of water [kJ/kgK]
$CapEx$	Capital Expenditure, i.e. initial cost of investment [€]
CF	Capacity Factor [-]
$CO_{2_{GridIntensity}}$	Carbon intensity of the grid $[kg_{CO_2}/kWh]$
CT	Carbon tax $[€/kg_{CO_2}]$
d	Day angle $[rad]$
$decay$	Decrease in performance factor [-]
DHI	Diffuse Horizontal Irradiance $[kW/m^2]$
DNI	Direct Normal Irradiance at its original direction $[kW/m^2]$
e	Solar elevation angle [°]
E_k	Kinetic energy $[J]$
E_t	Equation of time $[min]$
Exp_{grid}	Expenditure for grid electricity [€]
f	Probability density function [-]
F	Cumulative probability density function [-]
FC	Fuel Consumption [kW]
$FuelCost$	Expenditure for fuel [€]
GHI	Global Horizontal Irradiance $[kW/m^2]$
GTI	Global Tilted Irradiance $[kW/m^2]$
h	Hour of the year [-]
k	Weibull distribution shape parameter [-]
k_t	Clearness index [-]
kW_{peak}	Peak power installed $[kW]$
kWh_{grid}	Annual electricity bought from the grid $[kWh]$
kWh_{PV}	Annual electricity produced by the PV plant $[kWh]$

kWh_{req}	Annual electricity requirement $[kWh]$
kWh_{wind}	Annual electricity produced by the wind plant $[kWh]$
LAT	Local Apparent Time $[hour]$
LST	Local Standard Time $[hour]$
m	Mass $[kg]$
$\dot{m}_A$	Air mass flow rate [kg/h]
$\dot{m}_{EG}$	Exhaust gases mass flow rate [kg/h]
$\dot{m}_{gas_{GT}}$	Gas flow rate used in the gas turbine [kg/h]
$\dot{m}_{gas_{SB}}$	Gas flow rate used in the secondary boiler [kg/h]
$\dot{m}_{NG}$	Natural gas mass flow rate [kg/h]
$\dot{m}_{s_{th}}$	Theoretical steam produced [kg/h]
$\dot{m}_s$	Heat Recovery Steam Generator steam output [kg/h]
$\dot{m}_w$	Feed water mass flow rate [kg/h]
n	Year [-]
NPV	Cumulative Net Present Value [€]
NPV_n	Annual Net Present Value in year n [€]
$OpEx$	Annual operational expenditure [€ $per\ year$]
P	Power $[W]$
$P_{el_{demand}}$	Electric power demand [kW]
$P_{el_{grid}}$	Electric power bought from the grid [kW]
P_{el}	Electric power [kW]
P_{th}	Thermal power [kW]
$price_{el}$	Price of grid electricity [€/kWh]
$price_{gas}$	Price of gas [€/kWh]
r	Discount rate [-]
T_{amb}	Ambient temperature [°C]
T_{EG}	Exhaust gases temperature [°C]
T_s	Steam temperature [°C]
T_w	Feed water temperature [°C]
v	Fluid speed $[m/s]$
v_{cut-in}	Cut-in wind speed $[m/s]$
$v_{cut-out}$	Cut-out wind speed $[m/s]$
v_{rated}	Rated wind speed $[m/s]$
z	Height of the meteorological tower $[m]$

Chapter 1

Introduction

1.1 Context for the research

Over the last century, human activities have warmed the planet and their environmental impact is continuously growing. The Intergovernmental Panel on Climate Change IPCC [1] has reported a rise in the Global Mean Surface Temperature (GMST) of approximately 0.2°C per decade. At the end of 2017 the GMST was 1°C above the pre-industrial level and it is estimated to reach 1.5°C between 2030 and 2050 if the current rate of increase is maintained. In order to limit climate-related risks for natural and human systems, the IPCC set an initial target of keeping the rise in temperature below 2°C, and recently reduced it to 1.5°C.

The main cause of global warming is the anthropogenic emission of greenhouse gases (GHG), consisting mostly (≃70%) of carbon dioxide (CO_2). The main emitter of CO_2 is the energy sector [2], which includes various sub-sectors such as electric and heating power generation, and transport [1] (Figure 1.1).

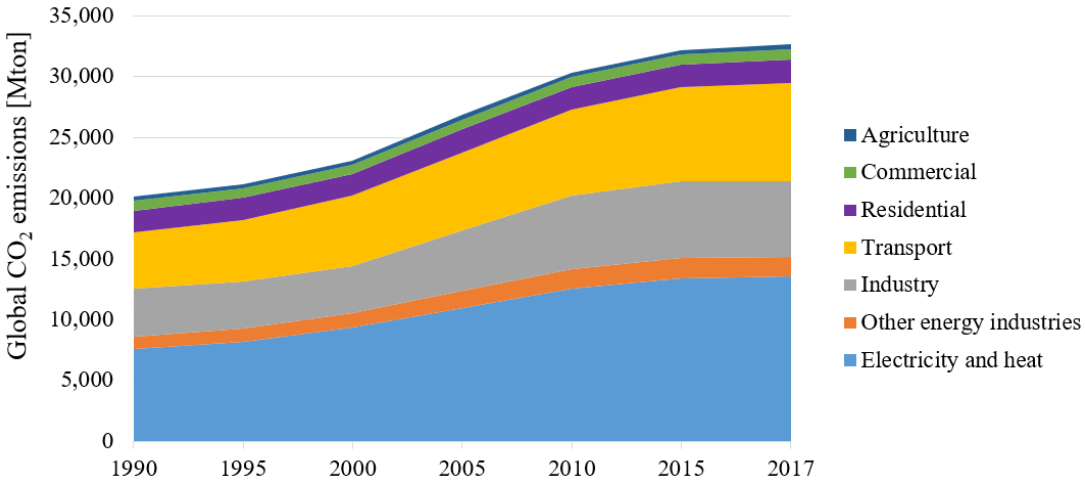

FIGURE 1.1: Global CO_2 emissions by sector
Based on data from the International Energy Agency [3]

[1] Electricity and heat are energy vectors used in the residential, commercial, and industrial end-use sectors.

In order to comply with the 1.5°C limit set by the IPCC, stronger and more coherent actions are needed rapidly to reduce the environmental impact of the energy sector. Despite progress in decreasing the amount of lost and wasted energy, the achievement of the necessary emissions reduction is still far away: a change towards a more sustainable way of both producing and consuming energy must occur.

While policies and incentives have been widely studied and already implemented to increase the sustainability of energy consumption in the residential sector, targeting the decarbonization of the industrial sector is more complex but also extremely important, given its key role in emissions reduction and in shaping the transition to a low carbon energy system. The industrial sector is, in fact, responsible for almost one third of the overall energy consumption [4] and accounts directly for 21% and indirectly (electricity taken from the grid) for another 11% of global greenhouse gas emissions [5]. By reducing the emissions associated with the industrial energy load, a considerable step forward could be made towards energy decarbonization. Options available to an industrial facility for reducing its environmental impact can be summarized as follow:

- adopt measures that increase the efficiency of the energy usage in the industrial facility, reducing overall wasted energy;
- purchase green (low-carbon) power to use on-site (e.g. through a corporate power purchase agreement with a renewable farm);
- produce on-site part/all of its energy load in a more sustainable way.

The latter is analysed in this thesis as option for reducing the environmental impact of the Irish manufacturing industry.

Manufacturing facilities have very different needs compared to the residential sector, requiring a continuous supply of thermal and electric energy that often cannot be altered based on the necessity of the grid. Therefore well-known solutions such as Demand Side Management (DSM) cannot be easily applied. These facilities are profit-driven entities and therefore economic parameters such as costs and Pay Back Time (PBT) are the main variables taken into account in the decision to invest capital. In fact, many industries operate in highly competitive markets and the transition to a low carbon economy should not damage their competitiveness. Therefore, as noted by the IPCC [5], in order to reduce the environmental impact of a manufacturing facility, the proposed solutions must be economically viable as well as technically feasible.

The main reason for the high level of emissions produced by the manufacturing sector is found to be the massive electric and thermal energy requirements to manufacture consumer products. While significant progress has been made in decarbonizing electricity generation, manufacturing industry has been slow in adopting solutions such as on-site renewable systems because the profitability of these investments is often dependent on environmental policies, that are difficult to predict in the long term [6–8]. Considering, on the other hand, the thermal energy demand of a manufacturing facility, there are fewer options for increasing

the sustainability of heating power generation due to more limitations. Heat is, in fact, a relatively carbon intensive end-use sector since it mostly relies on fossil fuels. There are low-carbon technologies for heating available on the market, however they are mainly suitable for low temperature applications such as space-heating, which represent the typical needs of residential end-users [9–11]. While these alternative technologies exist (e.g. heat pumps, thermal energy-storage, electric heaters), they are generally either significantly costlier or they require additional infrastructures that make them not economically viable for households [12]. There is a limited range of alternative solutions available at the moment for decarbonizing the thermal energy demand of manufacturing facilities, which is often significantly higher compared to an average end-user in the residential sector and is often required for high-temperature production processes [13].

1.2 Scope and contribution of the thesis

The overarching objective of the thesis is to investigate the viability for an Irish manufacturing facility to become an energy "prosumer" (i.e. both producer and consumer of energy) in a progressively decarbonized energy sector, by producing on-site part of the electric and thermal energy load in a more sustainable way and be actively involved in reducing industrial carbon emissions.

In order to achieve this goal, the following sub-objectives are identified:

- to determine the peculiarities, requirements and constraints of manufacturing facilities;
- to evaluate which technologies available on the market are suitable for on-site electric and thermal energy generation based on manufacturing facilities requirements;
- to develop a robust and flexible new tool in Matlab that allows the evaluation of the techno-economic feasibility of on-site energy generation for self consumption for different energy technologies for a generic manufacturing facility;
- to simulate through the implemented model the long term environmental benefits of the analysed on-site generation system, in terms of CO_2 emissions reduction.

The contribution of the thesis lies in:

- the development of a robust and flexible new model in Matlab that can be used to simulate the techno-economic and environmental feasibility of on-site energy generation for self consumption for a manufacturing facility;
- conducting the analysis, with the new implemented model, on a real Irish manufacturing facility to showcase the impact of technology adoption on a real end-user, in contrast to aggregated representations present in the literature that do not provide this insight;

- the identification of the constraints that characterize industrial end-users and may constitute an obstacle to becoming energy prosumers;
- the assessment of the techno-economic conditions in which on-site variable renewable energy generation would be a feasible option for an Irish manufacturing facility. This information could be relevant when establishing governmental policies with the goal of increasing the penetration of distributed renewable energy;
- the assessment of how the environmental benefits of on-site Combined Heat and Power (CHP) systems vary as the grid is progressively decarbonized. While it is widely known that CHP systems are currently an environmentally feasible solution for energy cogeneration in industrial sites, it is not clear whether they will still lead to positive carbon emission savings as the carbon intensity of the electric grid decreases;
- the study of the effect of introducing on-site energy generation on the residual electric load that the electric grid has to cover. As the penetration of distributed variable renewable energy increases, more flexibility will be required from the grid and balancing services will become increasingly important.

1.3 Outline of the thesis

The objectives listed in the previous section are addressed in the different chapters of the thesis as detailed below.

In Chapter 2, the evolution of the Irish industry sector and the main energy trends are discussed. The impact that climate policies have had on the Irish industry development are analysed along with the targets set by the European Union and Ireland for 2030. The main technical and institutional drivers of the transition towards a more sustainable energy sector are identified.

In Chapter 3, the different options currently available for decarbonizing the Irish manufacturing industry are discussed and the focus of the present thesis is highlighted. The new model implemented in this thesis and used as a tool to investigate the technical, economic and environmental feasibility of on-site energy generation in a manufacturing facility is presented.

An existing Irish manufacturing facility has been used as real case study to provide realistic data as inputs to the model. In Chapter 4, the peculiarities of this facility are evaluated to provide insights on manufacturing industry that have been then included in the model.

Its energy demand per all the different energy vectors is analysed. First, the hourly energy consumption profile over an entire year of each energy vector used in the facility is examined to better understand which technologies may be more suitable for on-site energy generation. A statistical study is conducted on the electric and steam demand to identify characteristics that

could be considered common peculiarities of manufacturing facilities. Possible inefficiencies in the current way of consuming energy are also investigated. The technologies considered better suited for reducing the carbon emissions associated with the manufacturing facility through on-site cogeneration of both electric and thermal energy are: renewable energy technologies such as solar photovoltaic (PV) and wind turbines, and a Combined Heat and Power (CHP) system. The state of the art of these technologies is presented in Appendix A.

In Chapter 5, the methodology used for assessing the technical, economic and environmental feasibility of on-site electricity generation through an on-site VRE system is described more in details. The procedure used to properly size the system and the equations used in the model, presented in Section 3.2, are stated in details. Then the results are presented: the technical feasibility is assessed in terms of electricity generation and overproduction; the economic feasibility is assessed by calculating the Pay Back Time (PBT) of the project in current and future scenarios, and the techno-economic conditions that would make the VRE system economically feasible are highlighted.

In Chapter 6, the integrated cogeneration system for on-site electric and thermal energy generation is described: it consists of the PV and wind system, a Gas Turbine (GT), a Heat Recovery Steam Generator (HRSG) and a secondary boiler. The contribution of every technology to the energy load of the facility is modelled hourly for the entire lifetime of the system. The technical, economic and environmental characteristics of this scenario are assessed and presented. The effect on apparent volatility of the net demand is also explored.

The limitations of the on-site integrated system are highlighted and potential solutions to these limitations are explored.

The effect of introducing on-site a battery storage system for reducing the variability of the net demand is assessed in Appendix B. The use of biogas instead of natural gas is proposed to overcome the temporal limit of the environmental benefit of the system: a brief overview of the current state of the art of biogas production, its supply potential and cost is given in Appendix C.

Finally, in Chapter 7 the conclusions of the thesis and suggestions for future work are presented.

Chapter 2

Decarbonization of the Irish industry sector

In this chapter the main industrial sectors active in Ireland are briefly presented. The evolution of the energy trends in the overall Irish industry sector and the impact that climate policies have had on its development are then analysed. The targets set by the European Union and by Ireland moving towards 2030 are discussed, along with the technical and regulatory barriers to a higher penetration of Variable Renewable Energy (VRE).

2.1 Energy trends in the Irish industry sector

From independence until the early 1930s the primary concern of the Irish government was the development of the agriculture sector. In the second half of the 30s, in order to establish a degree of economic independence, for the first time the government intervened in regulating the industrial sector. To allow for industrial development and reduce emigration of Irish citizens, home production was protected by establishing more extensive tariff walls to protect the newly established industries against foreign competition and by setting the requirement for new industrial enterprises of having at least 51% per cent of capital and the management of Irish origin [14].

Since then, the industry sector in Ireland has significantly evolved and can nowadays be described mainly as a knowledge economy[1], which focuses on financial service, high tech, and life science. Ireland registered a period of continuous economic growth between 1984 and 2007, but then it slowed down due to the 2008 financial crisis. The recovery of the economy in 2014, made Ireland the country with the fastest growing economy in the EU, growing by 4.8%. Several industries have contributed to the growth registered by the country [15]:

- Primary industries, which rely on the rich natural resources and include agriculture, mining, forestry, and fishing. Primary industries account for 5% of the country's GDP and employ about 8% of the total labor force. Agriculture has always had a strong potential for the Irish economy due to its large pasture, particularly in the southern and midland regions. However, agriculture contributes only 1% of the GDP. The mining

[1] Application of knowledge to generate tangible and intangible value.

industry relies mainly on the production of lead, zinc, alumina, and a small quantity of minerals such as copper, gold, limestone, and gypsum. Ireland is one of the major exporters of zinc. Extraction of natural gas takes place in Corrib and Kinsale Gas Fields where there are an approximately 20 billion cubic meters of proven reserves.

- Pharmaceutical and medical technology industries, which is one of the fastest growing industries in Ireland. This sector has over 100 companies with about 25,000 employees, generating 9.4 billion euros annually. The pharmaceutical industry registers nearly 50,000 employees and generates about 60 billion euros of export annually.

- Software and Information and Communication Tecnologies (ICT) industries. The success of this sector in Ireland is the result of the financial policies of the last few years which brought a number of foreign companies to set up their headquarters' offices in the country, especially in Dublin. This number is still growing, also due to the impending Brexit. The ICT sector employs over 35,000 people and generates about 35 billion euros per year. There are over 200 ICT companies, which includes most of the 10 largest ICT companies, including Facebook, Google, eBay, Amazon, LinkedIn, Twitter, Paypal, and Microsoft. The software sector generates over 16 billion euros annually and employs about 20,000 people. Ireland is the second-largest exporter of software in the world.

- Financial service industry, which has significantly recovered after the financial crisis of 2008. The sector employs nearly 35,000 people and generates an average of 2 billion euros in taxes. Ireland is Europe's 7th largest provider of wholesale financial services.

- Export and trade industry, which are the two main components of the economy of Ireland due to the sell of manufactured goods. Ireland is among the largest exporter of software-related goods, medical devices, and pharmaceuticals. The country is also the largest producer of zinc and the second-largest producer of lead in Europe. These minerals contribute greatly to Ireland's export earnings.

The industry sector in Ireland is a significant energy user (Figure 2.1). The economic activity and final energy use of industry in 2018 increased respectively by 9.6% and by 4.7% (reaching 2.6Mtoe) compared to the previous year [16].

As shown in the report produced by the Sustainable Energy Authority of Ireland SEAI [16], the final energy use in industry in 2018 was 50% higher compared to 1990 but 1.2% lower compared to 2005. The increase in final energy demand of the Irish industry peaked in 2006, with almost 2.7Mtoe, +55% compared to 1990. Between 2006 and 2009 there was an 18% fall in industrial final energy use and then, following a small increase in 2010 of 2.8%, the consumption in industry fell again until 2012. After 2012, the energy use in industry increased by 19% (Figure 2.2). The reduction trend that has characterised the last decade is due to both a reduction in the overall economic growth during certain periods of economic crisis (2008) and also to positive effects of governmental policies that promoted the switch to more efficient technologies in manufacturing production lines.

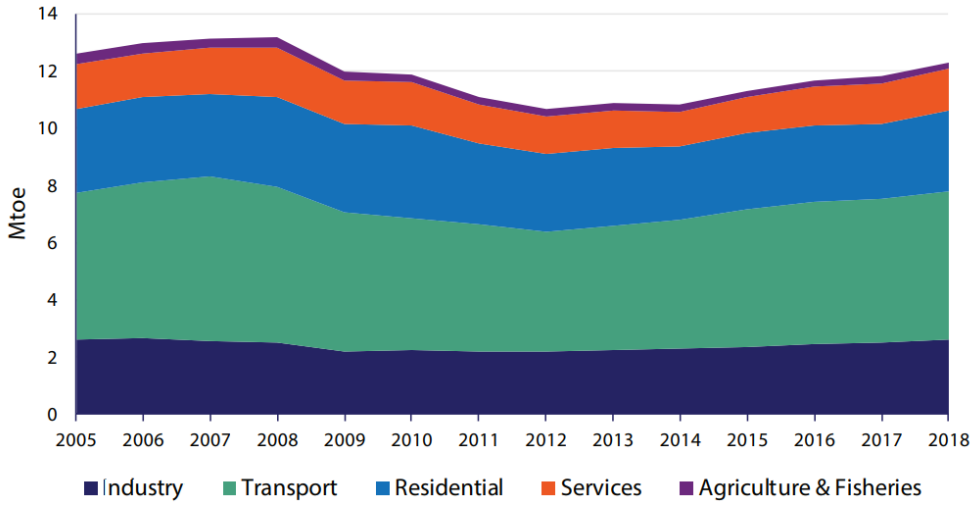

FIGURE 2.1: Total final energy consumption by sector in Ireland [16]

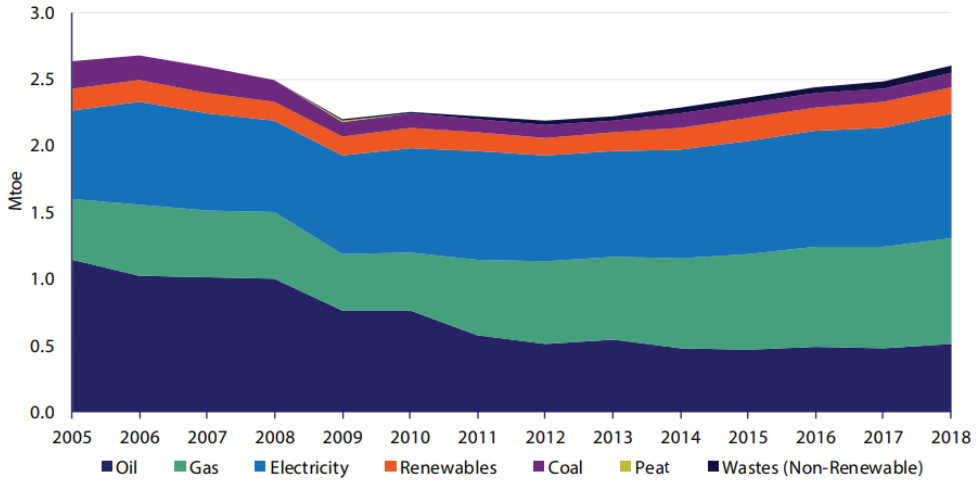

FIGURE 2.2: Total final energy use in industry bu fuel [16]

Over the period 2005–2018 only electricity, natural gas, wastes and renewables have increased their shares. The share of electricity has risen from 25% to 36%, natural gas from 18% to 30% and renewables from 6.2% to 7.6%. The increase in renewables is mainly due to the use of biomass in the wood-processing industry, the use of tallow in the rendering industry and the use of the renewable portion of wastes in cement manufacturing. Investments in on-site renewable plants from industrial facilities are still limited due to the dependency of their profitability on governmental policies, which are often variable and don't guarantee a low-risk investment.

The main trends in final energy use in industry in 2018 were:

- The consumption of all fuels increased with the exception of non-renewable wastes compared to the previous year.

- Oil use increased by 7.4%, to 516 ktoe, and accounted for around 20% of industry's energy use.
- Natural gas consumption in industry increased to 790 ktoe and accounted for 30% of industry's energy use.
- Renewable energy use increased to 198 ktoe and accounted for 7.6% of industry's energy use.
- Electricity consumption increased to 936 ktoe and accounted for 36% of industry's energy use.
- Coal use increased by to 105 ktoe and accounted for 4.1% of industry's energy use.
- The use of non-renewable wastes in industry fell by 3.7% to 55 ktoe, and accounted for 2.1% of industry's energy use.

Direct use of all fossil fuels accounted for 54% of energy use in industry in 2018 and grew by 4.8% in that year. Over the period 2005–2018, the use of fossil fuels in industry fell by 22%: while coal and oil consumption in industry fell over the period by 50% and 55%, overall fossil fuel did not fall at the same rate because of the increased use of natural gas (+71%). These changes in the fuel mix resulted in lower emissions from fuel-use in industry during this period.

The industry sector is responsible for a significant share of CO_2 emissions, as shown in Figure 2.3, that differentiates the on-site CO_2 emissions associated with direct fuel use and the upstream emissions associated with electricity consumption. The industry sector is, in fact, characterized by a high demand of both electric and thermal energy. While alternative technologies are available for producing low-carbon electricity that can be consumed by the industrial sector, lowering its environmental impact (e.g. renewable technologies), the heat energy use is more difficult to decarbonize. Direct energy use for heat in industry increased by 4.4% in 2018; heat is a relatively carbon intensive end-use sector that still relies mostly on fossil fuels and many manufacturing industrial processes are characterized by high-temperature thermal energy requirements, for which at the moment not many low-carbon technologies are commercially available and economically competitive.

In 2018 the industrial energy-related CO_2 emissions fell by 3.5%, to 8.1Mton and the electricity consumption was responsible for 50% of industry's energy-related CO_2 emissions. If upstream electricity-related emissions are omitted, then there was a 4.8% increase in CO_2 emissions from combustible fuels used on-site. This is as a result of changes in the volume and fuel mix used in industry, with increased oil (+7.3%), coal (+3.1%) and natural gas (+3.5%) countered by increased renewables (+3.5%).

The energy intensity of the Irish industry sector, defined as the amount of energy required to produce a unit of value added, fell by 1.2%, while value added increased by 146%, resulting in a reduction in intensity of 60% (Figure 2.4).

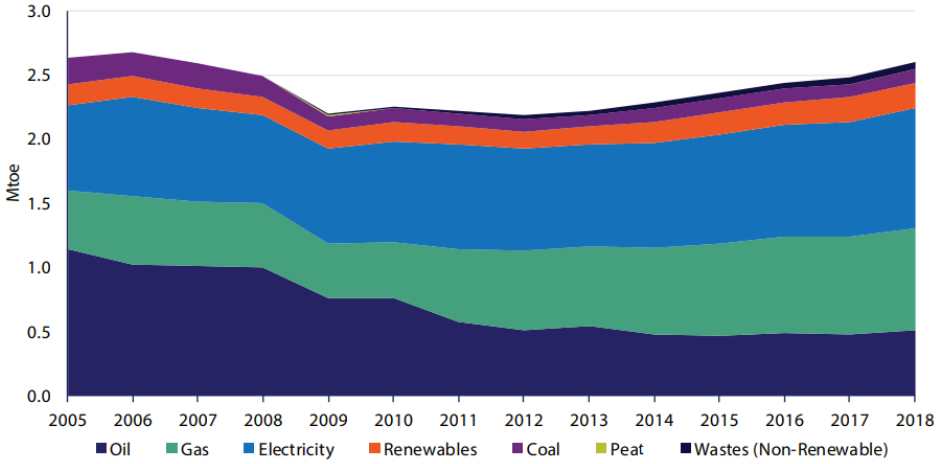

FIGURE 2.3: Industry energy-related CO_2 emission in Ireland [16]

The large increase in gross value added in 2015 is explained by a number of one-off factors, such as the transfer of assets into Ireland, and what are known as reverse takeovers. This increase in gross value added incurred no additional energy consumption. Energy intensity in this form is not a good indicator of energy efficiency, and variations may be the result of many factors, such as structural changes, or changes to the fuel mix or the volume [16].

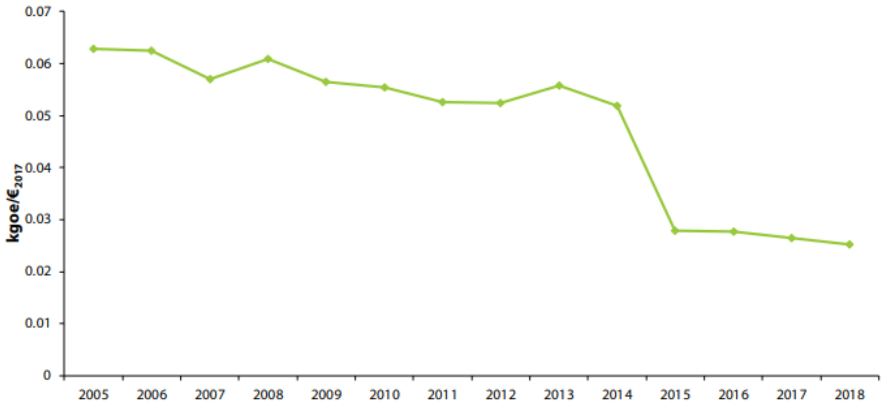

FIGURE 2.4: Industry energy-intensity in Ireland [16]

It has been shown that the Irish industry sector is responsible for a significant amount of energy demand and CO_2 emissions. In the next section, the policies that are targeting the decarbonization of this sector are analysed.

2.2 Climate policies targeting decarbonization of industry

The increasing scientific evidence regarding the contribution of energy use to climate change coupled with the growth in energy demand and related emissions have urged governments and policy makers to introduce policies designed to manage energy more effectively, to move towards less polluting fuels and to mitigate human impact on the environment.

This section briefly identifies the major policy developments that have had an impact on the industry sector.

The main policy that has been implemented by the European Union with the aim of reducing GHG emission is the EU Emission Trading Scheme (EU ETS). It currently is the world's first major carbon market and the biggest one. It operates in all the european Countries and also in Iceland, Liechtenstein and Norway, it limits emissions from more than 11,000 heavy energy-using installations (including power stations and certain industrial plants) and airlines operating between these countries; overall it covers around 45% of the EU's greenhouse gas emissions [17]. The EU ETS, set up in 2005 as the world's first international emissions trading system, works on the 'cap and trade' principle, i.e a cap is set on the total amount of greenhouse gases that can be emitted by installations covered by the system. By progressively reducing the cap, the total emissions fall. The companies which are regulated by the EU ETS scheme receive or buy their emission allowances (within the cap limit), which can then be either used or traded. At the end of each year, each company must have a sufficient amount of allowances to cover their annual emissions, otherwise heavy fines are imposed. If a company reduces its emissions, it can keep the spare allowances to cover its future needs or else sell them to another company that is short of allowances.The limited availability of allowances and the amount of emissions produced by companies that year influence the market value. This European policy incentivizes companies to invest in clean, low-carbon technologies, to limit their allowances requirement for future years.

The EU ETS has proved effective in reducing emissions from installations in the system: the European Commission's report [18] shows that in 2018 emissions from installations covered by the EU ETS decreased by 4.1%, about 73 million tonnes of CO_2 equivalents, compared to the previous year.

The system covers the following sectors and gases, focusing on emissions that can be measured, reported and verified with a high level of accuracy:

- Carbon dioxide (CO_2) from:
  - power and heat generation;
  - energy-intensive industry sectors including oil refineries, steel works and production of iron, aluminium, metals, cement, lime, glass, ceramics, pulp, paper, cardboard, acids and bulk organic chemicals
  - commercial aviation;
  - nitrous oxide (N_2O) from production of nitric, adipic and glyoxylic acids and glyoxal;
  - perfluorocarbons (PFCs) from aluminium production.

Participation in the EU ETS is mandatory for companies in these sectors, but presents some exceptions: in some sectors only plants above a certain size are included; certain small installations can be excluded if governments put in place fiscal or other measures that will

cut their emissions by an equivalent amount; in the aviation sector, until 31 December 2023 the EU ETS will apply only to flights between airports located in the European Economic Area (EEA).

Currently the EU ETS scheme is at its third phase and, compared to the precedent two phases, a single cap on emissions applies now to all the subjected Countries, with auctioning as the default method for allocating allowances and harmonised allocation rules. 300 million allowances are also set aside in the New Entrants Reserve to fund the deployment of innovative, renewable energy technologies and carbon capture and storage through the NER 300 programme. The fourth phase will begin in 2021 and will focus on increasing the pace of annual reductions in allowances to 2.2%, reducing the surplus of emission allowances in the carbon market, safeguarding the international competitiveness of industrial sectors at risk of carbon leakage through free allowances allocation,

The EU ETS scheme targets the Irish industrial sector, as has been discussed above, however it presents some limitations as shown by the fact that the decrease in emissions registered in the past years was mainly driven by the power sector, while emissions from industry decreased only slightly. The EU ETS, in fact, targets only certain Irish industrial activities, which have between the different requirements a high thermal energy demand (total rated thermal input exceeding 20 MW, as per S.I. No. 490/2012 [19]). The remaining industrial activities fall below the non-ETS scheme and only a limited amount of measures are taken to limit their emissions.

The present thesis, in particular, focuses on investigating available options for reducing CO_2 emissions in manufacturing industrial facilities with high electric and thermal demand and significant CO_2 emissions production that do not follow under the EU ETS scheme.

Industries that are not included in the EU ETS scheme, such as the facility analysed in this thesis, have to face the risk of deploying new innovative technologies based on governmental policies that are continuously evolving and this has resulted in manufacturing industry being slow in adopting solutions such as on-site renewable systems because the profitability of these investments is often dependent on environmental policies, that are difficult to predict in the long term [6–8]. In manufacturing facilities with high electric and thermal energy consumption in production processes, the challenges of decarbonization are greater since major changes in process technologies may be required and when going beyond marginal emission reductions, there seems to be relatively few, if any, co-benefits from decarbonisation [20]. The main issue is that adopting more significant changes such as innovative technologies for improving the energy efficiency of production processes or switching to non-fossil fuel energy sources, will likely lead to higher production costs that could threaten international competitiveness if not properly remunerated by tailored policies and may lead to carbon leakage (i.e. production relocated in countries with less strict climate policies). A new approach is required to reach the 2050 almost carbon neutrality, which should integrate innovation, aligned industrial, climate and energy policies that integrate international trade and foreign policies to ensure a fair competitiveness worldwide.

A measure from which all type of industrial facilities can instead benefit is the establishment of the Large Industry Energy Network (LIEN) [21]. The Large Industry Energy Network is a voluntary network, facilitated by Sustainable Energy Authority of Ireland, which involves companies working to maintain strong energy management and environmental protection practices. LIEN members collaborate on best practice and new technologies in energy management and benefits from the share of competences and progresses. LIEN's core aim is to support participants' goals for reducing the cost of energy. Investing in improving energy efficiency has shown not only environmental benefits to these companies but also social benefits and an improved firms' relationships with stakeholders. The share of knowledge and competences takes places through workshops and seminars, providing the possibility to socialize expertise. The stronger priorities that have been identified by the LIEN group are improving energy efficiency and the use of renewable energy and all the achievements reached by LIEN companies are recognised and contribute to national energy objectives ranging across efficiency, competitiveness, energy security and environmental protection.

2.3 Towards 2030

Ireland is contributing to the Paris Agreement via the Nationally Determined Commitment tabled by the European Union based on reductions in the ETS and non-ETS sectors of respectively 43% and 30% (compared to 2005). The non-ETS target, while not yet agreed, will present an enormous challenge for Ireland, which will require substantial investment by both the public and private sectors, as well as a broad range of non-financial policy tools, including regulations, standards, education initiatives and targeted information campaigns [22].

The European commitment to decreasing GHG emissions by 2030 of 55% compared to 1990 level will pass through a further decarbonizing of the energy system, critical to reach climate objectives in 2030 and 2050. The production and use of energy across economic sectors account for more than 75% of the EU's greenhouse gas emissions. Energy efficiency and further penetration of renewable sources are the priority identified by EU [23].

Ireland has put a lot of effort in progressively introducing more and more renewable energy into the electric system and electrify, where possible, the other energy sub-sectors committing to produce from renewable sources at least 16% of all the energy consumed by 2020 through a 40% target of renewable electricity, 12% of renewable heat and 10% of renewable transport [24].

Part of the European strategy to reach a significant decarbonization by 2050 is, in fact, to cover 95% of the electricity consumption by Renewable Energy Sources (RESs) and electrify as much as possible the other two sub-sectors, heat and transport [25].

A large share of renewable energy comes from Variable Renewable Energy (VRE) sources, such as solar and wind, defined variable sources because the electricity produced comes from stochastic energy flows and therefore is more variable and difficult to forecast. In fact, in

2018 wind generation accounted for 85% of all the Irish renewable electricity and for 28.1% of all the Irish electricity generated [16].

Variable Renewable Energy (VRE) has a key role in decarbonizing the energy sector by partially replacing highly polluting fossil fuels in the power generation mix. The penetration of VRE into the electric grid is, however, currently limited due to technical/physical and market/regulatory barriers. A brief overview of these barriers is provided in the next sections.

2.3.1 Technical barriers to further VRE penetration

Technical barriers to a deep VRE penetration lie in the fact that the electric grid needs to balance production and consumption at every spatial node in every instant of time to maintain a stable system frequency. When the electricity system was typically managed by a single vertically integrated company and electric power was mostly supplied by traditional centralized power plants, it was relatively easy to maintain the balance. With the liberalization of the electricity market (Electricity Directive 96/92/EC), the power generation was separated from the transmission segment, managed now by Transmission System Operators (TSOs), making it more difficult to guarantee the balance of the system [26]: a liberalized market, in fact, allows a larger number of participants to enter the market and has a positive effect on the competitiveness of the market but at the same time the increased quantity of power plants that participate to the market results in a higher complexity of the system that the TSO has to manage. In addition to that, balancing generation and demand becomes more challenging as a higher share of energy is produced from VRE systems, which are characterized by variability, uncertainty and locational-dependence. VRE systems, in fact, consist mostly of decentralized plants that exploit renewable sources, whose availability is strictly dependent on the weather in that geographical location.

The variability of renewable sources represents a technical limitation to the progressive increase in VRE penetration in the electric grid. With more energy coming from renewables, the residual electric load that remains to be covered by conventional power plants will have a more variable trend, with a consequent rise in the number of ramps.

Balancing the system is more challenging when the demand and the VRE production vary both very fast and in opposite directions:

- When the electricity demand drops while the VRE production increases to peak. As consequence, the dispatchable power plants will decrease their output, following the demand profile.
- When the electricity demand rises rapidly while the VRE production decreases. As consequence, the dispatchable power plants will increase their output as fast as they can to follow the demand profile.

When renewable sources are highly available and more energy than actually required would be produced, part of this energy has to be curtailed to maintain the balance of the

system, wasting clean and fuel-free energy. The case of Germany is shown as example in Figure 2.5: the amount of energy curtailed has increased every year since 2010 as the renewable penetration rises. In 2017 the energy curtailed reached 5,518GWh, of which 5,287 came from wind generators. This indicates that to reach the target of energy coming from renewables, the VRE capacity installed should be highly overdimensioned since the electric grid is currently not flexible enough to use all the renewable energy available and has to curtail a share of potentially clean and fuel-free energy.

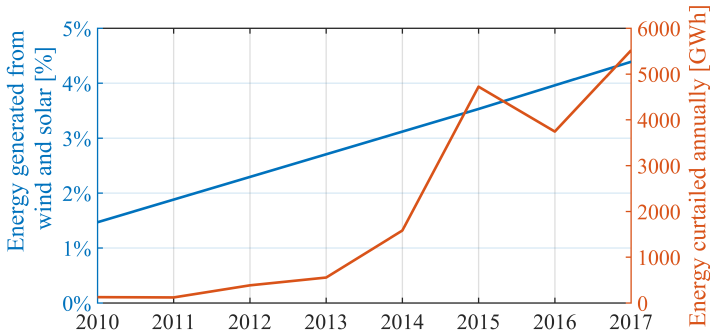

FIGURE 2.5: Annual curtailment and share of renewable energy sources in the final energy mix in Germany.
Based on data from the United States Department of Energy [27]

Another technical barrier is managing uncertainty. Uncertainty is not a new issue in the energy market, but, until the last decade, it was mostly related to the forecast of the energy demand, which included a statistical error. The demand profile is, however, more regular and easily predictable nowadays on a daily, weekly and seasonal base (Figure 2.6). Instead, the power output from VRE systems is highly unpredictable and very difficult to model.

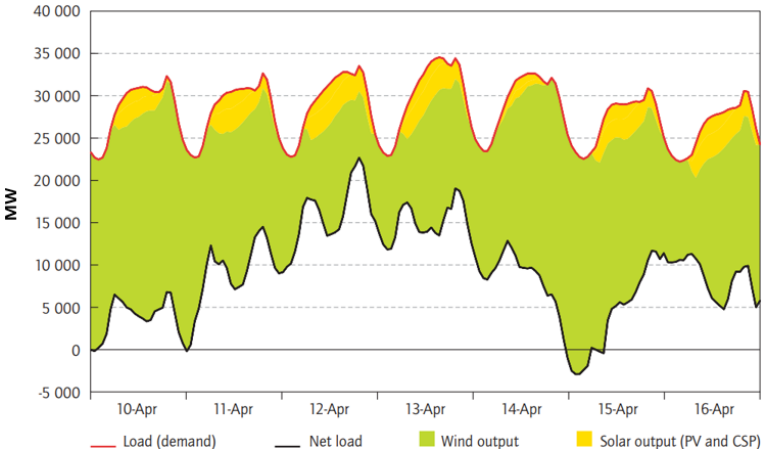

FIGURE 2.6: Effect of Variable Renewable Energy (VRE) generation on the net load [28]

Both these issues, high variability and uncertainty, lead to one of the most important features the future grid is required to have: flexibility, defined as how much the power system is able to modify its power output to adapt to the variability of the load.

IEA defines four forms of flexibility [28]: generation side, demand side, interconnection and storage. Concerning the flexibility on the *generation side*, flexibility in solar and wind systems lies in the possibility of curtailment, i.e. the possibility to curtail clean energy generation in case of excess availability of renewable sources compared to the electric load. Instead, flexibility of traditional power plants is identified through four parameters [29]: minimum load, ramp rate, start-up time and start-up cost. A larger share of intermittent renewable energy is estimated that will increase the variability of the residual load up to 38%. While nuclear and coal-fired power plants are design to operate at their optimum point, where they have the best performances, the modern gas-fired power plants are already very flexible and can provide fast start-ups in case of unexpected variations in the net load. They may represent a cost-effective solution to be used as back-up capacity in a high-RES scenario, if coupled with additional measures as Carbon Capture and Storage (CCS) for CO_2 emissions reduction.

The flexibility on the *demand side* lies in the "demand-side management and response": a percentage of the load is shifted dynamically over time to balance the scarcity/excess of electricity by reducing/increasing the consumption. Demand Response (DR) has been studied for decades and it is a particularly effective mechanism in the residential sector, while it is often not a suitable option for industrial facilities.

The third form of flexibility is found in the *interconnections of the network*. An increasing number of interconnections at European level can guarantee a higher flexibility of the grid by transporting the electricity from where it is produced to where it is needed most. In case a surplus of RES generation occurs, it can be exported, avoiding negative electricity price on the local market. It is a feasible solution only if the transmission and interconnection capacities are sufficient.

The last form of flexibility is the *storage*. Storage technologies are used to shift the production and consumption of energy in time: they store energy when cheap sources are available and the demand is low, and make it available when the load on the grid is high and problematic to satisfy. Given its important role in RES integration, many studies focus on storage systems. The current most economical and used utility-scale technology is pumped hydro storage. Batteries have a great potential especially for distributed medium and small scale applications, but the cost is still high.

The uncertainty and variability of VRE systems require additional capacity for supplying the power guaranteed by VRE systems in case the renewable sources availability differs from the forecast. This is where the current structure of the electricity market has to evolve: the availability of back-up generation capacity should, in fact, be properly remunerated to guarantee an increasing support to higher VRE penetration. The electricity market should properly consider the costs related to the increasing necessity of balancing services and modify its structure accordingly.

2.3.2 Market barriers to further VRE penetration

The regulation of the electricity market was build on a centralized electricity system characterized mostly by traditional centralized power plants connected to the electric grid in the context of a low VRE penetration. Therefore, the current structure of the electricity market may present barriers to higher VRE penetration, as the value of electricity drops rapidly as the VRE penetration rises.

An overview of the market design is given to better understand where the possible regulatory barriers to a higher penetration of VRE lie. Hu et al. [30] provide a review of the market design, which is briefly summarized in this section.

The electricity market involves different sub-markets with different time-frames, as shown in Figure 2.7.

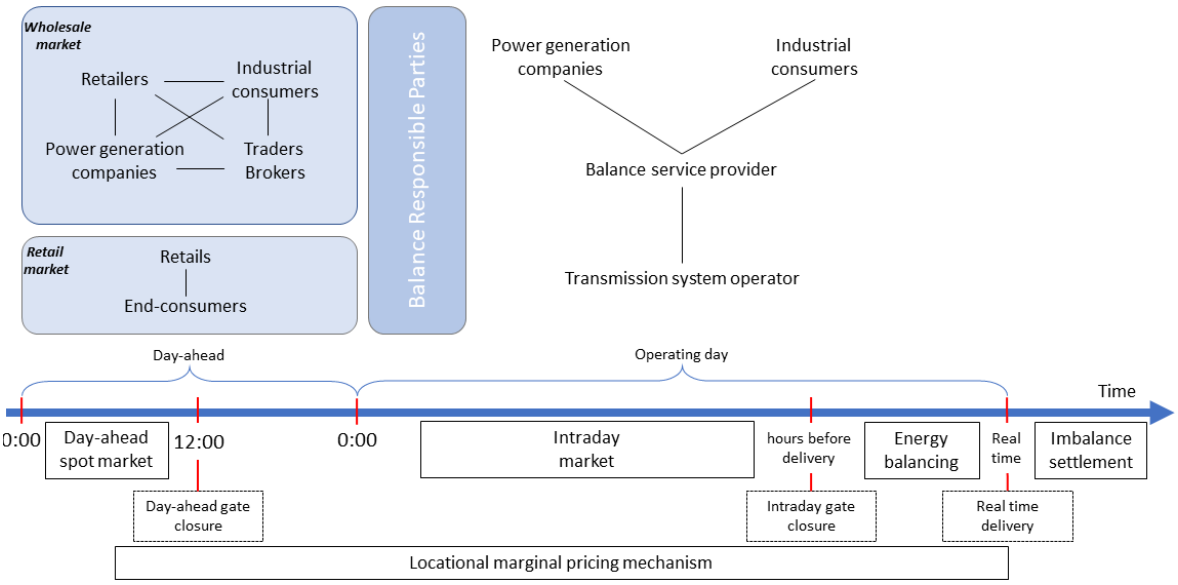

FIGURE 2.7: Structure of a competitive electric market and participants involved. Inspired by Hu et al. [30].

The electricity demand is forecast based on historical data; a high share of electricity generation to cover the estimated demand is sold to different suppliers on the year or month-ahead market through a bid system. Since long-term planning is subjected to uncertainty, getting closer to the moment of delivery other sub-markets come into play: the day-ahead spot market (DA), intraday market (ID), balancing market (BA) and the imbalance settlement. By the time of gate closure, generation and load parties must notify the TSO of their expected physical positions at real time and additional capacity is bought by the TSO to cover possible unbalances [31].

The DA spot market trades hourly power supply for the following day. All the bids are classified by ascending price (merit order) and the offers are classified by descending price. The demand with the highest willingness to pay goes with the supplier with the lowest willingness to sell. This procedure is repeated until a mutually approved price is found. The

highest price to be matched is defined "market clearing price" and it is the uniform price set for all the suppliers that won the bid. When the DA trading closes (12:00pm of the day-ahead), the bid winning parties have to commit themselves to ex-ante scheduling of power generation or consumption on a half-hour basis (in the specific case of Ireland). Every party chooses a balancing responsible party (BRP), which should have an overall balanced position before the delivery. Individual imbalances may be offset by other participants under the same BRP responsibility; if there are overall net imbalances in a BRP, they are settled financially [32].

The ID market is closer to the real time delivery, therefore market participants have new information (e.g. renewable sources availability updated forecast) relevant for their short-term planning. This market is organized in two different ways across European countries [33]: based on discrete auctions or on continuous trading. The first method, used in Spain, Italy and Portugal, establishes different auctions which are settled at different times. If the latter approach is applied (as in Nordic countries) bids and offers are not matched at a specific time but on a first-come-first-served order as soon as an offer matches the price of a bid. Therefore, every trade may have a different market price. Some countries as Germany, UK and Ireland combine the two mechanisms.

Since the time resolution of the DA market is of the order of one hour, even when all the market participants meet their DA commitment, it is not ensured that generation and consumption would be balanced within that period of delivery. The TSO reserves balancing capacity from Balancing Service Providers (BSPs) in the balancing market and activates it when imbalances are expected. Suppliers of active balancing power commit to supply energy if required at a certain ramp-rate, time-frame and for a specific duration. When BRPs don't meet their DA commitments, the cost paid by the grid for the activation of balancing capacity is allocated ex-post in the imbalance settlement. The trading product of this sub-market is the difference between the BRPs commitment and the real-time delivery; the time resolution varies between 15 and 60 minutes. The imbalance market can use a one-price or two-price system. The one-price system imposes the same price to BRPs with positive or negative imbalances: BRPs who produce less or consume more than declared (short) pay while BRPs that produce more or consume less (long) get paid. This method makes a long and a short BRP counteract and balance, aggravating system imbalances. The two-price system instead discourages imbalances by differentiating the imbalance settlement price from the DA price. This could, however, lead to strategic behaviour from BRPs that could submit production plans depending on the pricing system [33].

With the progressively increasing penetration of VRE, more imbalances are occurring due to the difficulty to accurate forecast renewables availability. There is, therefore, a pressing need for the electricity market to properly consider the costs related to the increasing necessity of balancing services and imbalance settlements and to modify its structure accordingly.

Integration costs, i.e. the costs for settling imbalances, have been analysed by Hirth et al. [35], who decompose them in three key components, based on the main characteristics of VRE: temporal variability, uncertainty and location-dependence.

Integration costs are high if renewable technologies are used at large scale and not considering them could strongly bias results. The largest integration cost component has been identified by Hirth et al. in the reduced utilization of the capital embodied in thermal plants. VRE systems have a zero fuel cost and can often bid with a very low DA price, which sometimes is even negative if they receive incentives that exceed their marginal costs; therefore they are dispatched in priority, replacing in part thermal plants and causing a lower spot price. As consequence, the final uniform DA price decreases bringing lower marginal revenues to VRE compared to the case where thermal plants set the spot price. This reduces the market value of additional VRE generation. At the same time, the marginal revenues of traditional power plants are even lower since they are dispatched after VRE and have higher operational and fuel costs. They become more useful to the grid as back-up capacity providers and therefore are often activated to run the power generators at partial loads, which results in a reduction of the thermal and economic efficiency of the system. In Europe over 20GW of gas-fired power plants were mothballed in 2013 and this figure is estimated to increase in the next years [30]. De Jong et al. [36] show that the overall wholesale power price decreased between 2008 and 2014 in Germany, France, Italy and Spain while the retail price increased due to a rise of taxes and levies. In fact, the costs of integrating more VRE are often socialized between all power generators and the grid; this further penalizes traditional power plants and could also lead to an increase in the electricity price for end-users (worsening energy poverty [37]). This is the paradox the electricity sector is facing: more renewable energy is needed to decarbonize the energy sector but the electricity market needs to display the integration costs as a clear and separate line of expenditure in order to not over-incentivize RES generation, leading to a reduction in its market value (death spiral of utilities [38]), and support the less polluting traditional power plants (e.g. gas turbines) in providing the back-up capacity needed to make the grid more flexible.

It is important that all the potentially externalities are carefully considered by governments when implementing energy policy to support the decarbonization of the energy sector [39].

The tariff structure has to include the price for the grid flexibility as a clear and visible separate item. The current market structure is price-based, i.e. its aim is to create the mix of energy sources that guarantee the lowest marginal cost. This market structure should change from kWh-based to capacity-based to provide a proper remuneration to conventional power plants that guarantee capacity availability and support higher VRE penetration by increasing the flexibility of the grid.

Chapter 3

A new model for investigating on-site energy generation feasibility

In this chapter, the options currently available for decarbonizing both the electricity and heat demand of manufacturing industrial facilities are discussed and the focus of the current thesis is highlighted. The new model implemented in Matlab in the present thesis is described through flow diagrams.

3.1 Options for decarbonizing the industrial electricity and heat demand

The necessity of decarbonizing the energy sector presents some challenges, as has been shown in the previous chapter. The complexity of the energy system and of its architecture makes it difficult to actualize all the required actions to reduce its environmental impact in a relatively short time (targets set for 2020, 2030 and 2050).

The industry sector is globally responsible for almost one third of the overall energy consumption [4] and specifically manufacturing industry accounts for more than 20% of energy-related carbon emissions. While policies and incentives have been widely studied and implemented to increase the sustainability of the residential sector, the industry sector is more difficult to target [40]. In Ireland, the industrial electricity demand represents a third of the total electricity consumption, more than the residential sector (Figure 3.1-a). The Irish industrial sector is also characterized by a significant thermal demand which is almost twice its electric demand, as shown in Figure 3.1-b, and is mainly provided by natural gas and oil.

Overall, while one household has an average consumption of 480W$_{el}$ and 1,255W$_{th}$ [41], a medium size manufacturing plant has an average demand of $2{,}500\times10^3 W_{el}$ and $5{,}000\times10^3 W_{th}$, equivalent to approximately 5,000 residential consumers. Making one single manufacturing plant consuming cleaner energy and reducing energy waste could have the same impact as convincing thousands of people to adopt more sustainable solutions. Therefore progress in the decarbonization of the industrial sector would give a significant contribution to emissions reduction.

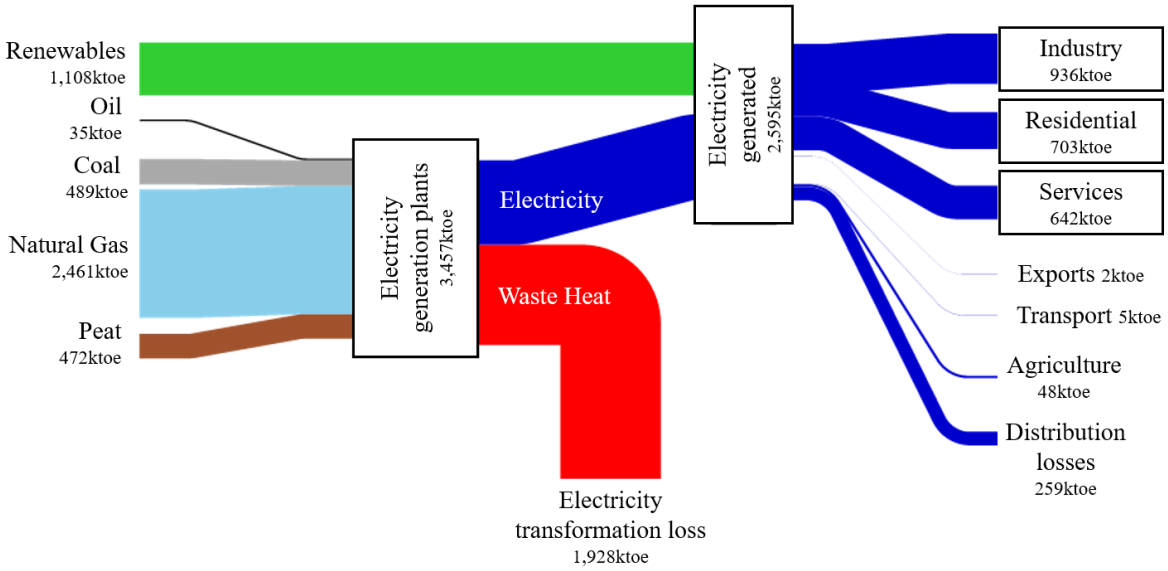

(a) Electricity generation by source and consumption by sector in Ireland in 2018

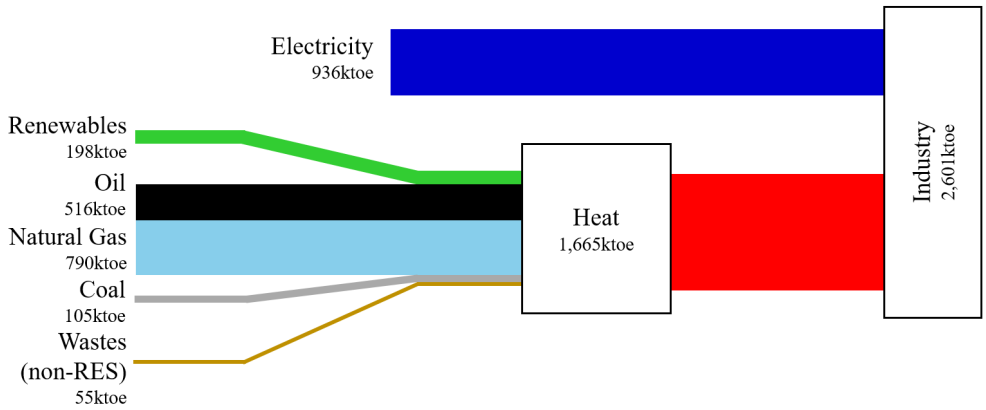

(b) Final consumption in industry by source in Ireland in 2018

FIGURE 3.1: Electricity and heat consumption in Ireland in 2018, with a focus on industry. Based on data from the Sustainable Energy Authority of Ireland [16]

Different options are available to a manufacturing facility for reducing the environmental impact of its electric energy load. They can be grouped and summarized in three categories:

- adopt measures that increase the efficiency of energy usage, reducing wasted energy;
- purchase low-carbon power from third parties, e.g. through a power purchase agreement (PPA) with a renewable farm;
- produce on-site part/all of its energy load in a more sustainable way.

Many manufacturing facilities have already implemented internal measures to increase the energy efficiency of their production lines. Often the first step a facility takes when

targetting energy waste reduction, is the creation of a "Energy Management" unit, responsible for controlling where possible energy waste may lie and improve the detected production process. Then, facilities with higher financial resources invest in innovative technologies that can guarantee more energy savings and an overall increase in energy efficiency.

The second option listed is also used by certain plants that do not have the financial resources to invest in either of the two remaining options. However, purchasing low-carbon power from a third party links the environmental impact of the facility to the carbon emissions produced by the third party. In addition, considering the challenges that are being currently faced to make the electric grid suitable for a higher penetration of VRE and considering the larger demand for low-carbon PPAs from companies, the cost of this option may increase in the future.

Due to all these considerations, the focus of this thesis is on the third option.

The decarbonization of the industrial heating demand is more challenging compared to the electric demand, especially if considering that many manufacturing facilities continuously require a significant amount of high temperature thermal energy. There are low-carbon technologies for heating available on the market, however they are mainly suitable for low temperature applications such as space-heating, which represent the typical needs of residential end-users [9–11] and while these alternative technologies exist (e.g. heat pumps, thermal energy-storage, electric heaters), they are generally either significantly costlier or they require additional infrastructures that make them not economically viable for households [12]. Only a limited range of alternative solutions is available for high-temperature production processes [13] and can mainly be identified within:

- use of renewable gas instead of natural gas in boilers on-site;
- combined generation on-site of both electricity and heat through an integrated technology such as Combined Heat and Power, that has a high overall energy efficiency.

Given that the purchase of renewable gas from a facility would be subjected to the development of technologies and decrease in cost of production of biogas on a national scale and it would depend on to the government decision to use gas infrastructures to provide biogas, the second option is analysed.

The objective of this thesis is therefore to investigate whether it is technically and economically feasible for a manufacturing facility to produce electric and thermal energy on-site reducing the environmental impact of its energy demand. To do so, a new model has been implemented in Matlab which simulates, given as inputs the energy demand of a facility and the techno-economic parameters of the selected on-site generation technologies, the technical and economical viability of on-site energy generation, and the emissions savings achievable with the new on-site system in current and future scenarios.

The first technologies investigated with the model for on-site energy generation are solar PV and wind turbine. Manufacturing facilities typically occupy larger spaces in non-residential areas compared to commercial sites in urban areas since they require open spaces

for production machinery, parking facilities, appropriate routes for supply and delivery, dedicated connections to national utility grid and other environmental considerations (e.g. noise pollution). This represents a good opportunity for installing renewable power plants, usually based on low "power density" technologies [42], that could produce clean energy on-site, reducing transmission and distribution losses. They also have dedicated connections to the national utility grid that could be used for selling extra power produced on-site to the grid [43]. Figure 3.2 shows the geographical area occupied by the manufacturing facility considered in this thesis as real case study and the large available space surrounding it that confirms the above statements.

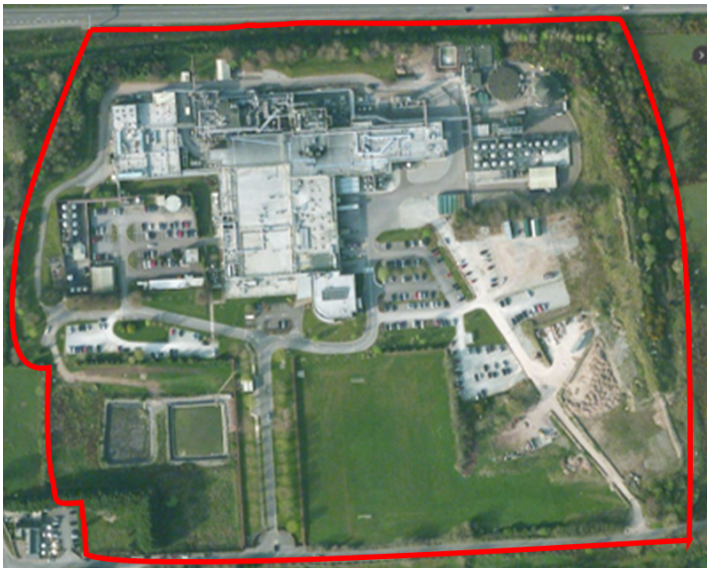

FIGURE 3.2: Aerial photography of the analysed manufacturing plant

The other technology considered for decreasing the emissions associated with the high-temperature heat demand of a manufacturing facility is a Combined Heat and Power system composed by a gas turbine and a Heat Recovery Steam Generator, for highly-efficient production of both electricity and steam.

3.2 Overview of the new model

In the present thesis a new model has been implemented and developed in Matlab that allows the execution of the techno-economic and environmental feasibility analysis of on-site electric and thermal energy generation. The technologies considered for on-site energy generation are a VRE system (solar PV and wind turbines) and a CHP system (gas turbine and heat recovery steam generator). The logic behind these technologies choice is described more in details in Chapter 4, 5 and 6.

The model is designed in a way that allows to replicate the analysis to any manufacturing facility worldwide, by simply providing as inputs to the model the hourly electric and thermal demand of the analysed facility, economic parameters such as technology costs, subsidies and

commodities prices, and geographical/meteorological data. An immediate feedback is then provided by the model on the feasibility of on-site energy generation through a VRE and CHP system for the specific analysed facility in the current conditions and for possible future scenarios.

The main inputs are briefly summarized below:

- Hourly electric and thermal energy demand of the facility for a sample year;
- Hourly solar irradiation at the geographical location for a sample year;
- Hourly wind speed at the geographical location for a sample year;
- Key performance parameters of the selected VRE and CHP system;
- Carbon intensity of the electric grid;
- Key economic parameters, such as cost of technologies, commodities prices and possible subsidies.

The main outputs generated by the model are:

- Hourly electric and thermal energy generation for each technology investigated for the entire lifetime of the on-site system;
- Pay Back Time (PBT) of the on-site system;
- Sensitivity of the PBT to different variables;
- CO2 emissions avoided.

Two flow diagrams are shown below: Figure 3.3 shows how the feasibility analysis is conducted for the VRE system; Figure 3.4 shows how the analysis is conducted for the integrated system. While the same logics and calculations apply for the VRE study, the additional calculations, inputs and logics used for the CHP analysis are shown more in details.

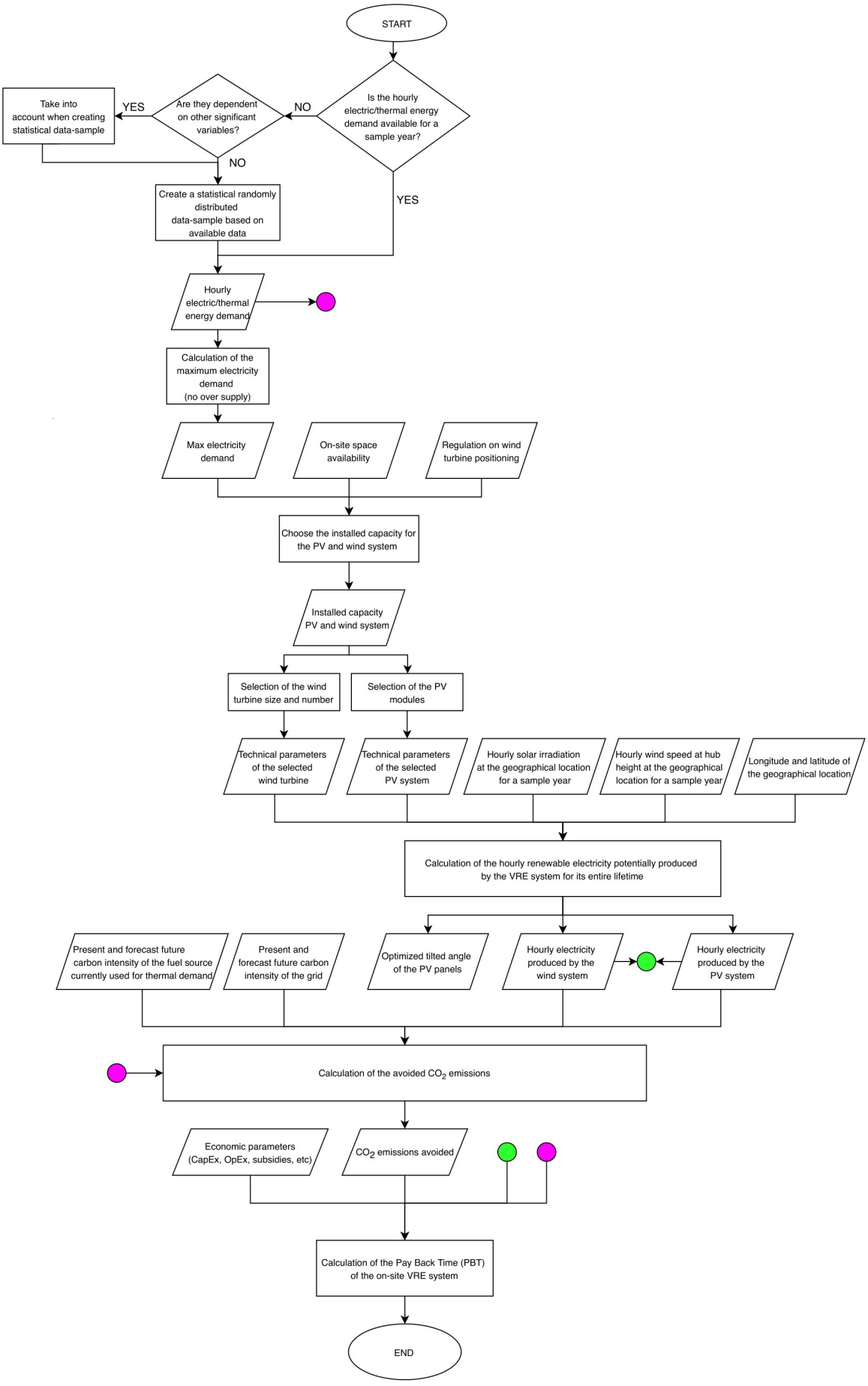

FIGURE 3.3: Flow diagram of the model: VRE feasibility analysis

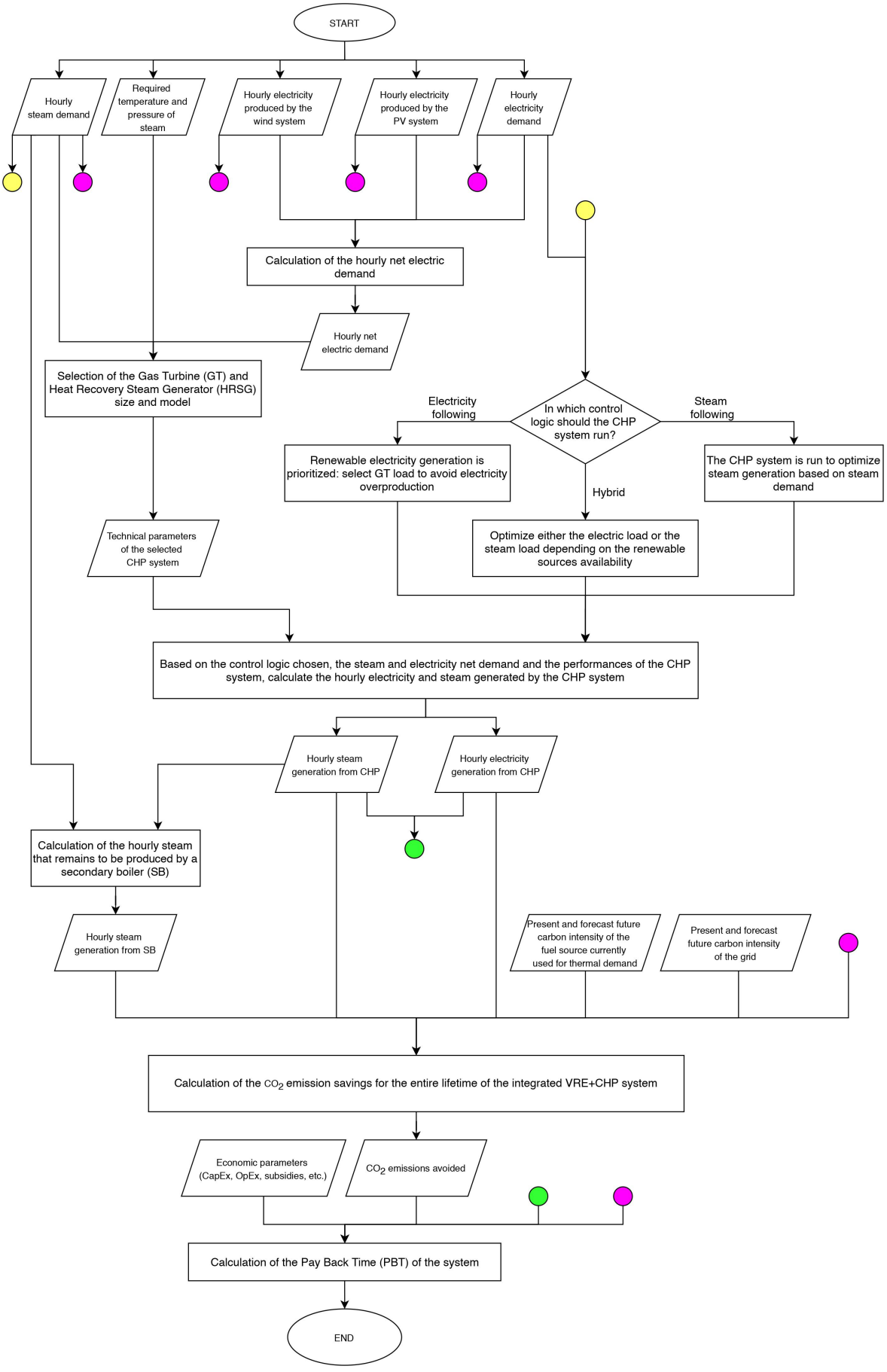

FIGURE 3.4: Flow diagram of the model: integrated VRE and CHP feasibility analysis

Chapter 4

Case Study

In order to provide realistic data as inputs in the model, an existing Irish manufacturing facility has been used as real case study. The peculiarities of this facility are discussed and the energy demand per all the different energy vectors is analysed.

4.1 Analysis of an Irish manufacturing facility

As explained in the introductory chapters, the aim of this thesis is to assess the feasibility for the Irish manufacturing industry to take on the role of energy "*prosumer*" (producer and consumer) by actively producing on-site energy for self-consumption to reduce the overall environmental impact by using cleaner energy sources and/or reducing energy waste.

A real manufacturing facility located in Ireland has been chosen as case study to investigate the techno-economic and environmental feasibility of on-site energy generation for the Irish manufacturing industry. The chosen facility is part of an international pharmaceutical company with 69,000 employees all over the world. The Irish manufacturing site counts more than 800 employees. It has a 24/7 batch production process with no shut-down during the year except for one short scheduled maintenance period.

In order to better understand the peculiarities of the energy needs of manufacturing facilities, the consumption profiles of the different energy vectors used in the selected facility during a typical year are presented in this section. The first step has been to identify all the energy vectors used, which are electricity, natural gas and water[1], and analyse their consumption trends. When data are taken from real facilities, the most common problem that has to be faced is the limited access to data and the unavailability of the devices used to take the needed measurements. This is one of the biggest hurdles to go over in this type of studies. To overcome this problem, data from both internal meters and bills have been compared and integrated.

[1] Water can be considered as an energy vector as it is used to distribute heat, but also because energy is embedded in water filtration before and waste water treatment after use in the manufacturing process.

4.1.1 Electric energy demand

The first energy vector considered is electricity. In Figure 4.1, the monthly electricity consumption and price paid by the company in 2015 and 2016 are shown. These data are taken from bills and the annual variation of consumption and price is detailed in Table 4.1.

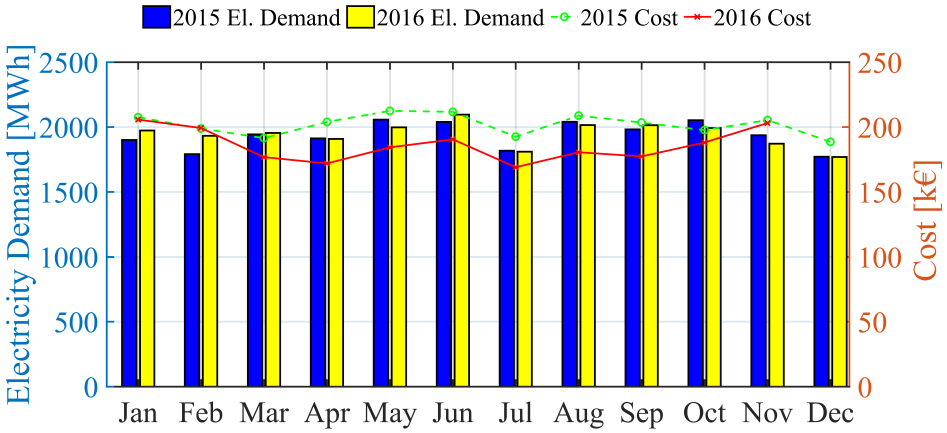

FIGURE 4.1: Monthly electricity consumption and correspondent price paid in 2015 and 2016

In Figure 4.2-a the electricity consumption internally monitored every hour of 2016 is displayed. The two datasets have been compared in order to fill possible gaps caused by unavailability of metering information.

The total amount of electricity consumed in 2016 registered by internal metering was 23,296MWh. The bills provided by the facility report a total consumption of 23,247MWh in 2015 and 23,331MWh in 2016. The two sources registered consistent data, differing by less than 1%, suggesting that the internal meters are reliable.

The electric load in 2016, displayed in Figure 4.2-a, is almost constant during the year without seasonal variations. The periods with an unusual trend during the year are marked in Figure 4.2-a by 4 ovals: these regions represent cumulatively 9 weeks of consumption. The electricity demand drops at the beginning (week 1) and at the end (week 52) of the year are caused by a reduction of the working shifts in the facility for Christmas holiday. The electricity demand does not drop to zero: a base-load demand is still present, even if reduced. The other highlighted regions (weeks 12, 13, 29) show the electricity consumption dropping to zero in late March and again in July. The event in March is an isolated data point, and seems to be a problem with the data logging. The event in July, however, spans 29 consecutive hours. The internal monitoring and external billing data are consistent, and so it is concluded that it is due to plant outage.

The range of hourly electricity consumption (maximum to minimum difference) and its standard deviation for every week of 2016, using both raw hourly data and a 1-week moving average to remove rapid fluctuations, are displayed in Figure 4.2-b and 4.2-c. Most of the time during the year, the fluctuations in the electricity consumption during a week are low. In fact, if the 9 weeks with the unusual high drops are excluded, the gap between the maximum

and minimum power load relative to the average registered in that week is below 33% for raw data while using a 1-week moving average it decreases below 7%.

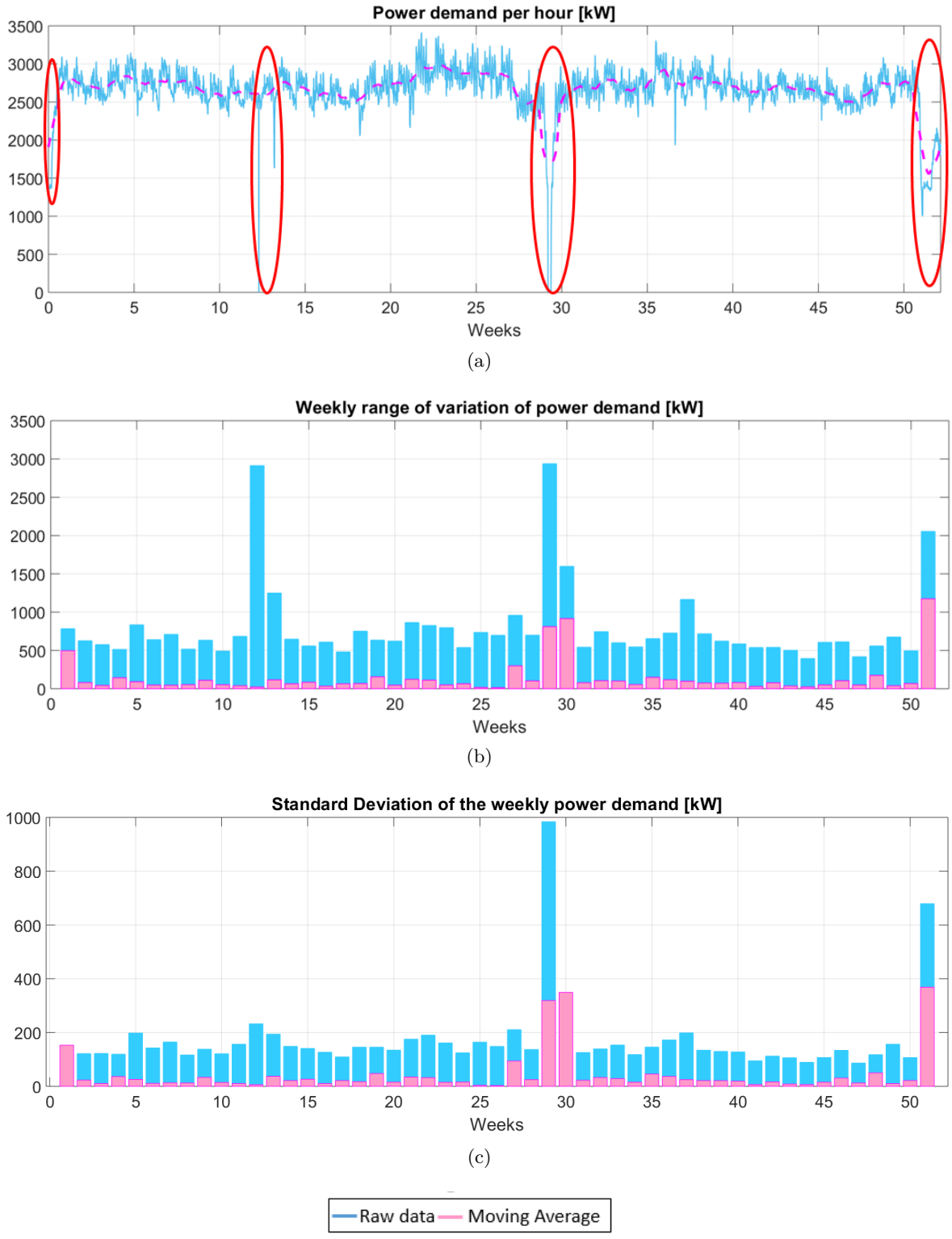

FIGURE 4.2: Electricity demand profile in 2016

The ensemble average of hourly and daily consumption over 2016 is shown in Figure 4.3.

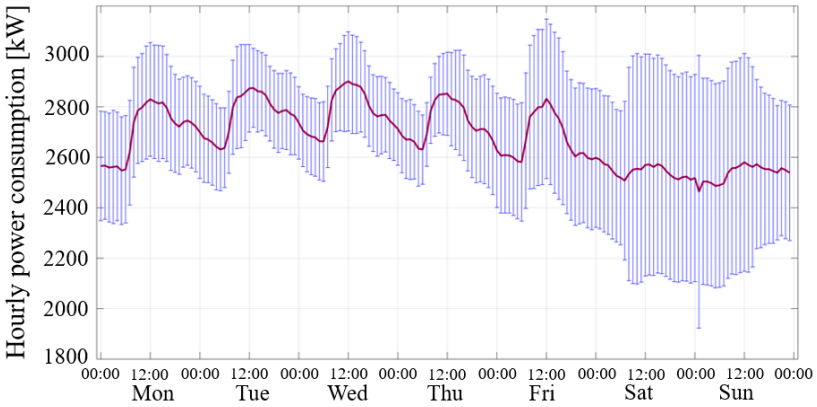

FIGURE 4.3: Electricity demand profile in 2016: Monday-Sunday hourly ensemble average

A diurnal variation is seen on weekdays (Monday-Friday), while the weekend hourly average is flat. The weekdays are comparable to each other both in terms of hourly trend and range of variation. The weekday diurnal trend is more or less additional to the weekend average and is approximately 5% of the mean electricity consumption. The range of variation at the weekend is twice that of weekdays and is approximately 15% of the mean consumption. This suggests that the diurnal variation during weekdays is not related to changes in manufacturing processes which will continue on a 24/7 basis, but rather reflects secondary activities, such as back-office operations, although there is no operational data to support this.

From the analysis conducted, given the almost constant trend and the overall relatively small diurnal, weekly and seasonal variability of the electricity demand, it is concluded that the electricity consumption profile of a manufacturing site differs from that of a typical residential consumer and the nature of on-site manufacturing processes is that deferred consumption is not viable[2]. Therefore, the commonly adopted strategies for Demand Side Management (DSM) are not easily applicable in this case.

4.1.2 Water demand

The second analysed energy vector is water, which is required in the production lines for different manufacturing processes. The majority of the water goes through different energy intensive chemical treatments (which are beyond the scope of this study) and then reaches the production lines, while around 7% is used as feed water for the boiler present on-site for the generation of steam. In Figure 4.4 and Table 4.2, the cubic meter of water consumed in 2015 and 2016 are shown, based on available billing information.

[2]This is based on a clear statement of the energy manager of the manufacturing facility analysed in this thesis, however it is clarified that this may not always be the case

Month	Electricity Consumption [MWh]		Consumption	Specific price 2016
	2015	2016	2016 vs 2015	[€/kWh]
Jan	1,900	1,973	3.85%	0.104
Feb	1,791	1,932	7.87%	0.103
Mar	1,943	1,954	0.53%	0.090
Apr	1,912	1,908	-0.21%	0.090
May	2,057	1,997	-2.91%	0.092
Jun	2,039	2,095	2.76%	0.091
Jul	1,817	1,809	-0.45%	0.093
Aug	2,040	2,015	-1.26%	0.090
Sep	1,981	2,014	1.65%	0.088
Oct	2,052	1,992	-2.95%	0.094
Nov	1,936	1,871	-3.37%	0.108
Dec	1,771	1,768	-0.15%	0.108

TABLE 4.1: Electricity consumption and specific cost in 2015 and 2016

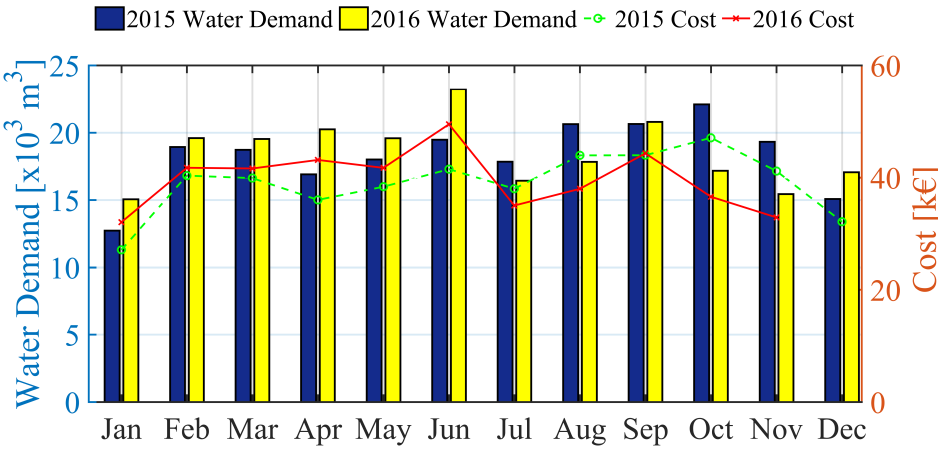

FIGURE 4.4: Monthly cubic meters of water consumed and correspondent price paid in 2015 and 2016

The specific price paid for cubic meter of water was the same in the two analysed years, 2.13€/m^3, with an additional operational expenditure of around 500,000€ per year. The amount of consumed water increased in 2016 registering a total consumption of 222,030m^3, around 20% more than 186,040m^3 consumed in 2015.

4.1.3 Thermal energy demand

The monthly thermal energy demand of the manufacturing facility for the same years is shown in Figure 4.5 and detailed in Table 4.3. It is measured in MWh which indicates the energy potentially produced by burning the quantity of natural gas bought. A small percentage of the thermal energy coming from the natural gas is used for space heating and other applications, while the largest share (around 80%) is used in a boiler to heat the feed water and produce the steam needed in the production lines.

Month	Water Consumption $[m^3]$		Consumption	Specific price 2016
	2015	2016	2016 vs 2015	$[€/m^3]$
Jan	12,733	15,053	18.22%	2.13
Feb	18,942	19,598	3.46%	2.13
Mar	18,731	19,538	4.31%	2.13
Apr	16,912	20,253	19.76%	2.13
May	18,012	19,589	8.76%	2.13
Jun	19,477	23,235	19.29%	2.13
Jul	17,848	16,441	-7.88%	2.13
Aug	20,634	17,837	-13.56%	2.13
Sep	20,644	20,802	0.77%	2.13
Oct	22,107	17,173	-22.32%	2.13
Nov	19,321	15,444	-20.07%	2.13
Dec	15,084	17,067	13.15%	2.13

TABLE 4.2: Water consumption and specific cost in 2015 and 2016

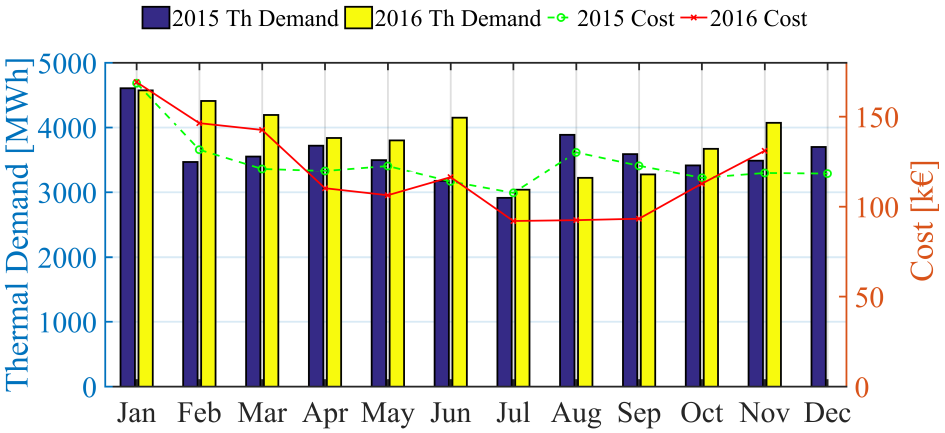

FIGURE 4.5: Monthly thermal energy demand and correspondent price paid in 2015 and 2016

Month	Thermal energy consumption $[MWh_{th}]$		Consumption	Specific price 2016
	2015	2016	2016 vs 2015	$[€/kWh_{th}]$
Jan	4,605	4,571	-0.73%	0.037
Feb	3,467	4,408	27.13%	0.033
Mar	3,551	4,193	18.08%	0.034
Apr	3,718	3,839	3.24%	0.029
May	3,497	3,800	8.68%	0.028
Jun	3,177	4,151	30.64%	0.028
Jul	2,914	3,039	4.31%	0.030
Aug	3,886	3,222	-17.09%	0.029
Sep	3,589	3,276	-8.72%	0.028
Oct	3,414	3,670	7.49%	0.031
Nov	3,487	4,072	16.78%	0.032
Dec	3,700	-	-	-

TABLE 4.3: Gas consumption and specific cost in 2015 and 2016

This energy vector, as opposed to electricity, presents a visible seasonal variation as expected, since the thermal energy needed to produce steam is influenced by the inflow water temperature and by the external temperature of the air used as oxidant in the combustion process. The total amount of thermal energy consumed, based on billing data, was 43,011MWh$_{th}$ in 2015 and 42,247MWh$_{th}$ in the first 11 months of 2016. The specific cost of the purchased natural gas was, on average, lower in 2016 by a factor of 12%, 0.031 instead of 0.035€/kWh$_{th}$.

In Figure 4.6, the natural gas flow rate measured by the internal meter located at the inlet of the boiler is displayed from the 11^{th} August 2016 to the 17^{th} March 2017 with a 10-minute step. It was not possible to analyse the full year trend because of the limited available data of the internal meters located in the boiler room. Unfortunately, there is also a high number of consecutive hours with no information available that results in a visible empty area in the graph.

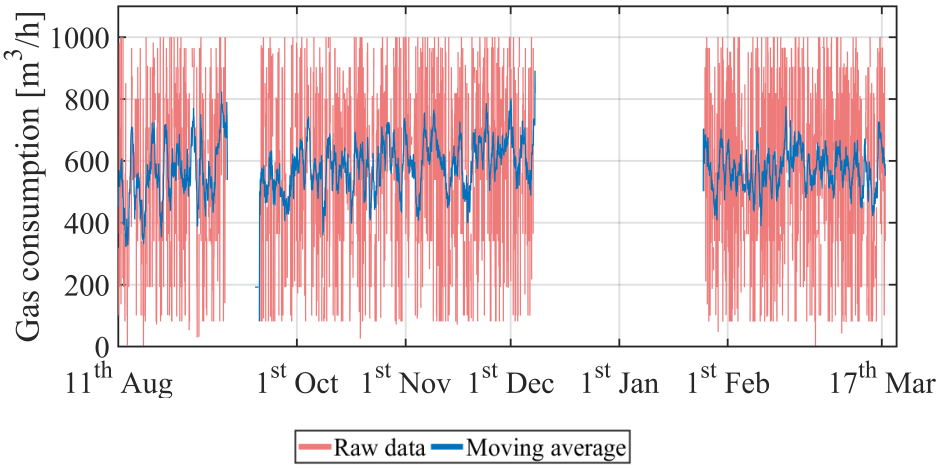

FIGURE 4.6: Natural gas flowing inside the boiler

The majority of the natural gas bought by the facility in a year ($36.5\times10^3 MWh_{th}$) is burned in a vertical boiler for producing the required steam flow at 14bar, which is sent to the designated production lines. The current process used for steam generation is displayed in Figure 4.7: the temperatures shown in the figure are based on average data; they can vary during the year depending on the ambient temperature.

The steam flow rate is registered by an internal meter with a 10-minute resolution. The available data, however, do not cover a whole year: they go from the 11^{th} of August 2016 to the 17^{th} of March 2017, as shown in Figure 4.8.

While the electric load is continuously registered, the steam load presents some gaps. In order to simulate a plausible continuous steam load over one year, a statistical analysis has been conducted on the available data. First, the relationship between the electricity and the steam load is investigated. As shown in Figure 4.9, the correlation between the two variables is weak therefore it is reasonable to study the steam load as an independent variable.

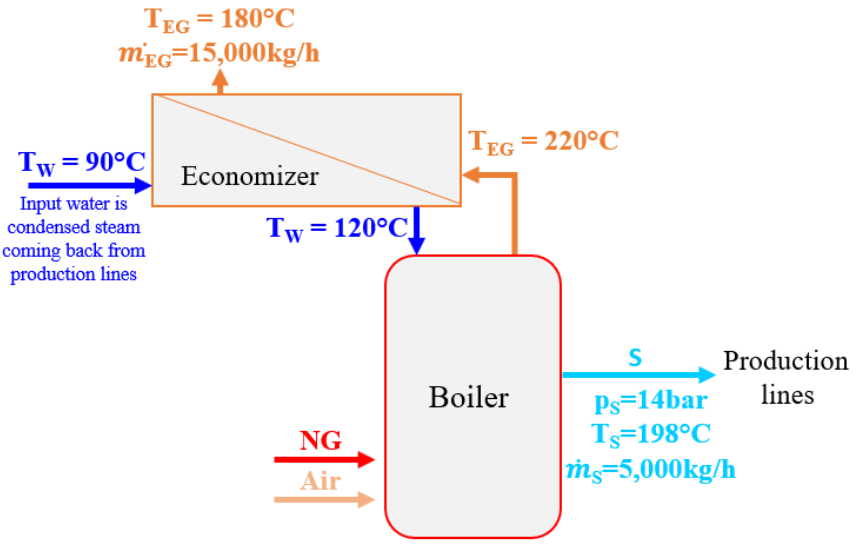

FIGURE 4.7: Existing boiler configuration with annual average parameters W=water; S=steam; NG=natural gas; EG=exhaust gases

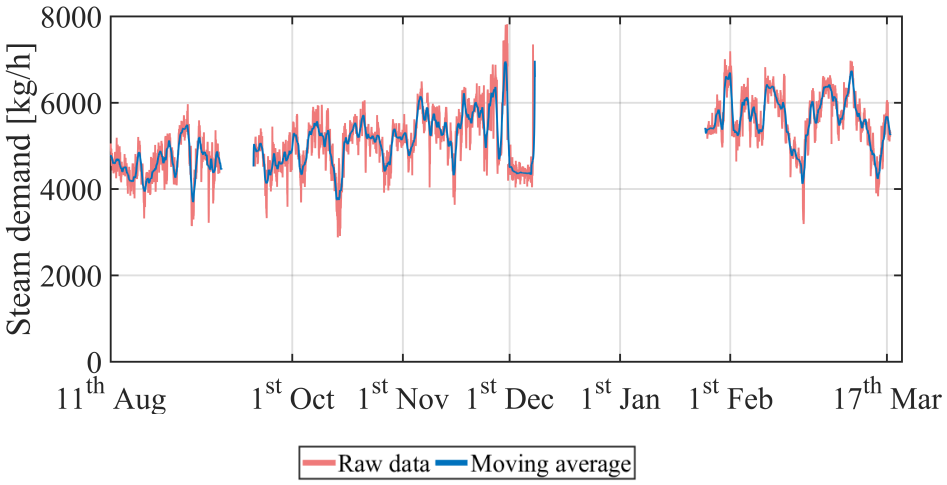

FIGURE 4.8: Steam load

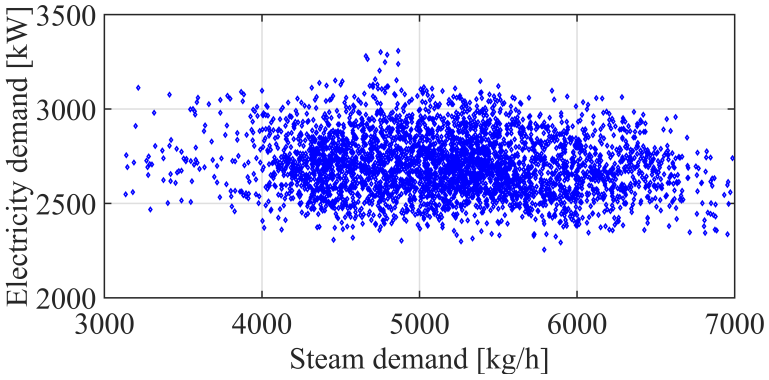

FIGURE 4.9: Steam demand vs electricity load

The probability distribution of the available steam data has been compared to three different statistical distributions to identify an appropriate model. As shown in Figure 4.10, none of the statistical distributions considered closely approximates the probability distribution of the steam load. For example, the null hypothesis of a normal distribution is rejected with a 5% significance level.

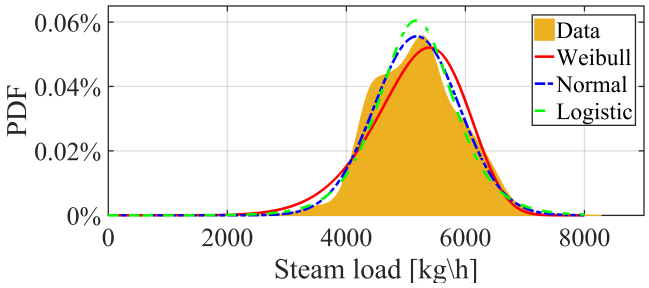

FIGURE 4.10: Probability Density Function (PDF) of the steam load

The week ensemble average has been calculated hourly based on the original available data. The weekly profile obtained does not show a significant diurnal or daily trend, suggesting that the temporal distribution of the data can be neglected. Therefore, a synthetic data set has been generated by randomly resampling the available measurements to cover one entire year. The steam demand has been set to zero for the 29 hours in July when the annual scheduled maintenance of the plant is conducted. The Probability Density Function (PDF) of the synthetic and of the original data is estimated using the Kernel Density Estimation (KDE). KDE model is based on the available observations of a random variable whose distribution function is unknown; it estimates the density function of the random variable without introducing any hypothesis nor requiring prior knowledge on the data distribution. This model is widely used in load and RES availability forecasting [44–46].

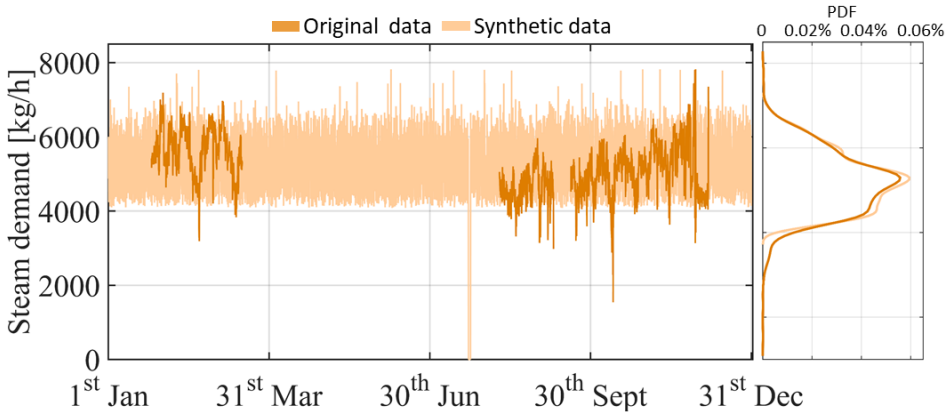

FIGURE 4.11: Annual profile and Probability Density Function (PDF) of the synthetic and original steam demand [kg/h]

As shown in Figure 4.11, the PDF of the synthetic data set well approximates the PDF of the original data set therefore this profile is used to simulate the annual steam demand of the manufacturing facility. In order to heat the water and generate the steam required

by the production lines, the facility is currently burning natural gas in a traditional vertical boiler that releases exhaust gases at high temperature (120°C) to the atmosphere. The energy content of the natural gas could be better exploited.

The annual energy demand of the facility and the correspondent CO_2 produced is summarized in Figure 4.12.

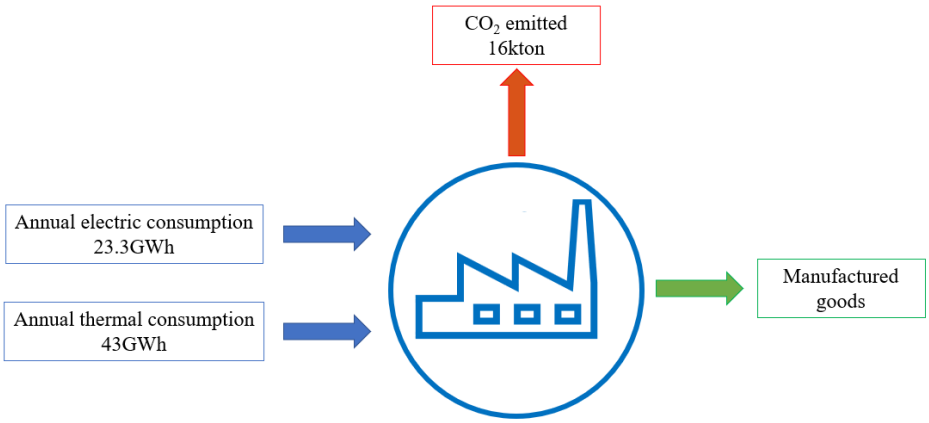

FIGURE 4.12: Summary of the annual electric and thermal energy consumption and CO_2 emissions

Having analysed the energy requirements of the facility, different technologies are investigated for decreasing the environmental impact of the manufacturing facility through on-site energy generation.

Chapter 5

On-site renewable electricity generation

In this chapter, the feasibility of on-site electricity generation from renewable sources in the analysed manufacturing facility is assessed. First a brief overview of different approaches presented in the literature for modelling renewable energy sources is given. Then the methodology used for the feasibility study is described and the results are presented: the technical feasibility is assessed in terms of electricity generation and overproduction; the economic feasibility of the project is assessed by calculating the Pay Back Time (PBT) in current and future scenarios. An overview of the state of the art of the chosen renewable technologies is provided in Appendix A.

5.1 Modelling of available renewable sources

In order to assess the feasibility of RES generation in a selected site, it is essential to first estimate the overall energy that can be produced by quantifying the availability of the chosen renewable sources. The methodology to assess solar and wind potential can be generically described, while for dispatchable renewable sources, e.g. hydro, it is strictly site-specific. For that reason, this section focuses on the estimation of solar and wind resources.

When the solar irradiance reaches the atmosphere part of it is reflected, part is absorbed and part is scattered. Three different types of irradiance get to the surface of a PV panel: beam, diffuse and reflected. The beam component is the solar irradiance that maintains its original direction travelling through the atmosphere; the diffuse component is scattered and therefore it is spread in every direction and it does not depend anymore on the position of the sun; the reflected component is the solar irradiance that reaches other surfaces, which then reflect part of it on the panel. The reflected component is usually negligible.

The data registered by meteorological stations usually are expressed as the radiation on a horizontal surface, Global Horizontal Irradiance (GHI). It is important to identify correctly the different contribution of the beam and diffuse components in order to optimize the tilt angle of the panel. If this is not a known input, it is possible to use the clearness index, defined as the fraction of radiation at the top of the atmosphere which reaches the surface

of the earth, to identify the beam and diffuse components [47–50]. Instead, when the two components of the radiation are already known as real measurements, there are different ways to calculate the global radiation on a tilted surface, as discussed in the next paragraphs.

Demain et al. [51], evaluate the performances of the 14 most used models (described in details in the article) for estimating the solar radiation incident on a tilted surface using horizontal radiation data. Real measurements have been used to validate the study. The first result of the analysis is that the largest contribution in PV systems oriented towards south is given by the diffuse component of the radiation, therefore it is suggested to choose a model with an accurate estimation of the diffuse radiation. The accuracy of the tested models under different sky conditions have been assessed by the Mean Bias Error (MBE) and Root Mean Square Error ($RMSE$). Considering all the possible sky conditions, every model tends to overestimate the radiation on the tilted panel; the isotropic models (i.e. models that assume an uniform distribution of the diffuse radiation) generate however very small statistical errors. Bugler model [52], among the others, offers the best result for all sky conditions both in term of MBE and $RMSE$. Considering, instead, the under overcast situation the smaller $RMSE$ is given by the Perez model [53]. The standard deviation between the models' results is small with extreme values of the clearness index, therefore all the models provide not widely different results when the sky is very cloudy or very clear; model discrepancies are larger for intermediate sky conditions.

Gueymard [54] compares the real radiation measured on a 40° tilted panel with predictions from 10 different models. Performances are tested both with optimal and suboptimal input data, i.e. when all the information about the radiation are available and when only the global irradiance is known. Also in this case, results are divided in all-sky conditions and clear-sky conditions only. The all-sky results show that the best performance is given by Gueymard [55] and Klucher [56] models. The registered RMS errors are lower in case of a clear sky and Perez and Gueymard models are the most accurate. The uncertainty introduced by suboptimal data is then discussed. Similar results are presented also by Evseev et al [57].

It is widely proved by the articles mentioned before that the major source of uncertainty in estimating the solar resource availability is attributable to the separation methods for the evaluation of the diffuse and beam components of the global irradiation.

Wind speed is highly variable over time and space and presents less predictable trends than solar. As with solar irradiance data, wind speed values are registered in meteorological stations with different time steps at the height of the monitoring tower (usually 10 m). The kinetic energy and the available power of an air mass that flows at a speed v with a density ρ through a cross section A are given by the following equations [58] :

$$E_k = \frac{1}{2} \times m \times v^2 \tag{5.1}$$

$$P_{av} = \frac{1}{2} \times \rho \times A \times v^3 \tag{5.2}$$

In the process of converting the kinetic energy of the air mass in another form of mechanical energy, i.e. blade rotation, there are some energy losses. The maximum power coefficient (C_p), defined as the percentage of wind kinetic energy that is extracted by a wind turbine, is given by the Betz limit under the assumption of infinite number of blades in one-dimensional theory with no turbulence taken into account and it is equal to $\frac{16}{27}$ (59%). Recently, a more accurate method has been developed by Okulov and Sørense [59, 60] to assess the maximum power that can be extracted from wind as function of the number of blades and the Tip Speed Ratio (TSR), i.e. the dimensionless rotation velocity normalized to the wind speed. They estimate the effect of a finite number of blades on the efficiency of an ideal wind turbine: the maximum C_p is given by a 3-blade wind turbine, which has the optimum trade-off between interference with wind flow (aerodynamics) and dynamic issues (weight balance, vibrations, etc.). The maximum C_p achievable by a 3-blade wind turbine is around 49% (Figure 5.1).

Nowadays, manufacturers give the C_p variation for the selected wind turbine as function of wind speed; therefore, it is possible to evaluate the power produced by the system for any wind speed. Other energy losses have to be taken into account to evaluate the electricity produced: the mechanical efficiency of the turbine, the generator's rotor and the gearbox, and the electrical efficiency of the generator and auxiliary system. The power generated by the wind turbine is calculated with equation 5.3.

$$P = C_p \times \frac{1}{2} \times \rho \times A \times v^3 \times \eta_{mec} \times \eta_{el} \tag{5.3}$$

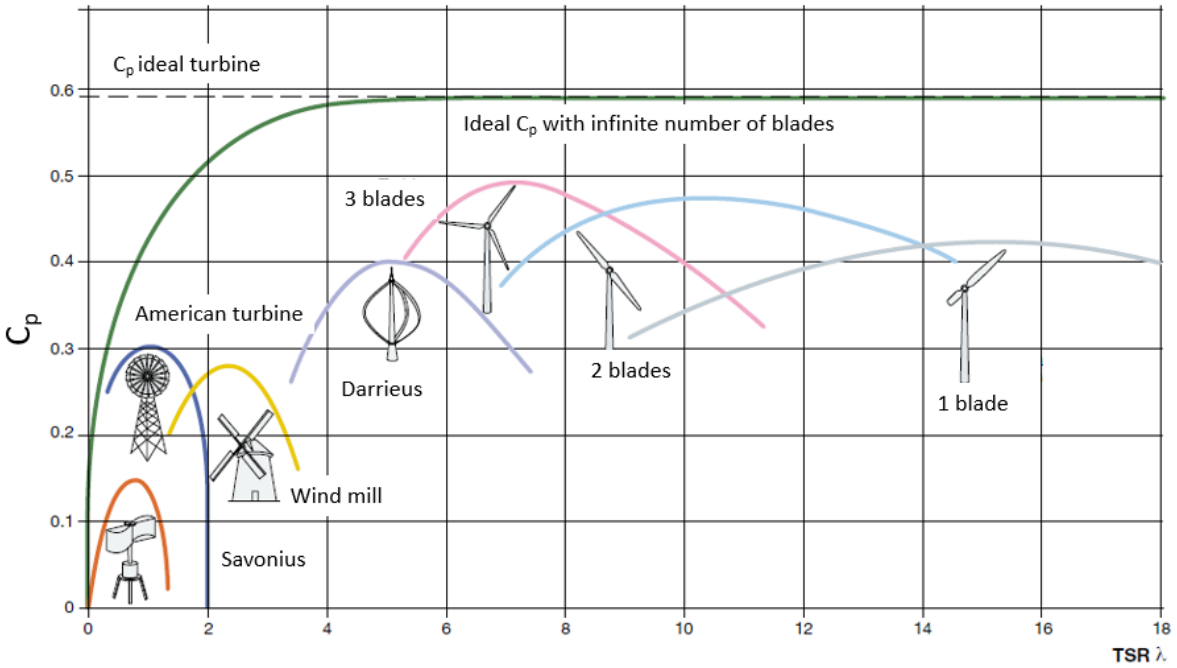

FIGURE 5.1: Power Coefficient C_p as function of Tip Speed Ratio (TSR) [61]

In order to estimate the wind energy potential of a site, the first step is to estimate the wind speed distribution in time. The statistical distribution most widely used in literature

is the Weibull distribution. The analysis of its two parameters is used to determine if an area is potentially a good site for a wind farm [62–66]. Other statistical distributions are also used in the literature, such as the Rayleigh distribution [67], Extended Generalized Lindley (EGLD) [68], Log-normal, Gamma, Exponential, Inverse Gaussian distribution [69, 70], mixture distributions [71–73] and flexible distributions based on MaxEnt and MinxEnt principles [74, 75].

As briefly mentioned before, the wind speed data are available only at the height of the meteorological tower that is often very different from the height of the wind turbine rotor hub. The following formula is used for a simplistic and approximative evaluation:

$$v_i = v_0 \times \left(\frac{z_i}{z_0}\right)^{\alpha_w} \tag{5.4}$$

where v_i is wind speed at the required height z_i, v_0 is the wind speed at the available height z_0 and α_w is a coefficient that depends on the site (close to 0 for an open and undisturbed environment, its value increases with the presence of obstacles). This coefficient has a consistent impact on the wind speed (Figure 5.2) and is very difficult to estimate exactly therefore for wind farm feasibility studies more reliable methods are currently researched.

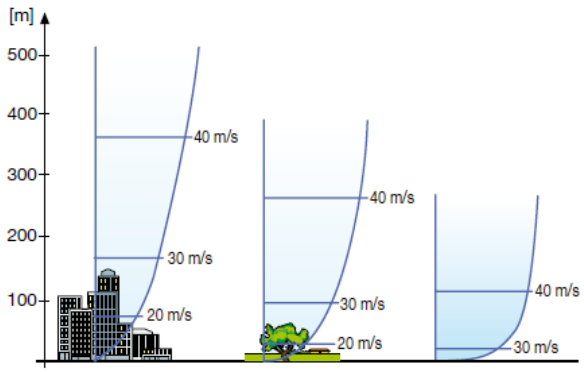

FIGURE 5.2: Wind speed variation as function of height for different types of location [61]

Detailed suggestions and guidelines for wind energy integration studies [76] and for wind energy project development and feasibility studies in the specific context of Ireland [77] are also widely present in literature.

5.2 Methodology

As explained before, given the high availability of land near manufacturing facilities, the first energy sources to be considered for on-site self energy production are renewable sources, which are often based on low power density technologies. The selected renewable sources for this analysis are solar and wind, which are less site-specific and therefore are more suitable for a widespread deployment that could be applied to different facilities located elsewhere. The implemented model, introduced in Chapter 3.2, that calculates the technical and economic

feasibility of on-site electricity generation in different scenarios requires the inputs shown in Figure 5.3: the electricity demand is based on the real data provided by the company.

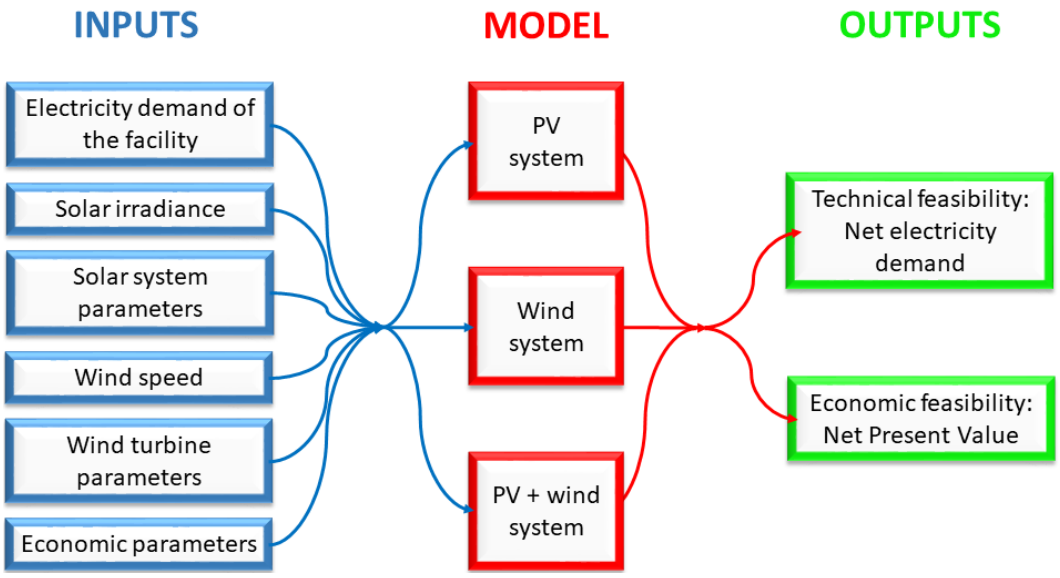

FIGURE 5.3: Inputs and outputs of the implemented model

The trend of the facility's electricity demand during a typical year is analysed and constitutes the first input of the model. Since the PV and wind systems convert solar and wind energy into electricity, the focus is on this particular energy vector.

A preliminary study has been done with the software HOMER ENERGY PRO [78] to compare the technologies chosen by the software as most suitable for the site with the one the author has chosen to implement in the model. The preliminary analysis conducted with the software shows that the best economic solution that minimizes the cost of the overall system in the current techno-economic conditions is to use only wind turbines, which are less expensive than PV systems for the same peak power installed. However, there are other factors that are not taken into account in the preliminary analysis as the strong regulations and physical limitations that apply to wind systems [79, 80]. Wind turbines have to be at least at a distance equal to the height of the turbine and blade from national and regional roads, and railways and at least 23m far from power transmission and distribution lines. The site has to be selected properly in order to avoid the shadow flicker effect in buildings nearby: at a distance of 10 rotor diameters this effect can be considered very low. In case the designed system includes more than a single wind turbine, the minimum distance between them to ensure optimal performance is considered to be three times the rotor diameter in the crosswind direction and seven times in the prevailing downwind direction. Spatial limitations and the morphology of the territory are not variables considered in the HOMER ENERGY PRO analysis. These limitations and constraints have, instead, been considered in implementing the model.

Based on these considerations and to promote a differentiation of renewable sources, both a solar and a wind system have been considered for distributed electricity generation and the

potential benefits of their integration have been studied.

The first system to be simulated is the solar PV system. The available data from meteorological stations are:

- NASA data [81]: daily Global Horizontal Irradiance and clearness index for the selected location from 1986 to 2004;
- Met Eireann [82] data, requested via email communication: Global and Diffuse Horizontal Irradiance per hour from 1986 to 2007, measured in a meteorological station less than 100km away from the facility. It has been verified that the difference in latitude between the facility and the meteorological station does not substantially influence the solar irradiance.

The Erbs model [49] has been used with the NASA data sample to evaluate the beam (DNI_h) and diffuse (DHI_h) components of the Global Horizontal Irradiance GHI_h depending on the clearness index value, k_t, through equation 5.5, 5.6 and 5.7.

$$k_t > 0.8 \qquad DHI_h = GHI_h \times 0.165 \tag{5.5}$$

$$0.22 \leq k_t \leq 0.8 \qquad DHI_h = GHI_h \times (0.951 - 0.160k_t + 4.388k_t^2 - 16.64k_t^3 + 12.34k_t^4) \tag{5.6}$$

$$k_t < 0.22 \qquad DHI_h = GHI_h \times (1 - 0.09k_t) \tag{5.7}$$

There is no need to apply this procedure to the Met Eireann irradiance data because the diffuse component is available from real measurements. Once the diffuse component is known, the beam component DNI_h can be obtained with a simple subtraction:

$$DNI_h = GHI_h - DHI_h \tag{5.8}$$

In order to optimize the angle of the panel it is necessary to calculate the beam irradiance at its original direction (DNI) and not projected on a horizontal surface. Therefore, the following equations have been used to asses the position of the sun for every hour of a year by using solar geometry (Figure 5.4). Since NASA data are averaged over a day, they are not accurate enough for this application. Therefore, the following equations, widely used in literature [83–85], have been applied to the Met Eireann data sample which has one-hour time step.

$$d = 2 \times \pi \times \frac{(day\ of\ the\ year - 1)}{365} \tag{5.9}$$

$$\delta = 23.45 \times \sin\left[\frac{360}{365} \times (day\ of\ the\ year + 284)\right] \tag{5.10}$$

$$E_t = [0.0000075 + 0.001868\cos(d) - 0.032077\sin(d) + \\ - 0.014615\cos(2d) - 0.040849\sin(2d)] \times 229.18 \quad (5.11)$$

$$LAT = LST + \frac{E_t}{60} + \frac{\psi_s - \psi}{15} \quad (5.12)$$

$$\omega = 15 \times (LAT - 12) \quad (5.13)$$

$$\theta_z = acos(\sin(\phi)sin(\delta) + cos(\phi)cos(\delta)cos(\omega)) \quad (5.14)$$

$$\cos(\theta_z) = \sin(\phi)sin(\delta) + cos(\phi)cos(\delta)cos(\omega) \quad (5.15)$$

$$e = asin(\sin(\phi)sin(\delta) + cos(\phi)cos(\delta)cos(\omega)) \quad (5.16)$$

$$DNI_h = \frac{GHI_h - DHI_h}{\cos(\theta_z)} = \frac{DNI_h}{\cos(\theta_z)} \quad (5.17)$$

The solar azimuth angle α_s has been estimated with the online tool Solar Geometry Calculator [86] that uses as convention 0°= North, 90°= East, 180°= South, 270°= West. The corrected solar azimut angle α is derived from α_s so that it is equal to zero at noon and it varies between -180° and +180°:

$$\alpha = \alpha_s - 180^o \quad (5.18)$$

The hourly Global Tilted Irradiance (GTI_h) on a tilted panel is given by equation 5.19, valid under the assumption of a negligible reflected radiation. It is a reasonable assumption since the PV panels are designed to be placed on the facility's roof far away from other buildings.

$$GTI_h = DNI_h \cos(\theta) + DHI_h \frac{1 + cos(\beta)}{2} \quad (5.19)$$

The angle θ is the angle between the beam radiation on a surface and the normal to the panel surface and it is equals to:

$$\theta = acos\left(sin(\theta_z)sin(\beta)cos(|\alpha - \gamma|) + \cos(\theta_z)\cos(\beta)\right) \quad (5.20)$$

It is now possible to optimize the pitch angle of the panel β, maximizing the annual GTI. The optimum pitch angle found for this location is 30°.

The available irradiance varies every year and it is not possible to predict ahead how much it changes. The hourly GTI_h on a 30° tilted PV panel has been calculated based on Met Eireann data for every year from 1986 to 2007. The global tilted irradiance of the last available year (2007) is chosen as input for the feasibility study since it differs less than 2% from the average yearly solar irradiation estimated in the same conditions by System Advisor Model (SAM) [88] and PVWatts Calculator [89], two software implemented by the National Renewable Energy Laboratory NREL. The values of the different input parameters for the PV system are shown in Table 5.1.

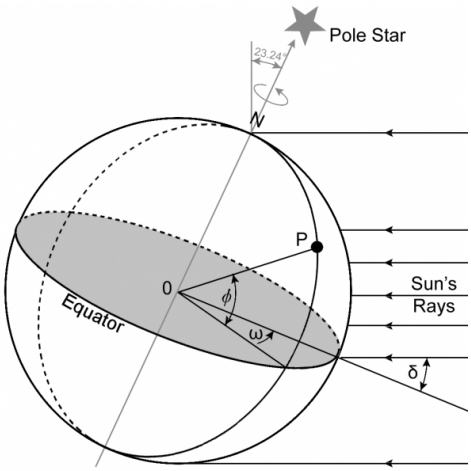

FIGURE 5.4: Solar geometry [87]

Description	Parameter	Value
Peak power installed	kW_{peak}	2020kW
Total area of the PV system	$Area_{pan}$	10,700m^2
Efficiency of PV panels	η_{panel}	19%
Performance decay		0.3% per year
System losses		14%
Annual electricity produced	kWh_{PV}	1,883,500kWh
Capital expenditure	$CapEx_{PV}$	3,721,100€
Operational expenditure	$OpEx_{PV}$	138,022€ per year
Discount rate	r	0.06

TABLE 5.1: PV System

The investment cost and the total area are determined with the SAM software. The accuracy of technical and economic parameters' estimations has been verified in the literature [90–92].

The total electricity produced every year n by the photovoltaic system is calculated with the following formula:

$$kWh_{PV} = \sum_{h=1}^{8760} (GTI_h) \times A_{PV} \times \eta_{PV} \times \eta_{inv} \times (1 - 0.003(n-1)) \times (1 - 0.14) \tag{5.21}$$

The efficiency curve of the inverter, η_{inv}, is included in the calculations [88]. The effect of temperature on the panel efficiency is considered negligible for the purposes of this study. The overall annual cost paid for the electricity bought from the grid, taking into account an increase in electricity price of 1.5% every year, is:

$$Exp_{grid} = kWh_{grid} \times price_{el} \times (1 + 0.015(n-1)) + OpEx \tag{5.22}$$

Therefore the saving can be calculated as:

$$Saving = (kWh_{req} - kWh_{grid}) \times price_{el} \times (1 + 0.015(n-1)) \tag{5.23}$$

The overall cost of the PV system is the sum of the capital cost ($CapEx_{PV}$) and of the annual operational cost ($OpEx_{PV}$), which is estimated to increase every year by 1.5%. It is assumed that the facility has no additional cost for land use.

$$OpEx_{PV} = (85,826 + 28,856 + 20 \times kW_{peak}) \times 0.89 \times (1 + (0.015(n-1))) \tag{5.24}$$

The other system simulated is the wind system. The installed power is chosen so that there is no significant overproduction of electricity if the wind and solar systems are integrated (less than 1% of the time during the year). A wind turbine model is chosen for this study: Enercon E-44 [93]. The characteristic parameters of the wind system are listed in Table 5.2.

Description	Parameter	Value
Power installed	kW_{peak}	2 × 900kW
Cut-in speed	v_{cut-in}	3.0m/s
Rated speed	v_{rated}	16.5m/s
Cut-out speed	$v_{cut-out}$	34m/s
Swept area	A_{swept}	2 × 1521m^2
Hub height		50m
Performance decay		1.6% per year
Annual electricity produced	kWh_{wind}	3,609,800kWh
Capital expenditure	$CapEx_{wind}$	2,768,675€
Operational expenditure	$OpEx_{wind}$	100,000€ per year
Discount rate	r	0.06

Table 5.2: Wind System

Wind speed data are available online on the Met Eireann website [82] for a meteorological station less than 20km away from the manufacturing facility. The hight of the measurement tower is 10m while the turbines hubs are located at 50m from the ground. The equation 5.4 is suggested in literature for estimating the variation of wind speed with height but it is difficult to estimate exactly the coefficient α_w. Therefore, a different method is proposed. MERRA-2 [94] data have been requested through private correspondence with Dr. Conor Sweeney, lecturer in Applied and Computational Mathematics in the School of Mathematical Sciences, UCD, and member of the Meteorology and Climate Centre, the UCD Earth Institute and the UCD Energy Institute.

These data are available for a location less than 100km away from the facility both at 10m and 50m height.

The wind speed v at 50m height can be calculated for a certain moment in time as:

$$v_{MetEireann@50m} = v_{MetEireann@10m} \times \frac{v_{MERRA@50m}}{v_{MERRA@10m}} \tag{5.25}$$

By using equation 5.4, it is now possible to calculate the value of the coefficient α_w every hour of the year. As shown in Figure 5.5, α_w results to be very variable over time therefore it is more accurate to use in the calculation its value in the specific moment of time considered, instead of the average value over a year.

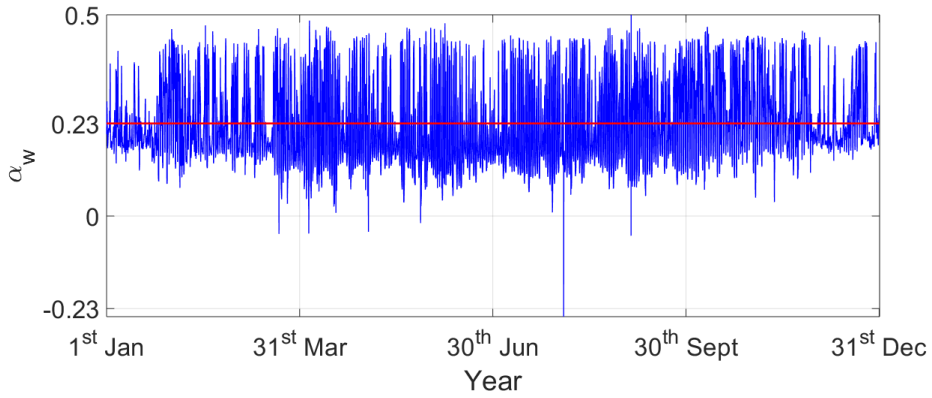

FIGURE 5.5: Variation of the coefficient α_w during the analysed year

As already explained in section 5.1, the Weibull Statistical Distribution is a widely used method to analyse wind speed and assessing wind energy potential of a specific site.

The probability density function f and the cumulative distribution function F of a generic Weibull variable $x \geq 0$ are calculated respectively with equation 5.26 and 5.27. They can be used to forecast wind speed and density and the energy potential of a wind plant.

$$f(x;\lambda,k) = \frac{k}{\lambda}\left(\frac{x}{\lambda}\right)^{k-1} e^{-(\frac{x}{\lambda})^k} \tag{5.26}$$

$$F(x;\lambda,k) = 1 - e^{-(\frac{x}{\lambda})^k} \tag{5.27}$$

The wind speed at 50m for the analysed location can be well approximated by a Weibull statistical distribution with a scale parameter λ of 7.59 and a shape parameter k of 2.07 (Figure 5.6).

The power P potentially produced by the wind turbine is function of the wind speed as shown in the following equations.

$$v < v_{cut-in} \qquad P = 0 \tag{5.28}$$

$$v_{cut-in} \leq v < v_{rated} \qquad P = \frac{1}{2} \times Cp \times \rho \times v^3 \times A_{swept} \tag{5.29}$$

$$v_{rated} \leq v < v_{cut-out} \qquad P = kW_{peak} \tag{5.30}$$

$$v \geq v_{cut-out} \qquad P = 0 \tag{5.31}$$

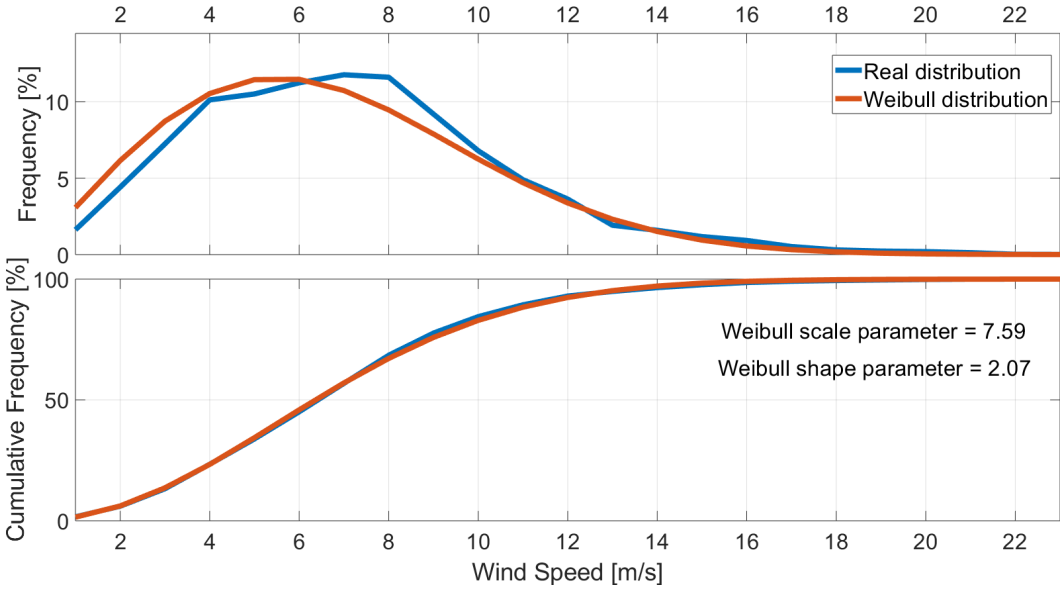

FIGURE 5.6: Frequency distribution of real wind speed measurements and Weibull distribution

Cp is the coefficient of performance and its curve, shown in Figure 5.7, has been taken into account in the calculations.

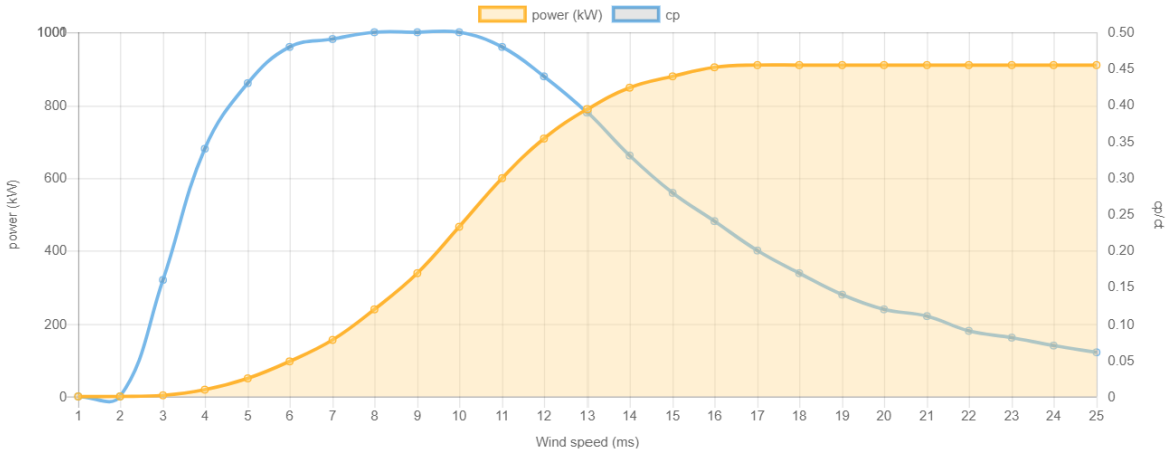

FIGURE 5.7: Power and Cp curve of Enercon E-44 wind turbine [93]

The performance decay factor is assumed to be 1.6% per year based on the conclusion of the study conducted by Staffell and Green [95]. The investment cost and the operational cost, $CapEx_{wind}$ and $OpEx_{wind}$, are estimated based on available information on existing plants [96]. To assess the economic feasibility of the wind and PV systems the Net Present Value NPV is calculated:

$$NPV = \sum_{n=1}^{lifetime} NPV_n = \sum_{n=1}^{lifetime} \frac{(Saving_n - CapEx_n - OpEx_n)}{(1+r)^n} \tag{5.32}$$

While the savings and the operative and maintenance costs vary every year n, the $CapEx$ is different from zero only the first year, when the initial capital investment is done. It is noted that there is typically also a cost of financing that should be considered, however it has been decided in this thesis not to make any assumption on the way the initial investment is financed by the facility given the numerous options and agreements that could be available to different facilities located elsewhere or with different resources and liquidity.

The Pay Back Time (PBT), or Return On Investment period (ROI), is defined as the number of years required to reach a $NPV = 0$€. The PBT is function of different technical and economic parameters that are likely to change in the near future; therefore to make this model comprehensive of potential future changes, the NPV is calculated for a wide range of parameters' values and not just for the actual estimated conditions. Since the cost of investment ($CapEx$) for PV and wind systems is likely to decrease [97] and the electricity price paid by the company is likely to increase in the future [98], the model considers a normalized $CapEx$ (€/W_{peak} installed) that ranges from 50 to 110% of the actual one and an electricity price that varies between 0.08 and 0.35€/kWh.

5.3 Feasibility analysis of the VRE system

5.3.1 Technical viability

With the introduction of on-site renewable electricity generation, the electric load is provided by both the RES systems (based on the renewable sources availability) and by the grid. The quantity of electricity that would be produced by the simulated PV and wind systems and the resulting net demand profile are respectively shown in Figure 5.8 and 5.9 for every hour of 2016. The electricity potentially produced by the PV plant (Figure 5.8-a) increases during summer, following an overall seasonally predictable trend. The electricity produced from wind, instead, is very unstable and not predictable (Figure 5.9-a). Given the unsteady nature of wind speed, the variance of the wind output is almost double that of the photovoltaic plant. However, the high peaks in wind speed allow the wind turbines to produce more energy than the PV plant, even though the nominal capacity is lower. The difference between the electricity consumption and production represents the net demand for the grid as shown in Figure 5.8-b and 5.9-b. This is negative (i.e. power sold into the grid) mainly for the wind plant on rare occasions in the winter months (76 hours over the year), resulting in a curtailment of 0.84% of the total wind power if net metering is not applicable. As explained before, the event in March may be due to a problem with the data logging while the event in July is due to plant outage. It is also worth noting that problems with unavailable or mistaken data happen frequently in SCADA systems in large manufacturing operations and this is a real world complication that has to be faced. Nonetheless, these data drop-outs will not significantly affect the net impact on the grid, which is summarized in Table 5.3.

The variability of the solar and wind resources on a monthly and weekly basis in the analysed location is shown in more detail in Figure 5.10. Visibly, the wind resource has wider fluctuations within a month but overall a lower daily variation.

	PV System	Wind System
Electricity requirement	23,296	23,296
RES generation	1,884	3,610
Electricity from grid	21,426	19,717
Electricity over produced	14	30

TABLE 5.3: Renewable energy generated in the first year [MWh]

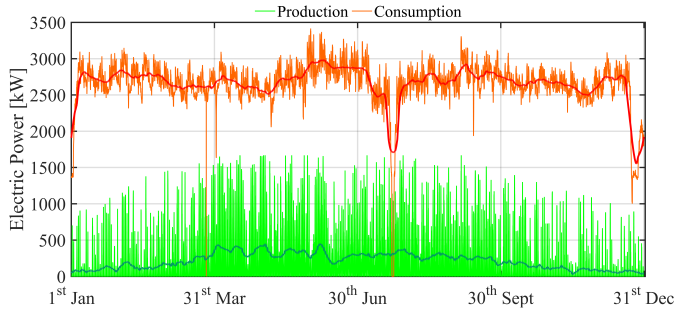

(a) Electricity demand and PV electricity generation: raw data (lighter line) and 1-week moving average data (darker line)

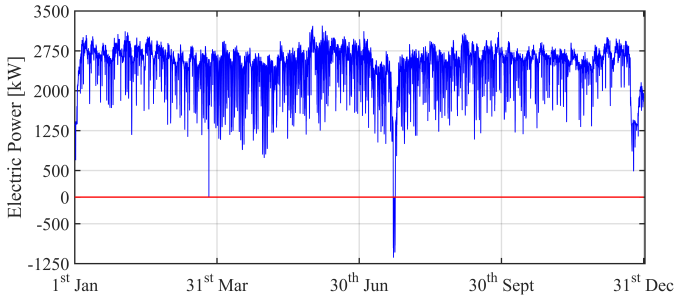

(b) Net demand

FIGURE 5.8: PV system: RES electricity generation and net demand in 2016

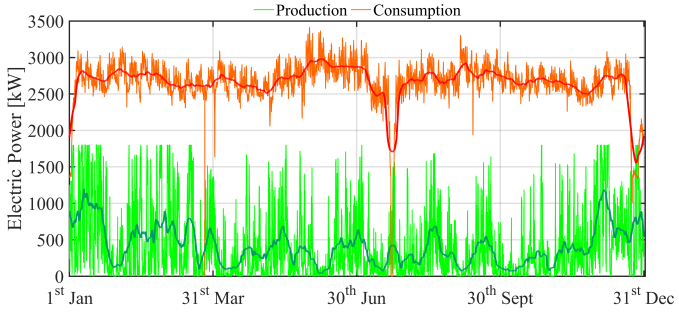

(a) Electricity demand and wind electricity generation: raw data (lighter line) and 1-week moving average data (darker line)

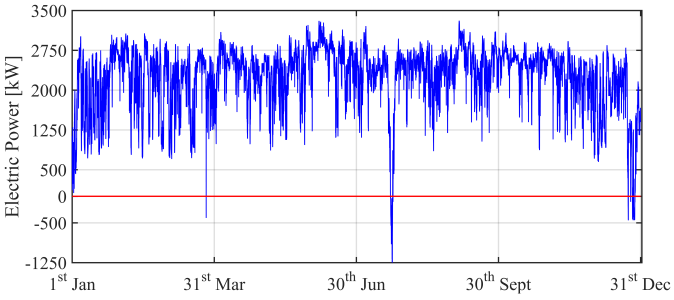

(b) Net demand

FIGURE 5.9: Wind system: RES electricity generation and net demand in 2016

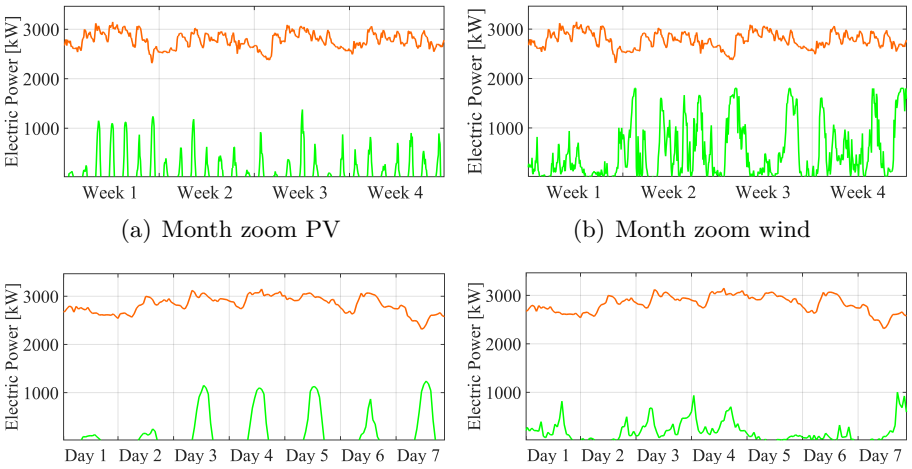

(a) Month zoom PV

(b) Month zoom wind

(c) Week zoom PV

(d) Week zoom wind

FIGURE 5.10: RES generation profile: one month zoom of (a) Figure 5.8-a and (b) Figure 5.9-a; one week zoom of (c) Figure 5.8-a and (d) Figure 5.9-a

5.3.2 Economic viability

The economic parameter that is usually calculated for assessing the economic viability of an investment project is the cumulative Net Present Value, NPV. This takes into account the investment cost and all the annual costs and savings as shown in equation 5.32. However,

when manufacturing facility managers evaluate an investment they consider the Pay Back Time (PBT) of the project. The two parameters are directly related: the PBT is the number of years required to get back on the initial investment and therefore reach a NPV=0€. After a number of years $n = PBT$ the NPV is positive and the savings have compensated the costs. When the NPV of the renewable plant reaches 0€, the Levelized Cost of Energy $LCOE$ of the renewable system equals the price of grid electricity, since the total cost of building and operating the RES plant equals the savings from the electricity not bought from the grid. In general, managers in the manufacturing sector are not likely to invest in a project with a PBT over 10 years (often as low as 5 years) therefore this is considered as the main requirement in the economic analysis.

Figure 5.11 shows the PBT of the PV, wind and integrated system for different prices of grid electricity and different normalized capital cost (€ per Watt installed) in the base case scenario. The effect of some form of carbon pricing is also included (Figure 5.11-d). For reference, the current price paid for grid electricity is indicated with a dashed line parallel to the x-axis, and the normalized $CapEx$ value based on current commercial prices is indicated with a dashed line parallel to the y-axis. If the PBT exceeds the expected lifetime of the system (25 years) the region of the graphs is white. The project is considered to be economically viable for a manufacturing facility if the PBT is less than 10 years (often as low as 5). This criterion is arbitrary and it is based on the economic decisions of facility managers.

Figure 5.11-b shows that wind technology can be economically viable if small incentives are provided for the electricity sold to the grid or even just with a reduction in capital cost but only for long payback periods. It is highlighted that the wind speed data used for this simulation are taken from the year 2007, characterized by an average wind speed profile. The PBT decreases from 25 years up to 5 years if periods with a particularly high wind speed profile are chosen. This is the case of 1986, when the wind energy potentially produced would be 7,156MWh (compared to 3,610MWh in 2007). Furthermore, a slight variation in the specific electricity price paid by the facility could change the PBT from 25 to 15 years.

On the other hand, for the PV system (Figure 5.11-a), a stronger support policy would be needed. By combining the two systems, the weak points of both are mitigated. The long PBT of the solar system is reduced by the more economical technology of the wind turbine (Figure 5.11-c). The wind system's variability and aleatory nature is balanced by the photovoltaic plant (Figure 5.10).

Different market conditions can improve the investment, leading to a positive NPV:

- Decrease in normalized $CapEx$ (learning curve for solar technology, e.g. improved PV efficiency);
- Decarbonization incentives, effectively acting as subsidies for renewable energy generation;
- Incentives for electricity sold to the grid;
- Increase in electricity price.

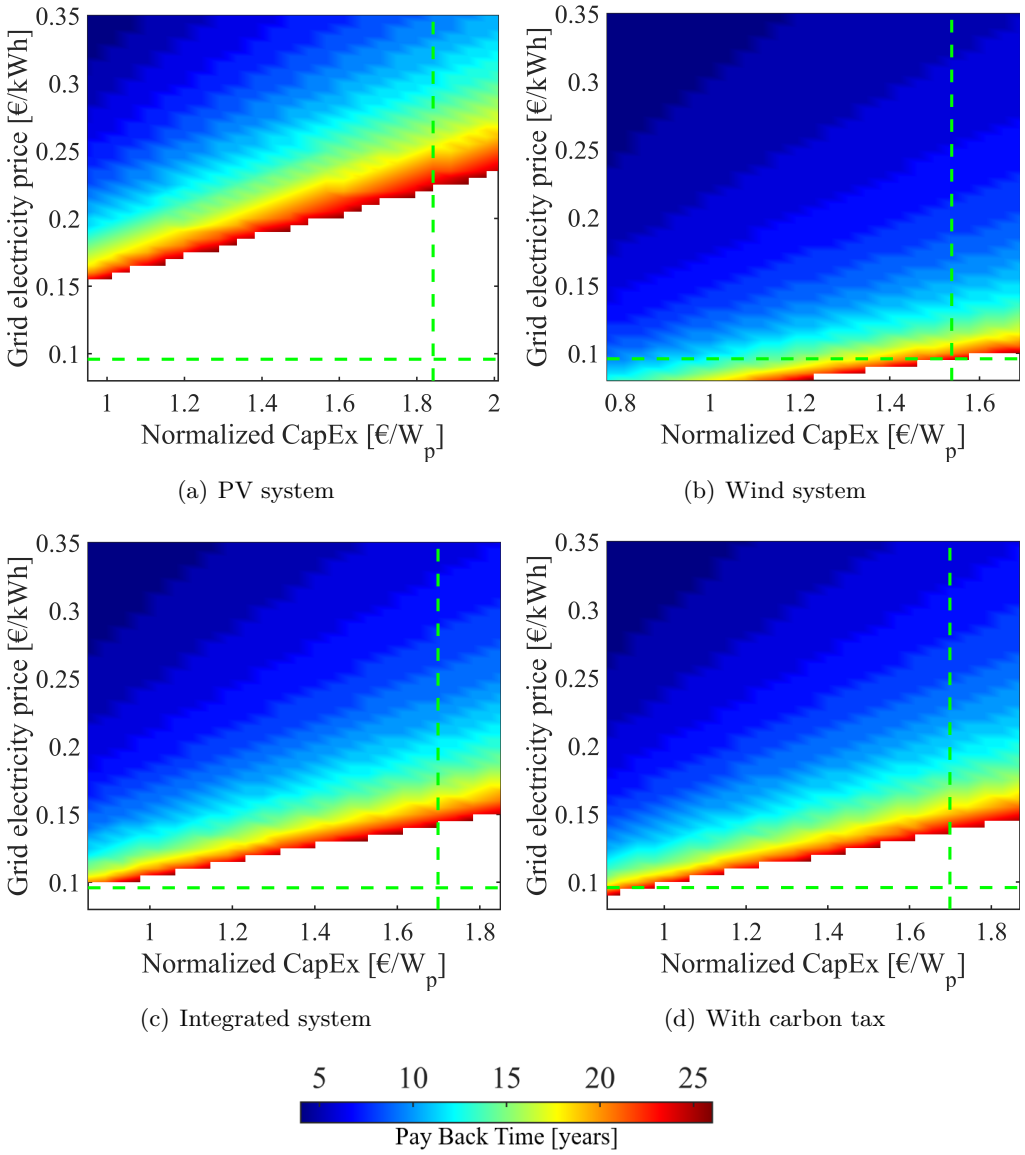

FIGURE 5.11: PBT as function of normalized $CapEx$ and cost of electricity

Figure 5.12, 5.13, 5.14, 5.15 and 5.16 show the sensitivity of the PBT of the PV and wind systems as function of the price of grid electricity and of the normalized $CapEx$ for different discount rates r, carbon taxes CT and PV modules efficiency η_{PV}.

While a technical opportunity to integrate solar, wind and the grid does exist, the PV system does not appear to be economically viable even with higher electricity prices and a significant reduction in the normalized $CapEx$. The introduction of an additional carbon tax, acting as a subsidy, or the reduction in the discount rate (Figure 5.12 and 5.13) would lead to a 10 year PBT only with an electricity price of around 0.35€/kWh, which is more than 3 times the current price paid by the company. In addition, a 50% reduction in the normalized $CapEx$, if acting in isolation, would still not give a PBT lower that the lifetime of the system.

A PV panel efficiency of $\eta_{PV} = 0.19$ and a discount rate of $r = 0.06$ would lead to a PBT of 10 years with a minimum electricity price of 0.355€/kWh. Assuming a learning curve for PV modules that would lead to an efficiency of $\eta_{PV} = 0.3$, a 10 year PBT could be achieved with a price of electricity of 0.25€/kWh (Figure 5.14), and with a 50% reduction in the normalized capital cost it would decrease to 0.165€/kWh.

The PBT of the wind system in the current economic conditions (carbon tax $CT = 0$€/ton and discount rate $r = 0.06$) is around 25 years. However, the introduction of an additional carbon tax of 60€/ton (Figure 5.15) or a lower discount rate of 0.035 (Figure 5.16) could lead to a PBT close to 5 years if coupled with an increased electricity price or with a reduction in the normalized $CapEx$, which is unlikely to happen given that wind turbines are now a well-developed technology.

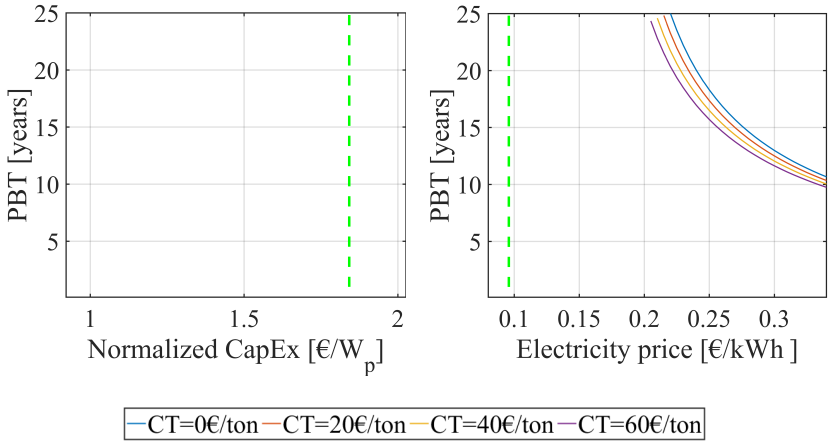

FIGURE 5.12: PBT of the PV system with different carbon taxes CT

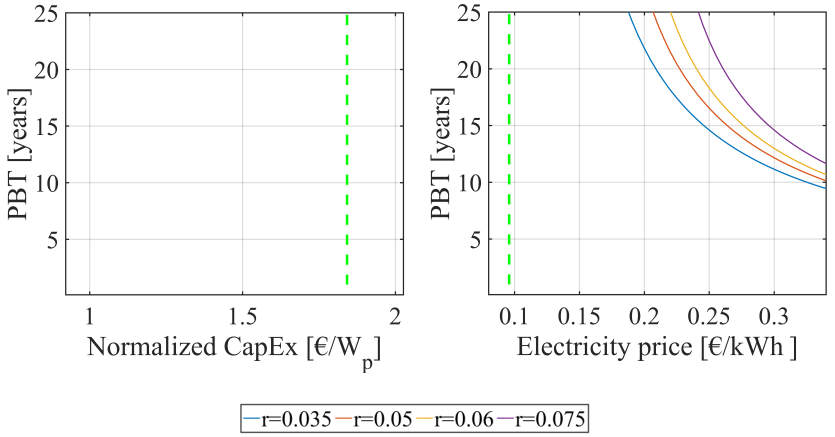

FIGURE 5.13: PBT of the PV system with different discount rates r

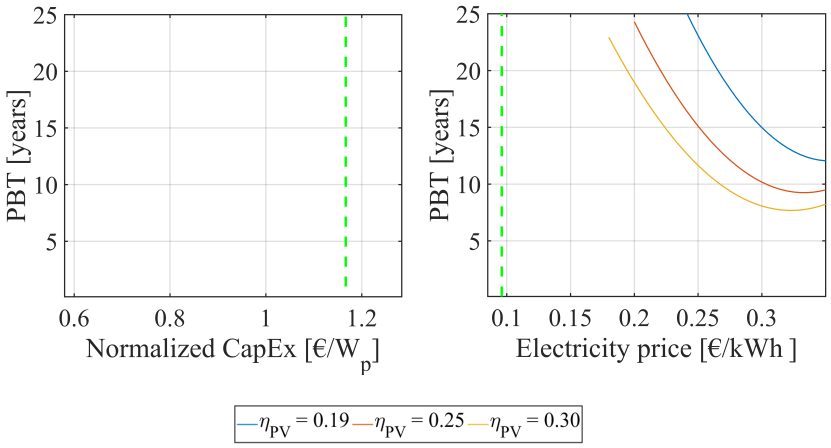

FIGURE 5.14: *PBT* of the PV system for different values of modules efficiency η_{PV}

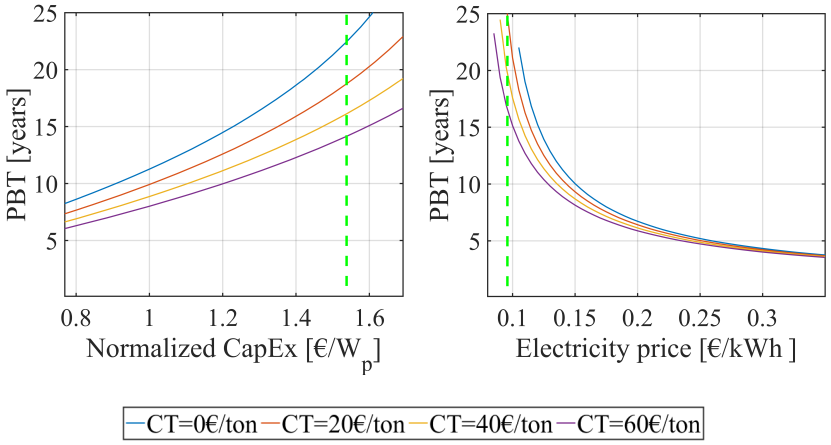

FIGURE 5.15: *PBT* of the wind system with different carbon taxes *CT*

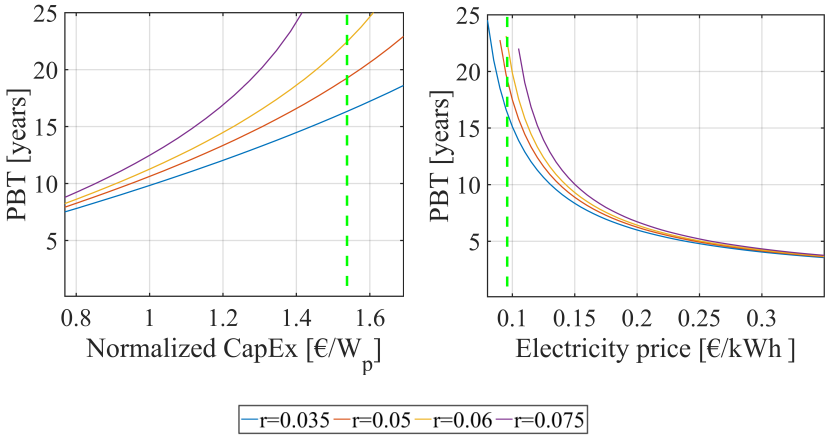

FIGURE 5.16: *PBT* of the wind system with different discount rates *r*

While there is a strong sensitivity of the PBT to the carbon tax and discount rate for a wide range of normalized $CapEx$, the sensitivity to these parameters decreases rapidly if the electricity price paid by the facility increases. If the electricity price reaches 0.2€/kWh then the PBT is not significantly influenced by the considered environmental and economic policies. The PBT could potentially decrease to a minimum of 3.5 years. The main driver to reach an acceptable PBT (lower than 5 years) is therefore the price of grid electricity. In order to make on-site wind generation economically viable, promoting and contributing to the decarbonization of the grid, an economic subsidy (e.g. additional carbon tax) is needed. The penetration of renewable energy would then increase, causing a reduction in the wholesale prices and therefore in the electricity network owners' revenues, and an increase in the reserve requirements that would lead to additional charges on the electricity price. The increase in electricity price paid by the final users would make on-site renewable generation even more profitable but their system value (i.e. value to the wider electricity system) would decrease [99]. In this scenario, the subsidies would become worthless as previously explained. The introduction of a carbon tax could have the effect of reducing the PBT of wind (in the range of electricity price currently paid) but it would have a negative effect on conventional power plants, which would see a further reduction of their revenues. The same positive effect on wind systems could be achieved by increasing directly the electricity price, making VRE more profitable, increasing the revenue for all the power suppliers and making more money available for balancing operations.

5.3.3 Integration of the PV and wind systems

Since solar and wind have complementary advantages and disadvantages, it is interesting to study a complex integration of the grid with both these renewable sources.

By integrating these two systems, the average electric power taken from the grid decreases to 2,040kW (2,445kW with the solar system and 2,250kW with the wind system) since a higher share of the electric load is covered by the two decoupled sources combined together (Figure 5.17).

The addition of wind plant introduces high variability, increasing the fluctuation of the net demand. The system has a signal variance of 1.9×10^5 $(\text{kWh})^2$ for solar, 3.6×10^5 $(\text{kWh})^2$ for wind and 4.5×10^5 $(\text{kWh})^2$ for both combined. It can be expected that the performance of PV and wind plant will gradually decrease over time, increasing the electricity requirement from the grid. Furthermore, while the manufacturing site is a net consumer of grid electricity, there are times when it is an electricity producer (see Table 5.3), which leads to curtailment of the extra renewable energy or to the increase in the total non-synchronous penetration on the grid.

A benefit of installing both wind and PV plant is visible in Figure 5.11-c. While the wind plant increases the variability of the net demand for the grid, it improves the overall viability of the project.

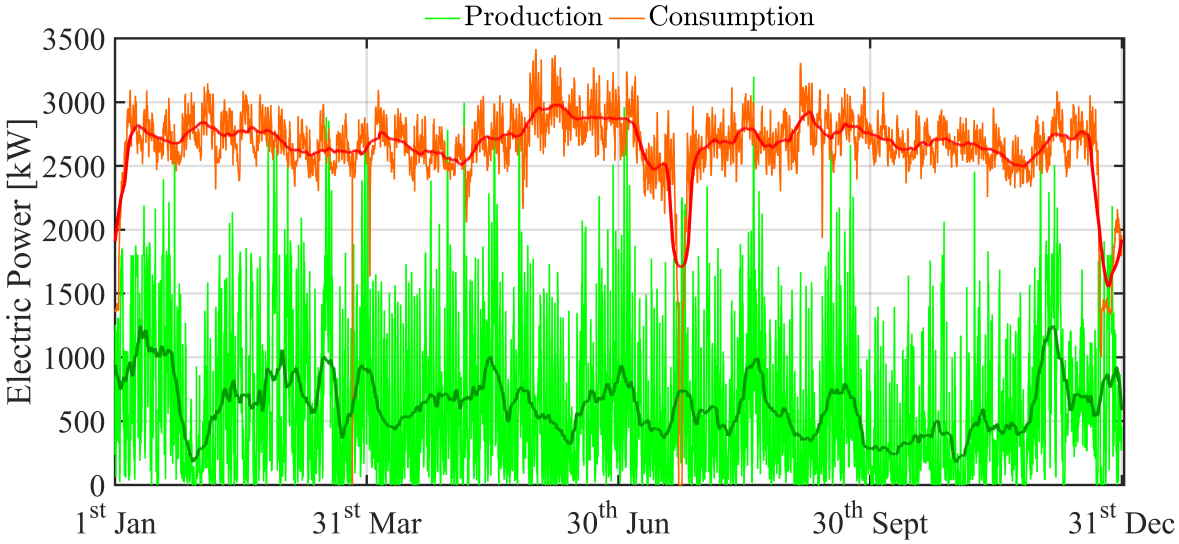

FIGURE 5.17: Electricity generated by the integrated system: raw data (lighter line) and 1-week moving average data (darker line)

Assuming an additional carbon tax of 60€ per tonne of CO_2, or other effective subsidies for on-site generation, the achieved saving increases. With a PV panel efficiency of 0.30 and a discount rate of 0.035, the *PBT* is shown in Figure 5.18. A carbon tax would make the profitability of the project easier to achieve, but a significant reduction in *CapEx* would still be required. This scenario considers a fixed value for the carbon tax during the whole lifetime of the project. However, the economic profitability of the project may be reached in a longer time if it is taken into account that the benefit of a carbon tax, here acting effectively as a subsidy, decreases as the grid is decarbonized.

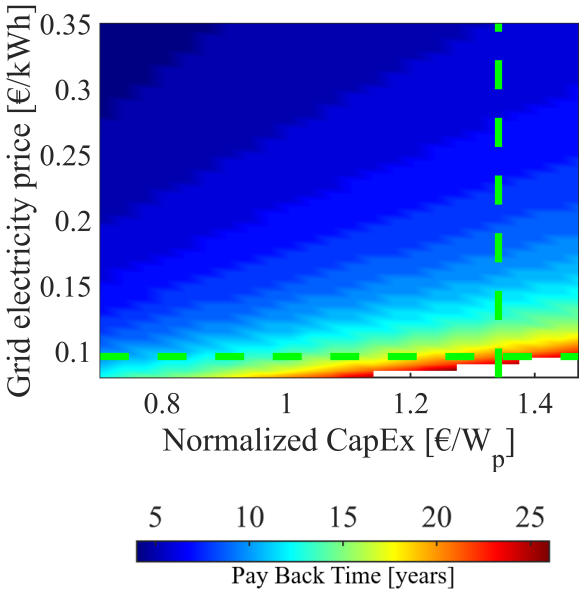

FIGURE 5.18: *PBT* of the integrated system in the best case scenario

5.4 Summary

This study suggests that the installation of PV and wind power plant on manufacturing sites for self consumption would be attractive only with a long Pay Back Time, a substantial subsidy (e.g. carbon tax), and the technological improvements yielding to a commensurate reduction in $CapEx$. Achieving all three conditions is probably unlikely, and so it is concluded that distributed renewable generation for manufacturing industry in Ireland does not make economic sense from a manufacturing facility commercial point of view when considered in isolation.

Nonetheless, it may still be a reasonable policy goal to help reduce the carbon intensity of the national economy. The manufacturing facility would, in fact, avoid over its entire lifetime the emission of 34kton of CO_2 over a total of 334kton of CO_2 otherwise emitted in the basecase (about 10% reduction in emissions). A progressive decarbonization of the grid has to be achieved to decrease the environmental impact of the energy sector and on-site renewable generation for the manufacturing industry would represent a good opportunity to move towards this goal, given its peculiar features such as dedicated connections to the national utility grid, high land availability, reduction in transmission and distribution losses with RES generation plants located near the consumption point.

Chapter 6

On-site electric and thermal energy cogeneration

In Chapter 5 it has been shown that distributed renewable generation for manufacturing industry in Ireland does not make economic sense in isolation. Therefore another option has been investigated in this chapter: the integration of a flexible and commercially mature technology for on-site cogeneration. An overview of the state of the art of the technologies suitable for on-site cogeneration is provided in Appendix A. An integrated system of a gas turbine and a heat recovery steam generator is proposed for cogeneration of both electric and thermal energy. This system would work in parallel with the grid and the on-site VRE system for providing the energy required by the facility (as previously introduced in Chapter 3.2). The technical, economic and environmental feasibility of the integrated system is analysed in different scenarios: the methodology and results are presented in this chapter.

It is noted that other options may be considered for decarbonizing the thermal demand of the facility, such as the use of biogas instead of natural gas. This would involve, however, a governmental decision on gas infrastructures and would not be limited to a solution implemented on-site by the facility itself, therefore is considered outside the scope of this thesis.

6.1 Methodology

To make the on-site VRE system economically viable and to decarbonize the thermal energy load of the facility, an alternative option is investigated.

Combined heat and power (CHP) is a mature and reliable technology that has been widely studied in literature and successfully applied in real industrial energy hubs for decades. CHP is recognized to be a particularly suitable solution for on-site energy generation for self consumption because the electricity produced can be used immediately, partially avoiding interactions with the grid, and the heat can be used locally, avoiding the necessity for distribution [100].

In order to assess the feasibility of the integrated cogeneration and VRE on-site system in the manufacturing facility, the electricity and steam demand have been analysed in Chapter 4.

As explained before, in order to heat the water and generate the steam required in the production lines, the facility is currently burning natural gas in a traditional vertical boiler that releases exhaust gases at high temperature (120℃) to the atmosphere. The energy content of the natural gas could be better exploited by a cogeneration system composed by a Gas Turbine (GT) and a Heat Recovery Steam Generator (HRSG). A Secondary Boiler (SB) is also included for providing the remaining steam load when needed.

Two sizes of GT have been considered based on the facility's requirements and models available on the market with a capacity of 1,600kW$_{el}$ and 800kW$_{el}$.

The GPB17D model of the Kawasaki industrial gas turbine has been chosen as an appropriate model available on the market and it has been used to provide typical performance data. The detailed data for the 1,600kW$_{el}$ gas turbine have been made available by the manufacturer; in order to make a direct comparison, the parameters have been scaled for simulating the equivalent performances of the 800kW$_{el}$ gas turbine. The parameters used in the calculations are listed in Table 6.1 and are available for different ambient temperatures (-20° C to 40° C) and different loads (50%, 75%, 90%, 100%). The data available have been interpolated to find a realistic value for all the variables listed at every ambient temperature and load.

Description	Symbol	Value	Unit
Electrical efficiency	η_{el}	26%	-
Electric power produced	P_{el}	1,630	kW_{el}
Exhaust gases mass flow rate	$\dot{m}_{EG}$	28,800	kg/h
Exhaust gases temperature	T_{EG}	526	°C
Fuel Consumption	FC	6,280	kW_{th}
HRSG steam output	$\dot{m}_S$	5,000	kg/h
HRSG thermal efficiency	η_{HRSG}	80.1%	-
Power to Heat Ratio		2.3	-

TABLE 6.1: GPB17D parameters at full load and $T_{amb} = 15$ ° C [101]

The detailed configuration of the GT coupled with the HRSG is shown in Figure 6.1. Every stage of the process involving natural gas is numbered from 1 to 6 while the different stages involving water are identified with letters. The feed water flows into the HRSG at a certain feed water temperature T_W (a) and is pre-heated close to the saturated temperature in the economizer (b), then it goes in the evaporator where the phase transition from liquid to vapour occurs (c). If a temperature higher than saturated is required, the steam flows into the superheater until it reaches the required temperature (d). In this case study the process lines of the facility require steam at a saturated temperature, therefore there is no need for the superheater and the process stops at (c). The addition of the superheater would not significantly change the PBT of the system because the cost estimated is based on average prices of HRSG which include this component.

In order to avoid waste of energy, the operation of every on-site technology is strongly interconnected to the rest of the system and is managed based on the availability of RES

sources (Figure 6.2).

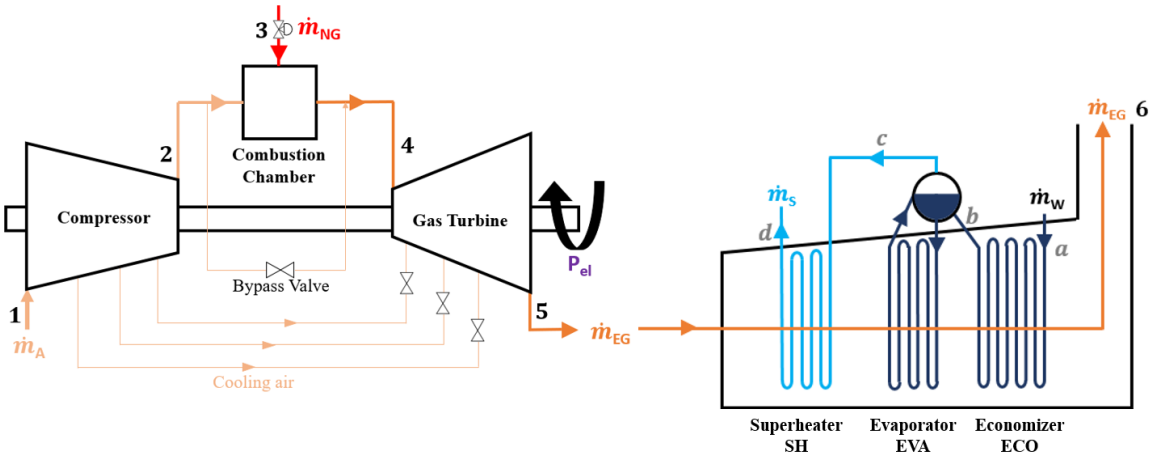

FIGURE 6.1: GT and HRSG detailed scheme

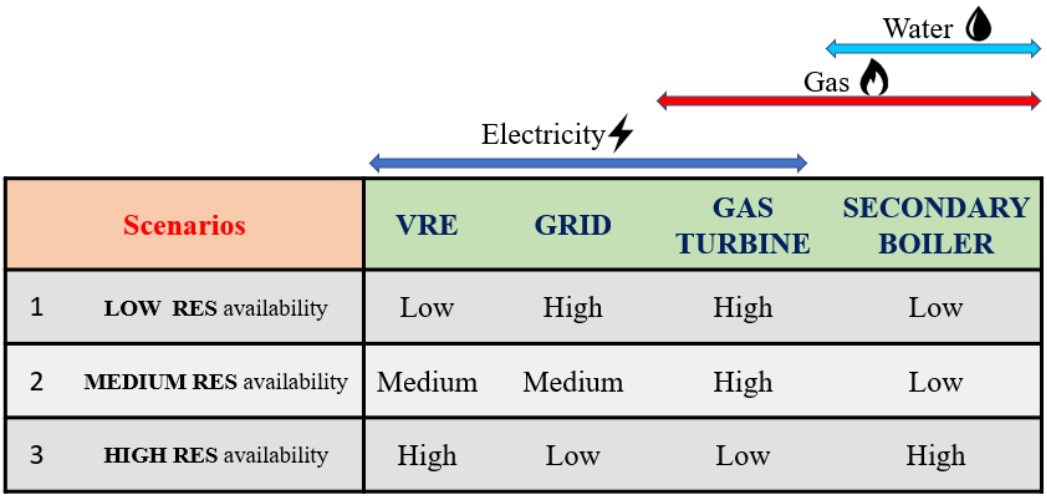

Scenarios		VRE	GRID	GAS TURBINE	SECONDARY BOILER
1	**LOW RES** availability	Low	High	High	Low
2	**MEDIUM RES** availability	Medium	Medium	High	Low
3	**HIGH RES** availability	High	Low	Low	High

FIGURE 6.2: Energy vectors scenarios based on RES availability

The VRE system is prioritized in order to minimize the curtailment.

In parallel with the VRE system, the gas turbine can be run with different control strategies: electricity following (to minimize electricity overproduction); steam following (to optimize the steam generation); or a hybrid of the two. Depending on the control strategy chosen, the residual load provided by the electric grid changes. The residual load is defined as the electricity demand minus the electricity produced on-site: it is positive when the facility needs more electricity than generated on-site and is negative when there is overproduction of electricity. The operation of the different energy systems on-site is strongly interconnected as shown in Figure 6.3. When renewable sources are poorly available (Figure 6.3-a), more fuel has to be burned to provide enough electricity, in parallel with the grid. As a consequence, a higher percentage of the steam required is produced by the HRSG and the secondary boiler may be turned off or work at minimum load. If slightly more electricity is available from the

VRE system (Figure 6.3-b), the GT load could be decreased, leaving the net load on the grid unvaried. If renewable sources are highly available (Figure 6.3-c), then the input from the grid and from the gas turbine has to decrease to avoid overproduction of electricity (negative residual load). As a consequence, the secondary boiler needs to increase its steam production to meet the steam demand.

During the maintenance period in July, both the electricity and steam demand are null therefore the cogeneration system (GT & HRSG) is turned off.

For the VRE system two options are possible:

- VRE system turned off: while for the wind turbine this would not represent a problem, the PV modules would still get solar irradiance without being able to produce and distribute electric power. This could lead to system damages and/or shorter lifetime.
- VRE system actively producing electricity that is sent to the grid: this could involve additional costs and operational constraints for both the facility and the grid due to additional necessary switchgear for two-way power flow.

The investigation of the consequences of either these two options is beyond the scope of this thesis. In both cases, the VRE generation for on-site consumption would be zero during the maintenance outage.

In order to decide at what load to run the gas turbine, the electric power and the steam that would be produced by the integrated system has been calculated for every hour of the year, considering the external ambient temperature (available from the Met Eireann website [82]). By comparing this with both the electric and steam demand of the facility it is possible to choose the necessary load of the gas turbine based on the selected control strategy. Since the time-step considered to be significant for the demand's variation is one hour, which is enough time for the system to reach a new steady state after a transient operation, a static approach has been adopted for the present study.

The steam flow rate theoretically produced by the gas turbine is calculated with equation 6.1, where FC is the fuel consumption, Δh_{eva} is the latent heat of evaporation, c_W is the specific heat of water and the coefficient *decay* takes into account the progressively decrease in the efficiency of the system during its lifetime.

$$\dot{m}_{S_{th}} = \frac{FC \times 3600 \times (1 - (\eta_{el} - decay)) \times (\eta_{HRSG} - decay)}{\Delta h_{eva} + c_W \times (T_S - T_W)} \tag{6.1}$$

If the steam following strategy is chosen, the GT load that produces the closest value to the steam flow rate required is selected. The remaining steam load is covered by the secondary boiler. If the electricity following strategy is chosen, the overproduction of electricity (negative residual load) is penalized and therefore the closest value that does not exceed the demand is selected. This is an internal decision of the manufacturing facility managers: the overproduction of electricity would, in fact, require additional investments either in storage facilities or in additional two-way connections with the grid subjected to both specific commercial and technical requirements.

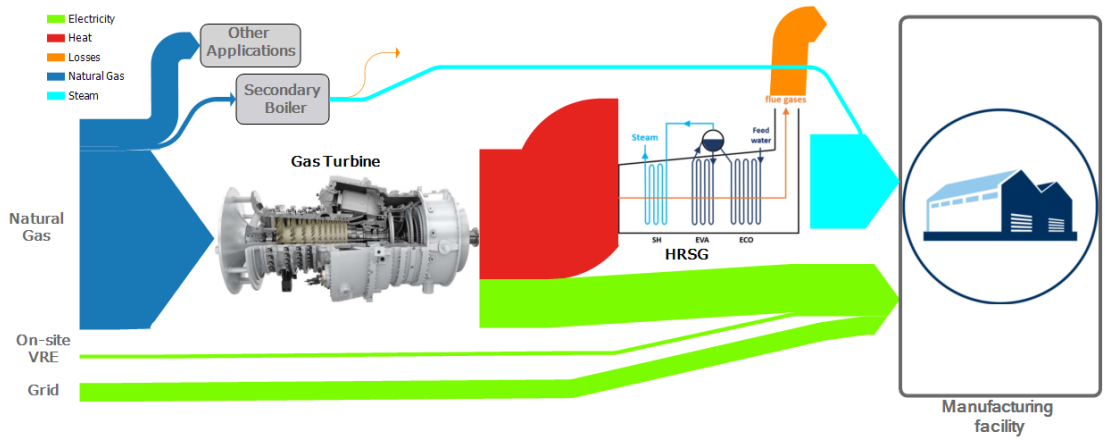

(a) Low RES availability

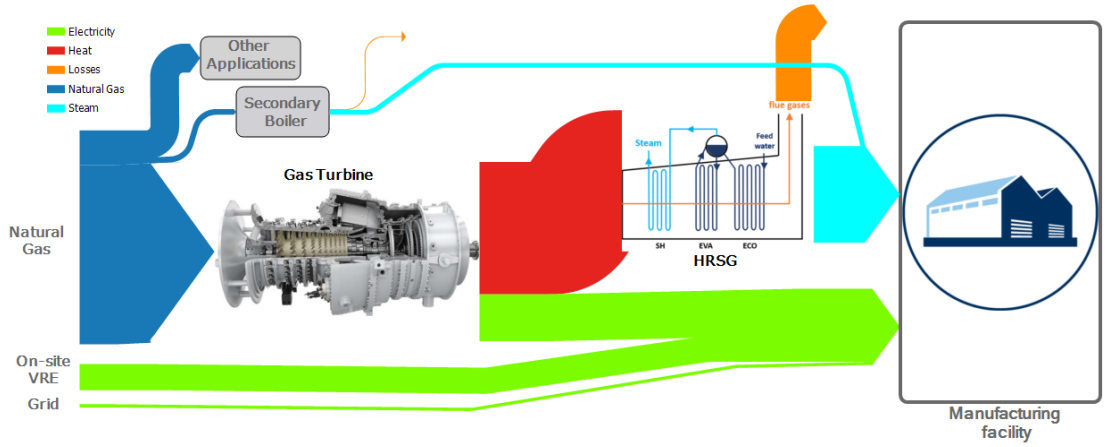

(b) Medium RES availability

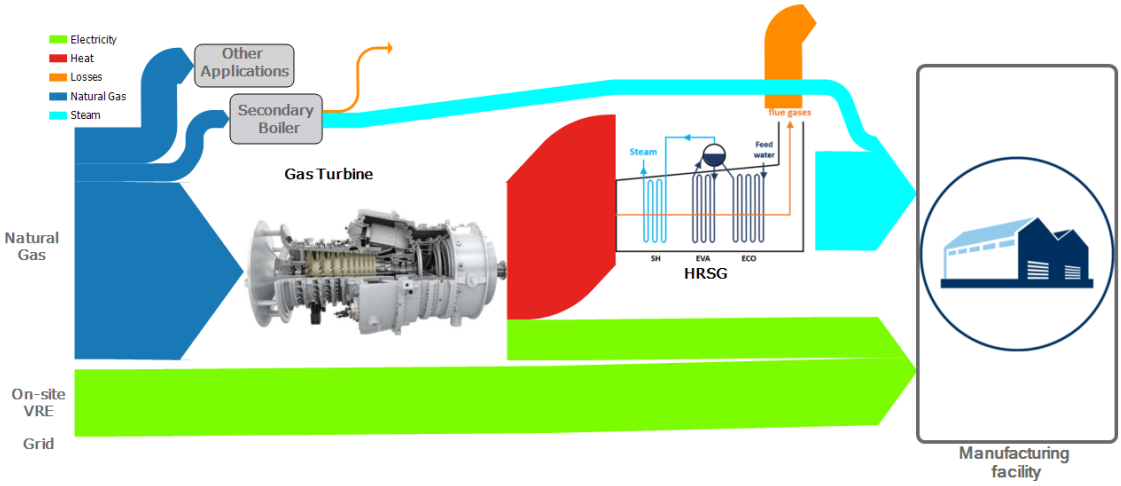

(c) High RES availability

FIGURE 6.3: On-site cogeneration system (Copyright www.siemens.com/press for the gas turbine image used for graphical purpose only)

The economic viability of on-site cogeneration has been evaluated through the cumulative Net Present Value (NPV). While the savings and the operative and maintenance costs vary every year n, the $CapEx$ is different from zero only the first year, when the initial capital investment is done.

$$NPV = \sum_{n=1}^{lifetime} NPV_n = \sum_{n=1}^{lifetime} \frac{(Saving_n - CapEx_n - OpEx_n)}{(1+r)^n} \tag{6.2}$$

The interest rate, r, is 0.06 in the base case scenario [90]. The savings are given by the electricity not bought from the grid and by a lower natural gas consumption and are calculated as:

$$Saving = FuelCost_{original} - FuelCost + OpEx_{original} - OpEx \tag{6.3}$$

The $CapEx$ is the total initial investment which is equal to:

$$CapEx = CapEx_{GT} + CapEx_{HRSG} + CapEx_{SB} + CapEx_{Wind} + CapEx_{PV} \tag{6.4}$$

The current fuel cost paid by the facility has been calculated for a given year n, considering a progressive increase in the commodity prices of 1.5% [90], as shown in equation 6.5.

$$FuelCost_{original} = \left\{ \sum_{h=1}^{8760} P_{el_{grid}} \times price_{el} + \sum_{h=1}^{8760} P_{th} \times price_{gas} \right\} \times (1 + 0.015 \times (n-1)) \tag{6.5}$$

The new cost of fuel, $FuelCost$, is evaluated in the same way as equation 6.5, considering that the electric power bought from the grid is lower because of the electricity produced by the gas turbine and the natural gas bought is overall reduced because it is used more efficiently to produce the same amount of steam. It is highlighted that fuel costs projections have a significant element of uncertainty and could be very volatile given their dependency on many factors that are difficult to forecast (e.g. geopolitical events), therefore a sensitivity analysis to different prices of commodities has been included in section 6.2.2.

$OpEx$ is the sum of all the operational costs. The current operational expenditures, $OpEx_{original}$, consist of the electric and gas distribution costs and operational costs of the boiler currently present on-site. The $OpEx$ in the new scenario with the integrated system is evaluated in equation 6.6:

$$OpEx = OpEx_{grid} + OpEx_{GT+HRSG} + OpEx_{SB} + OpEx_{Wind} + OpEx_{PV} \tag{6.6}$$

Table 6.2 details the additional costs the facility has to face for the on-site integrated system. There are no additional costs for the secondary boiler ($CapEx_{SB}$ and $OpEx_{SB}$ set to zero) since the facility already has an operating boiler on-site. The CHP $CapEx$ and $OpEx$ costs have been estimated based on average specific price (€/kW$_{peak}$) for the same range of electric power [102]. The costs related to the wind and PV systems are based, respectively,

on the study conducted by Kealy et al. [96] and on the estimation obtained simulating the PV system with the SAM software [88, 103].

Symbol	Value		Unit
	$800kW_{el}$	$1{,}600kW_{el}$	
$CapEx_{GT}$	1,324,000	2,648,000	[€]
$CapEx_{HRSG}$	100,000	200,000	[€]
$CapEx_{SB}$	0		[€]
$CapEx_{Wind}$	2,768,675		[€]
$CapEx_{PV}$	3,721,052		[€]
$OpEx_{grid}$	2,301,504		[€]
$OpEx_{GT+HRSG}$	299,662	555,359	[€]
$OpEx_{SB}$	0		[€]
$OpEx_{Wind}$	100,000		[€]
$OpEx_{PV}$	138,023		[€]
$price_{gas}$	0.031		$[€/kWh_{th}]$
$price_{el}$	0.096		$[€kWh_{el}]$

TABLE 6.2: Additional costs for the on-site integrated system

The system can be run with different strategies such as minimizing the thermal energy losses, the total gas consumption or the overall CO_2 emissions. The last parameter has been considered for establishing the environmental benefit of the integrated system.

The amount of CO_2 [kg/year] produced by the current system is calculated as in equation 6.7, where $\frac{44}{16}$ indicates the ratio of kg of CO_2 per kg of natural gas (CH_4) burned.

$$CO_{2_{BaseCase}} = \sum_{h=1}^{8760} P_{el_{demand}} \times CO_{2_{GridIntensity}} + \sum_{h=1}^{8760} \dot{m}_{gas} \times \frac{44}{16} \tag{6.7}$$

The amount of CO_2 produced by the integrated cogeneration system is calculated as in equation 6.8.

$$CO_2 = \sum_{h=1}^{8760} P_{el_{grid}} \times CO_{2_{GridIntensity}} + \sum_{h=1}^{8760} (\dot{m}_{gas_{GT}} + \dot{m}_{gas_{SB}}) \times \frac{44}{16} \tag{6.8}$$

The difference between the two CO_2 emissions estimates constitutes the annual emissions avoided. The criteria used to evaluate the environmental feasibility of the system is to have a positive cumulative CO_2 emissions reduction for the entire PBT of the system, considering that 3 years would be necessary to eventually design a governmental policy and 3 other years to implement, approve and build the system on-site. Different scenarios for the decarbonization trend of the grid have been considered.

6.2 Feasibility analysis of the integrated VRE and CHP system

6.2.1 Technical viability

The electric load of the manufacturing facility, shown in isolation in Figure 4.2-a, is also displayed for reference in Figure 6.4, 6.5, 6.8 and 6.10 where the electricity generated by the VRE and cogeneration system during one year is displayed.

The first analysis focuses on the integrated system of PV, wind, the 1,600kW_{el} GT coupled with the HRSG and a secondary boiler (SB). The same operational criteria are used for the 800kW_{el} GT: if the electricity following mode is selected, electricity overproduction is penalized; if, instead, the steam following control strategy is selected the closest value to the required steam is selected to limit the overproduction of excess steam. In this case, there is no restriction on the electricity side, which is the electricity generated at the correspondent load.

Figure 6.4 and 6.5 show the annual trend and the probability density function PDF of the electricity demand and of the on-site electricity generation for the VRE and the 1,600kW_{el} GT with two different control strategies: electricity following and steam following.

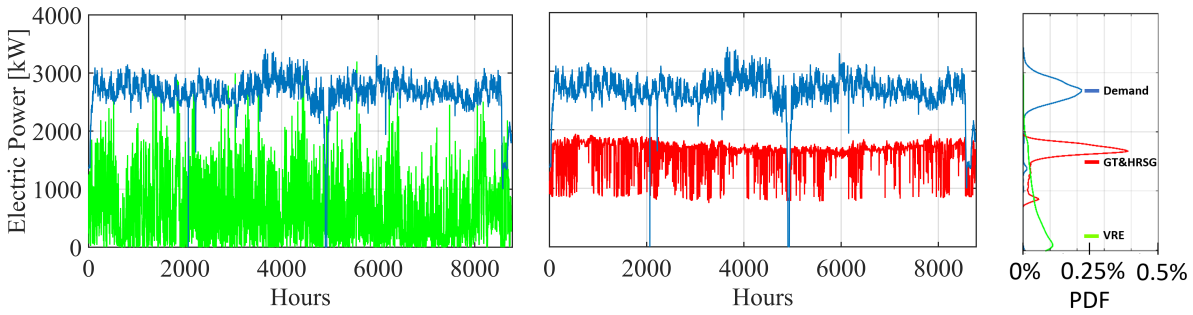

(a) VRE and electricity load (b) GT and electricity load (c) PDF

FIGURE 6.4: 1,600kW_{el} GT in electricity following control strategy: electricity generation profile and Probability Density Function

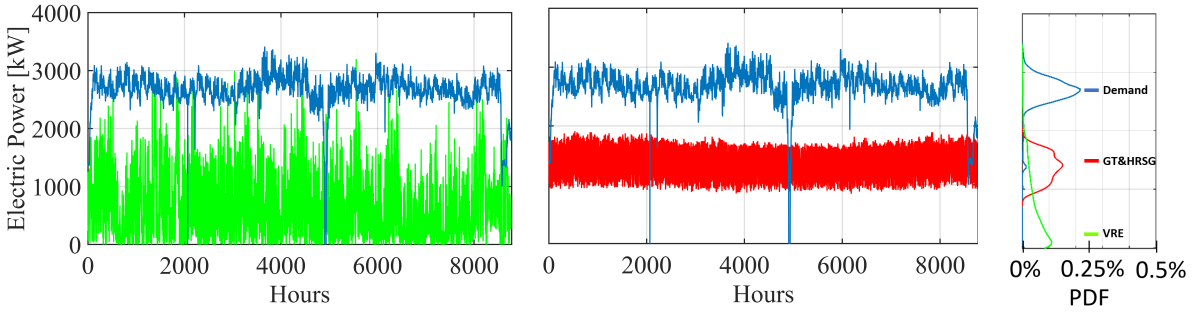

(a) VRE and electricity load (b) GT and electricity load (c) PDF

FIGURE 6.5: 1,600kW_{el} GT in steam following control strategy: electricity generation profile and Probability Density Function

The steam generated in the HRSG and in the secondary boiler in the same conditions is displayed in Figure 6.6 and 6.7.

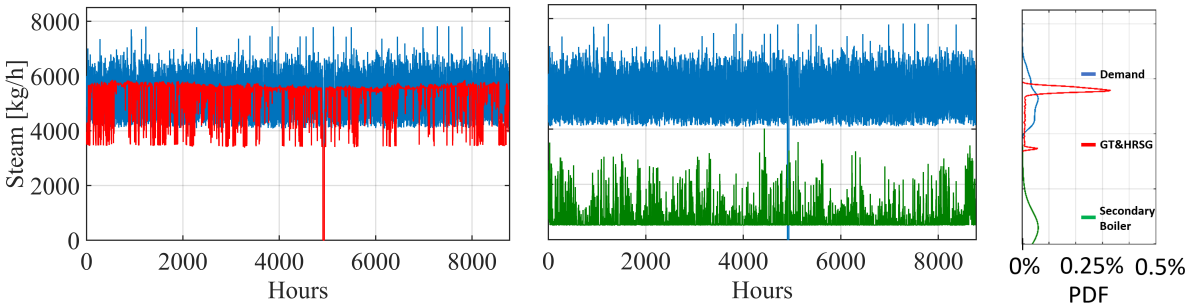

(a) GT and steam load (b) SB and steam load (c) PDF

FIGURE 6.6: 1,600kW_{el} GT in electricity following control strategy: steam generation profile and Probability Density Function

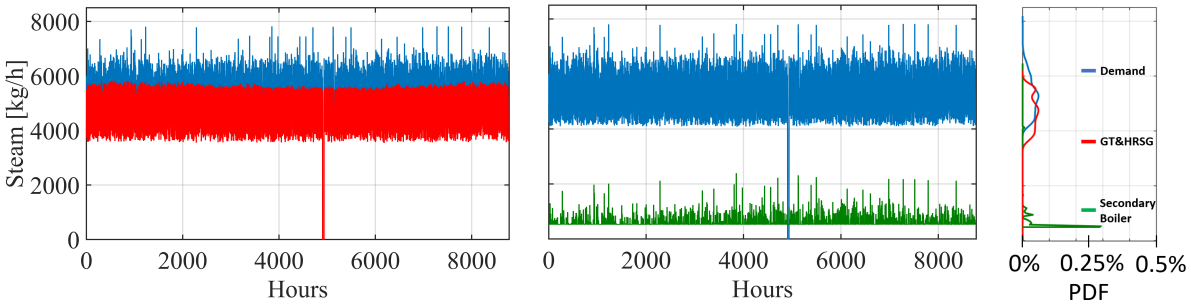

(a) GT and steam load (b) SB and steam load (c) PDF

FIGURE 6.7: 1,600kW_{el} GT in steam following control strategy: steam generation profile and Probability Density Function

The measured annual values are reported in Table 6.3: they show that if the electricity following control strategy is chosen the overproduction of electricity is reduced by more than 70% compared to the steam following case. On the other hand, the secondary boiler would have a wider range of steam flow rates to cover and the consequent additional cycling could reduce its lifetime (Figure 6.6). Also, a significant increase in the overproduction of steam is registered with the electricity following strategy.

A possible third option is a hybrid control strategy that takes into account the availability of renewable sources. If there is high availability of wind and solar (e.g. higher than the third quintile), the gas turbine can be switched to electricity following in order to optimize electricity generation. This solution gives improvements in the respective weak points of both control strategies but the overproduction of both steam and electricity is still significant (Figure 6.8 and 6.9, Table 6.3).

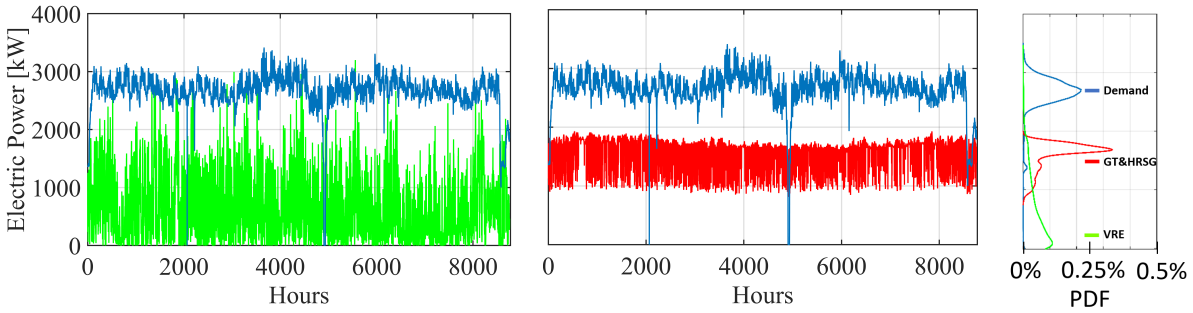

(a) VRE and electricity load (b) GT and electricity load (c) PDF

FIGURE 6.8: 1,600kW_{el} GT in hybrid control strategy: electricity generation profile and Probability Density Function

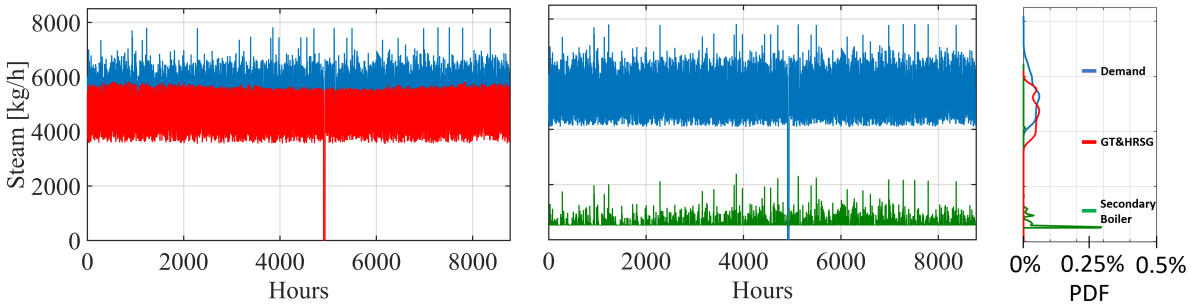

(a) GT and steam load (b) SB and steam load (c) PDF

FIGURE 6.9: 1,600kW_{el} GT in hybrid control strategy: steam generation profile and Probability Density Function

A smaller size gas turbine coupled with a bigger secondary boiler has been investigated. The system with a 800kW_{el} GT presents similar production trends with the different control strategies: the electricity and steam generation profiles are shown in Figure 6.10 and 6.11.

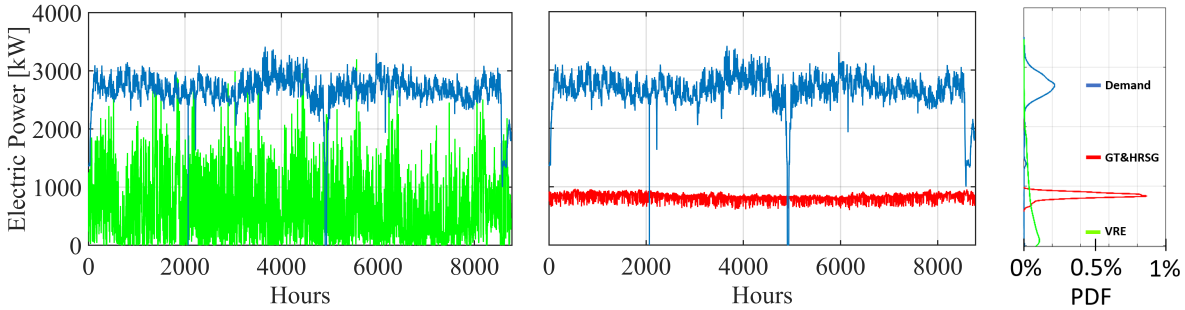

(a) VRE and electricity load (b) GT and electricity load (c) PDF

FIGURE 6.10: 800kW_{el} GT: electricity generation profile and Probability Density Function

By switching to a smaller GT size, the electricity bought from the grid significantly increases to 10.6×10^6kWh while the electricity overproduced decreases to 0.07×10^6kWh in the electricity following strategy (Table 6.4). The total amount of steam produced by the secondary boiler is almost three times higher than the previous case analysed.

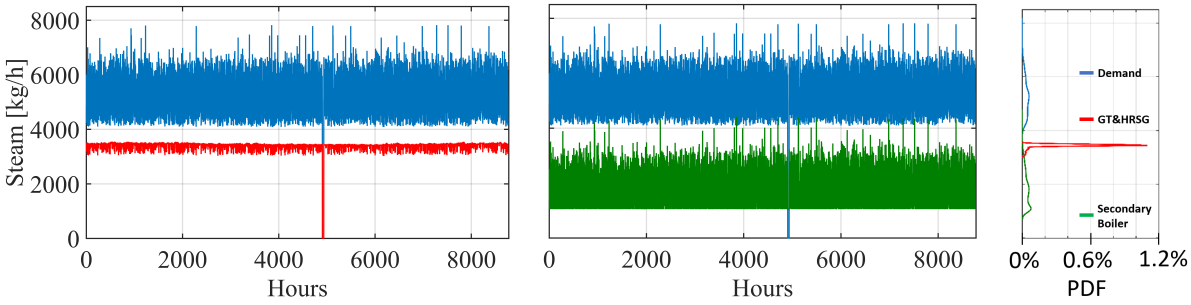

(a) GT and steam load (b) SB and steam load (c) PDF

FIGURE 6.11: $800kW_{el}$ GT: steam generation profile and Probability Density Function

In the steam following configuration there is no steam overproduced during the year. The CO_2 emissions avoided in the first year of the project are estimated to be 2.5×10^6kg. While this is lower than the carbon emission saving achievable with the larger GT size, they are estimated to decrease more slowly with a progressive decarbonization of the electric grid, given the higher share of the electric load covered by the grid.

The integrated system with the $800kW_{el}$ GT shows a better technical feasibility for on-site cogeneration in the manufacturing facility for the reduced amount of extra steam and electricity produced, therefore it is concluded that a technical opportunity does exist to improve the exploitation of the natural gas energy content, which is now partially wasted by releasing the exhaust gases at high temperatures.

Symbol	Electricity following	Steam following	Hybrid
Grid electricity [$\times10^6$ kWh]	4.2	6.6	5.9
Extra electricity [$\times10^6$ kWh]	0.18	0.63	0.2
Steam from SB [$\times10^6$ kg]	6.0	4.9	6.0
Extra steam [$\times10^6$ kg]	6.6	0.08	1.9
CO_2 avoided [$\times10^6$ kg]	3.5	3.7	3.7

TABLE 6.3: Annual values for the integrated system with the $1{,}600kW_{el}$ GT

Symbol	Electricity following	Steam following	Hybrid
Grid electricity [$\times10^6$ kWh]	10.6	10.7	10.7
Extra electricity [$\times10^6$ kWh]	0.07	0.16	0.07
Steam from SB [$\times10^6$ kg]	16	15.8	15.9
Extra steam [$\times10^6$ kg]	0.3	0	0.17
CO_2 avoided [$\times10^6$ kg]	2.5	2.5	2.5

TABLE 6.4: Annual values for the integrated system with the $800kW_{el}$ GT

The option of producing on-site electricity and steam only through the CHP system, and not in parallel with a renewable plant, has been investigated: after a preliminary assessment this option was discontinued due to the limited amount of carbon emissions saving achieved as the electric grid is progressively decarbonized.

6.2.2 Economic viability

The economic parameter that is calculated for assessing the economic viability of an investment project is the Pay Back Time (PBT). As underlined before, managers in the manufacturing sector are not likely to invest in a project with a PBT over 10 years (often as low as 5 years) therefore this is considered as the main requirement in the economic analysis. The PBT of the project has been calculated in the current conditions:

- grid electricity price, $price_{el} = 0.096€/kWh$;
- gas price, $price_{gas} = 0.031€/kWh_{th}$;
- discount rate $r = 0.06$;
- additional carbon tax $CT = 0€$/ton;
- secondary boiler already present on-site.

Under these conditions, the PBT of the integrated system is close to 7 years if the bigger gas turbine is selected and 6.2 years with the smaller one, independently from the control strategy chosen. By integrating the electricity and gas energy vectors it has been possible to design an economically viable system that reduces the overall CO_2 emissions by producing clean electricity from solar and wind and by fully exploiting the energy content of the burned natural gas. The well developed technology of gas turbine makes it possible to reduce the high PBT of the VRE system that would not be economically viable by itself [43].

However, in the near future the values of some parameters may significantly change as effect of governmental policies to promote the progressive decarbonization of the energy sector. It is difficult to forecast with accuracy how these parameters will change, therefore a sensitivity analysis has been done to evaluate in which scenario the integrated on-site cogeneration system is going to be a viable option for the manufacturing industry.

The first two parameters that are analysed are the electricity and gas prices paid by the facility. It is very difficult to forecast how these two prices will evolve in the next few years because they are inter-dependent and also depend on how the electricity market may change to support a higher VRE penetration. A range is estimated for both these variables in order to cover different scenarios.

The electricity price is simulated to vary $\pm 20\%$ with respect to the current price paid by the facility based on portfolio predictions by Poyry [104]. In this report, commissioned by EirGrid, the national Irish grid operator, various technology options for delivering a sustainable power are presented. Six possible generation portfolios were modelled from 2020 to 2035: two focused on fossil fuels alternatives, one on nuclear energy and three on renewable deployment. The impact of the six different options on the energy market and wholesale prices yields a range of electricity prices of $\pm 20\%$.

It is more difficult to select a gas price range. Looking toward a more decarbonized grid with a higher VRE penetration and a more integrated energy system it is possible that

natural gas will not only be an energy source but will also become an energy vector produced by using electricity (i.e. power-to-gas sector). Therefore, the price range selected has to take into account not only variation in the price of the primary source (fossil natural gas) but also a possible transition to different technologies, not commercially mature yet, for the production of gas from electricity. This would also impact the carbon intensity of the gas produced. The current efficiency of gas generation through electrolysis and methanation is respectively 0.7 and 0.75, therefore the price of gas produced with the use of these technologies would be $\frac{1}{0.7 \times 0.75} = 1.9$ times the price of the electricity used to produce it. If the current average price of electricity is considered, then the cost of producing gas would be $0.18€/kWh_{th}$. This price is almost 6 times the current price of gas paid by the company therefore it would not make sense to consider it in the analysis. On the other hand, if the gas is produced when there is an excess of electricity generation that has to be consumed, acting effectively as a storage and flexibility service, the price paid for electricity could be very low or even negative, leading to a lower price for gas. Assuming a 50% maximum penetration of power-to-gas in the gas supply, the range of gas price resulting would be between $0.031€/kWh_{th}$ (current price) and $0.1€/kWh_{th}$ ($0.031 \times 50\% + 0.18 \times 50\%$).

The sensitivity of the PBT to the commodities price is displayed in Figure 6.12. The PBT of the integrated system with the smaller gas turbine does not vary significantly with the control strategy chosen, therefore only one curve is plotted in the graphs.

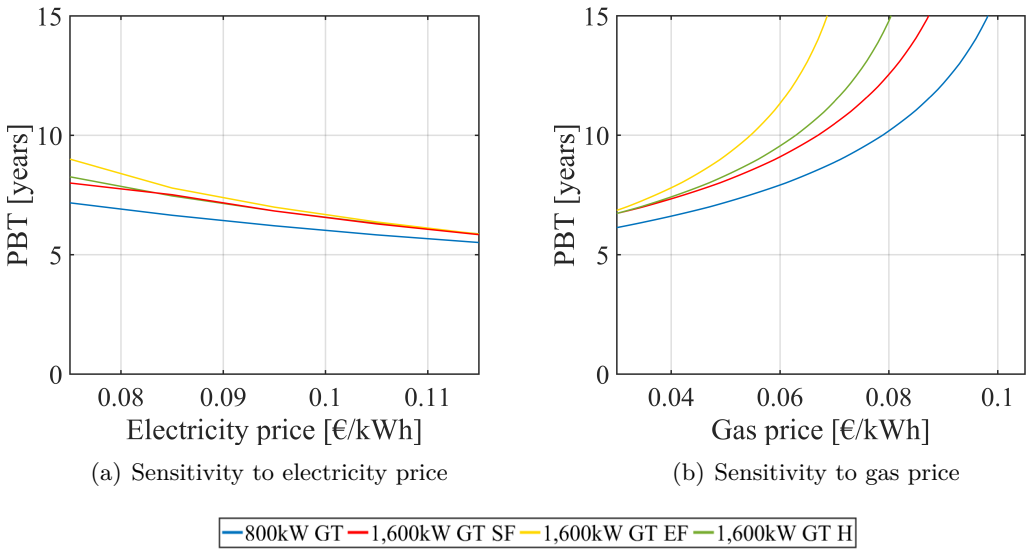

(a) Sensitivity to electricity price

(b) Sensitivity to gas price

FIGURE 6.12: Sensitivity of PBT to commodity price. Control strategies: SF = Steam Following; EF = Electricity Following; H = Hybrid.

The configuration with the lowest PBT in all the conditions simulated is the on-site integrated system with the $800kW_{el}$ GT.

If the electricity price increases, the system becomes more economically viable in all the analysed cases with a decrease in the PBT close to 5 years, as shown in Figure 6.12-a. The

sensitivity of the PBT to the electricity price for the integrated system with the bigger gas turbine is very similar for the three different control strategies.

The sensitivity of the PBT to the gas price is notable (Figure 6.12-b) and the cogeneration system becomes less viable with the progressive increase in gas price. The effect of an increase in the gas price is more evident on the bigger gas turbine run in the electricity following control strategy since there is a higher overproduction of steam, i.e. a partial waste of the natural gas energy content.

While the gas and electricity prices have been shown as two independent variables in Figure 6.12, in reality they influence each other. It is hard to make their relationship explicit and it is even more difficult to forecast the way they will interact in the future. A simplified approach is used and three scenarios are studied. The first scenario reflects the current economic conditions. The other two scenarios take into account possible variations in the commodities price due to the decarbonization of the energy sector.

The increasing penetration of variable renewable energy in the electric grid is causing additional costs for balancing and flexibility services which are currently not fully included in the electricity price: with the progressive rising in renewable penetration the final price of grid electricity will be driven up [105]. The future trend of gas price is more difficult to forecast. In the future, the power-to-gas (P2G) sector is forecast to grow as one possible efficient way to use the extra electricity produced by VRE when the demand is lower than the offer (acting as a storage service), reducing the need for curtailment. In this scenario, the price of gas would be directly influenced by the price of electricity: a higher VRE penetration will correspond to higher electricity and gas prices (Scenario 2). However, technical developments in this field will require time and the competitive price that currently characterizes gas as a fuel source is likely to maintain the use of gas as fossil fuel at the current level (Scenario 3), if not even higher (coal-to-gas switch).

The PBT has been simulated as function of the electricity and gas price. The results are presented for the two configurations of the on-site cogeneration system that show the best economic performances (lowest PBT): the cogeneration system with the $800kW_{el}$ GT and the cogeneration system with the $1{,}600kW_{el}$ GT run in the steam following control strategy. The results are shown in Figure 6.13 and Table 6.5. The integrated system with the smaller GT is more economically viable and requires less time to return on the initial investment. Currently the PBT estimated is 6.2 years (Scenario 1); if the electricity and gas prices increase, respectively, by 20% and 250% of the current prices (50% of gas produced from P2G), the PBT would increase to 10 years (Scenario 2). The effect of a rise in electricity price partially compensates the increase in PBT caused by higher gas prices. However, this scenario is unlike to happen in the immediate future given the technology developments that would require. The more likely scenario (Scenario 3), where fossil natural gas is used in traditional technologies such as boilers or turbines for energy generation, is characterized by the increase in the electricity price only, while the gas price remains competitive. The PBT decreases to 5.4 years in this scenario, making on-site cogeneration even more economically

viable. The PBT of the integrated system with the bigger GT follows the same trend but is higher in all the conditions analysed.

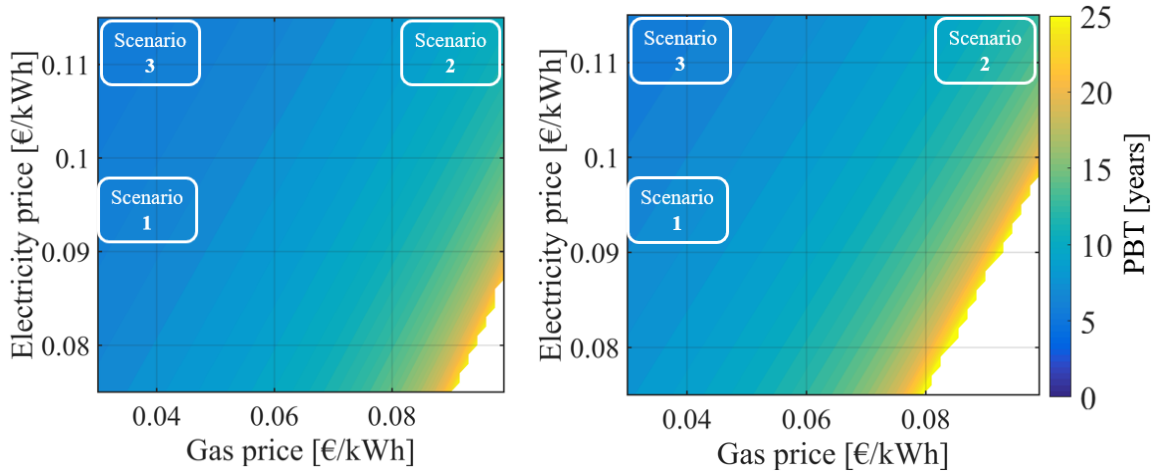

(a) Integrated system with 800kW$_{el}$ GT (b) Integrated system with 1,600kW$_{el}$ GT

FIGURE 6.13: Sensitivity of PBT to the electricity and gas prices. The three analysed scenarios in Table 6.5 are highlighted

It is interesting to note that the range of PBT achievable with different commodity prices is wide and may result in significantly different economic outcome for facilities subjected to different price agreements.

	Electricity price €/kWh$_{el}$	Gas price €/kWh$_{th}$	PBT [years] 800kW_{el} GT	PBT [years] 1,600kW_{el} GT
Scenario 1	0.096 (-)	0.031 (-)	6.2 (-)	6.8 (-)
Scenario 2	0.115 (+20%)	0.1 (+250%)	10 (+60%)	12.5 (+84%)
Scenario 3	0.115 (+20%)	0.03 (+0%)	5.4 (-13%)	5.8 (-15%)

TABLE 6.5: PBT of the integrated system in the three scenarios discussed

The economic viability of the project is dependent also on other economic parameters that may change in the near future. The sensitivity of the PBT to the discount rate r and to the introduction of an additional carbon tax CT has been studied and the results for the on-site cogeneration system with the 800kW_{el} GT are displayed in Figure 6.14 and 6.15. A lower discount rate has a positive impact on the PBT, reducing it by 30% when the price of gas is high (Figure 6.14). However, in the current conditions or even with an increase in the electricity price, the discount rate does not have a significant effect on the PBT. Similarly, the effect of an additional carbon tax on the PBT is small as shown in Figure 6.15. The system with the bigger gas turbine presents a similar sensitivity of the PBT to these parameters.

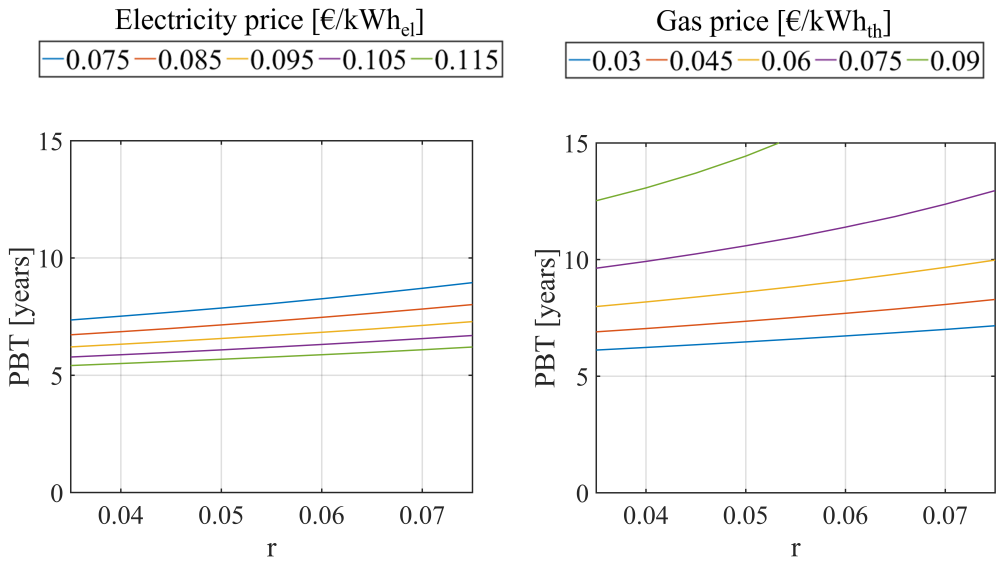

FIGURE 6.14: Sensitivity of PBT to the discount rate r

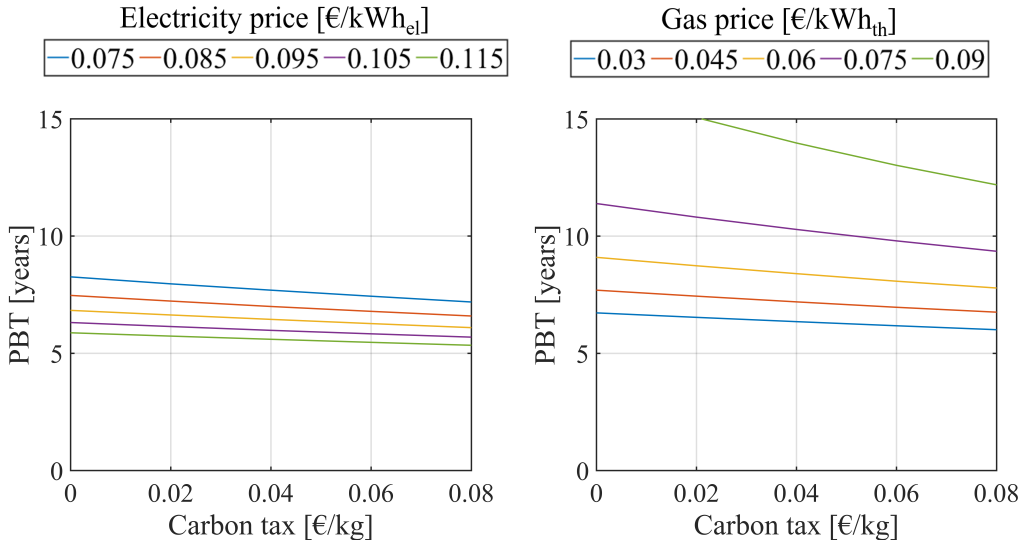

FIGURE 6.15: Sensitivity of PBT to the carbon tax CT

After studying the sensitivity of the Pay Back Time to different parameters, it is concluded that both a technical and economic opportunity does exist for on-site cogeneration (PV, wind and grid electricity with a gas fired plant) in the Irish manufacturing industry in presence of a more decarbonized energy market and the forecast increase in electricity price would make this option even more economically viable.

6.2.3 Environmental viability

It has been shown in the previous sections that the integration of on-site cogeneration with an on-site renewable energy system is a technically and economically viable option for manufacturing facilities in Ireland. However, policies to decarbonize the energy supply have a strong impact on the economic profitability of these projects. The key question is therefore whether this integrated system is compatible with the goal of decarbonization. Will such an installation avoid carbon emissions now and over its lifetime?

The cumulative amount of emissions saved during the entire lifetime of the project (25 years) can be calculated with eq. 6.7 and 6.8. The result is highly dependent on the trend of the grid carbon intensity forecast for the next decades. There are many studies in the literature that model different decarbonization pathways to achieve the 2030 and 2050 emissions reduction targets, however the analysis focuses mostly on total CO_2 emissions trajectories. Glynn et al. [106] characterize 38 scenario variants to account for the uncertainty in climate mitigation policies and other constraints. Chiodi et al. [107] propose 4 alternative scenarios to the reference one (no emissions reduction targets) and present the different measures required to reach more or less stringent targets. Both these studies, along with the majority of the literature, present pathways for the total CO_2 emissions and while they show the reduction target specific to the electricity generation sector, it is impossible to infer uniquely from these data the forecast carbon intensity of the grid. A distinction should be made, in fact, between the electricity generated and transmitted through the grid that would set out the grid carbon intensity and the electricity generated from decentralized systems for self-consumption, which would contribute to the total electricity generation but not to the grid carbon intensity. Given the absence of forecast trends for the carbon intensity of the Irish electric grid, different scenarios have been simulated. This is the methodology usually adopted in forecasting emissions trend [5].

SEAI [108] presents the average annual carbon intensity of the Irish grid. The values between 2005 and 2016 have been used as historical data and are plotted in Figure 6.16-a as circular dots. It is suggested to not include older data because the result could be affected by the positive effect energy policies have had in the first years after their implementation. Based on these data, three interpolation curves are used to forecast possible trends for the average carbon intensity of the grid until 2050, as shown in Figure 6.16-a. The three different fitting curves lead to the cumulative carbon emission savings shown in Figure 6.16-b. Two configurations of the cogeneration systems are considered: the system with the $800kW_{el}$ GT (case with lowest PBT) and the system with the $1{,}600kW_{el}$ GT in steam following control strategy (case with highest CO_2 emissions savings).

The exponential fitting curve takes into account that, after a first rapid decrease in the carbon intensity of the grid, the reduction rate slows down since it will be progressively more difficult to integrate more renewable or sustainable energy sources into the grid. This is the more realistic trend. In this scenario, the cumulative emissions saving has a peak after 14 years (small GT) and after 17 years (big GT) from the commissioning then it decreases

but it remains positive for the whole lifetime of the system, showing a positive environmental impact of the project. The progressive decrease in cumulative emissions avoided in the second part of the lifetime is due in part to a reduction of the energy efficiency of the technologies on-site. The other reason is that the carbon intensity of the grid is simulated to gradually decrease every year of the project and at a certain point this will result in the cogeneration system producing more CO_2 than would be produced by buying the electricity from the grid and generating steam in a natural gas boiler. The second method uses a linear interpolation. While this curve fits better the historical values, it is not likely to give a true representation of the future carbon intensity of the grid because it assumes a constant decarbonization rate. A third option is to consider a linear decrease in carbon intensity for the next decade, while there is still margin for increasing the penetration of renewable sources on the grid, and then to introduce an exponential fitting curve that simulates the progressively increasing difficulty in finding additional methods for further reducing the carbon intensity. The linear and hybrid interpolation curves lead to a neutral amount of cumulative emissions avoided before the end of the lifetime of the integrated system, reducing the time span in which this installation could be environmentally beneficial (Table 6.6).

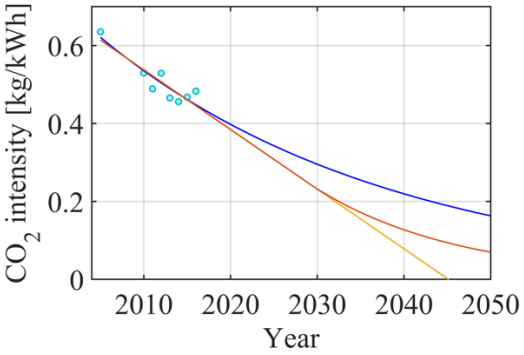

(a) Estimated carbon intensity of the electric grid based on the interpolation of historical data (dots)

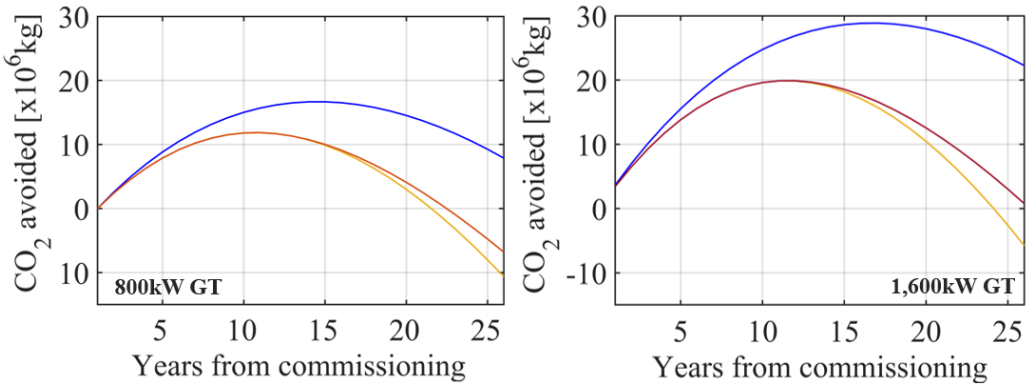

(b) Estimated cumulative emissions avoided

FIGURE 6.16: Estimated grid carbon intensity and cumulative emission avoided. Interpolation method used: — Exponential — Linear — Hybrid

Interpolation method	Neutral year	
	$800kW_{el}$ GT	$1{,}600kW_{el}$ GT
Exponential	>30	>30
Linear	21	24
Hybrid	22	26

TABLE 6.6: Neutral year after the commissioning with different interpolation method

These results are only based on the interpolation of historical data and do not guarantee an accurate forecast. Alternatively, the minimum carbon intensity of the grid required to guarantee a positive cumulative emission saving can be calculated.

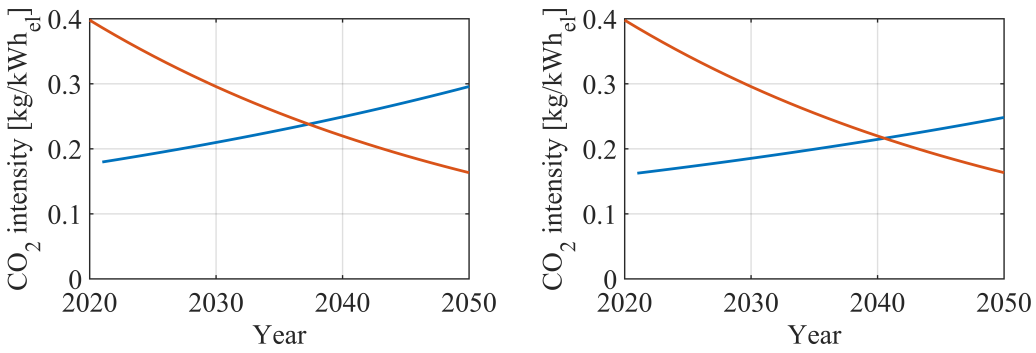

(a) Integrated system with 800kW$_{el}$ GT (b) Integrated system with 1,600kW$_{el}$ GT

FIGURE 6.17: — Minimum grid carbon intensity required to guarantee positive cumulative emission savings — Forecast grid carbon intensity based on exponential fitting

Figure 6.17 shows the minimum carbon intensity of the grid required to guarantee positive cumulative emission savings until that year if the project was implemented in 2020 and it is compared to the forecast grid carbon intensity. The intersection of the two lines shows that the requirement for a positive environmental impact of the project could be met until 2037 (2040 with the bigger GT) then it would be more environmentally sustainable to purchase electricity from the decarbonized grid and only produce steam on-site.

6.2.4 On-site CHP as balancing service provider

From the analysis conducted, it has been concluded that a technical opportunity for on-site cogeneration of electricity and high temperature steam through the integration of a gas turbine and a VRE system does exist for the targeted manufacturing facility, however its environmental feasibility is limited to the next two decades.

The use of CHP on-site may have another potential benefit: it may mitigate the high variability of the VRE generation with its flexible operation. The intermittency of renewable sources is a well known obstacle to high VRE penetration; it affects the operation of the electricity grid on all three time scales (minute-to-minute, intrahour, hour-to-day-ahead) and

may result in increasing operating costs to ensure power quality and network reliability [109]. An increase in VRE on-site generation in manufacturing facilities may lead to a shift from an almost flat demand, effectively considered by the grid as a predictable base-load, to a highly variable net demand with peaks that are likely to be registered when renewable sources are scarcely available. This could cause significant balancing issues at a local level, especially in highly industrialized areas with agglomerated manufacturing sites, where the amplitude of power fluctuations could increase. Figure 6.18 shows the facility's net electricity demand with and without VRE on-site, during two months of the year (January as example of winter months and June of summer). The introduction of an on-site VRE system leads to higher fluctuations in the manufacturing facility net demand. From the electricity grid point of view, an almost flat and predictable load is substituted by a more variable and unpredictable one that requires more flexibility from the grid.

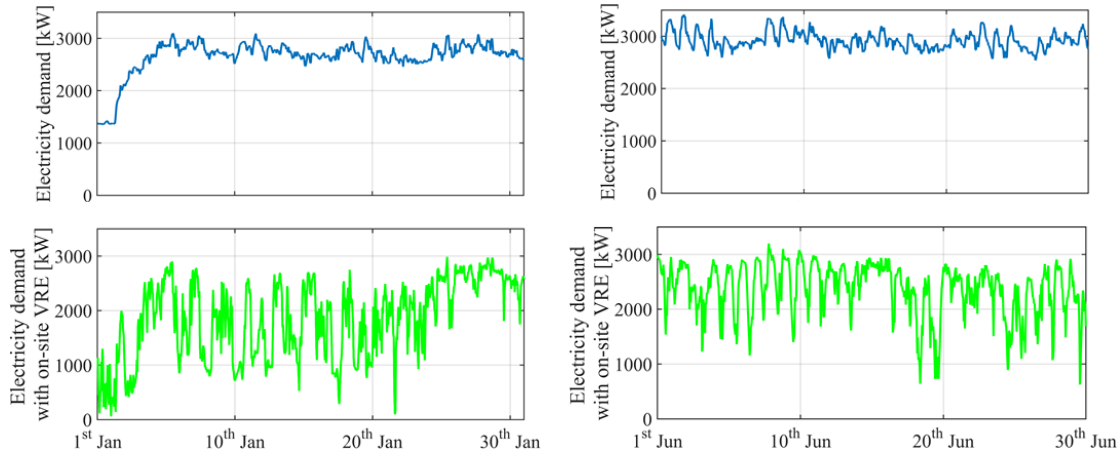

(a) January (b) June

FIGURE 6.18: Net electricity demand of the facility with and without the VRE system on-site

On-site CHP could support a higher penetration of distributed renewable generation by absorbing part of the intermittency of on-site VRE through its flexible operation, effectively acting as a local balancing service provider. While CHP has shown limited environmental benefits if considered only as an electricity and steam generator, it could result in a beneficial reduction of emissions (higher VRE penetration) and reduced need of balancing service on a grid level if considered also as a flexibility provider.

The effect of on-site cogeneration on the variability of the net demand for grid electricity is assessed by calculating the standard deviation σ_h of the net demand over a five-hour window spanning two hours before and two hours after every hour h of the year [110], as shown in equation 6.9:

$$\sigma_h = \sqrt{\frac{1}{5-1} \times \sum_{i=h-2}^{h+2} (x_i - \bar{x}_h)^2} \tag{6.9}$$

The parameter x_i represents the net demand for grid electricity at a specific hour of the year and $\bar{x}_h$ is the average net demand over the analysed 5-hour window centred in h as shown in eq. 6.10.

$$\bar{x}_h = \frac{1}{5} \times \sum_{i=h-2}^{h+2} (x_i) \tag{6.10}$$

The five-hour window around hours with null electric demand due to maintenance have been excluded from the calculation.

An indicator to qualitatively evaluate the variability of the net demand during the whole year is the mean of σ_h, $\bar{\sigma}_h$. It indicates how rapidly the residual electric load that the grid has to cover changes on average during the year: an increasing $\bar{\sigma}_h$ indicates that the net demand sees more rapid and higher fluctuations.

$$\bar{\sigma}_h = \frac{1}{8760} \times \sum_{h=1}^{8760} (\sigma_h) \tag{6.11}$$

This indicator has been normalized with respect to the base-case with no on-site cogeneration (eq. 6.12) in Table 6.7.

$$\bar{\sigma}_h^* = \frac{\bar{\sigma}_h}{\bar{\sigma}_{h_{basecase}}} \tag{6.12}$$

The purpose of this indicator is, in fact, to compare the different analysed cases and draw qualitative conclusions rather than creating a metric for quantifying the variability of the net electric load. A further discussion on the indicator and on the time window chosen for this analysis is presented in Appendix B.2.1.

	$\bar{\sigma}_h^*$
No on-site cog.	1
VRE only	4.34
VRE + $800kW_{el}$GT	
el. following	4.12
steam following	4.2
hybrid	4.22
VRE + 1,$600kW_{el}$GT	
el. following	2.86
steam following	5.46
hybrid	5.46

TABLE 6.7: Normalized mean variability of the net demand $\bar{\sigma}_h^*$

As shown in Table 6.7, the introduction of on-site VRE significantly increases the occurrence of rapid fluctuations during the year. The $800kW_{el}$ GT does not have a significantly positive effect on the variability of the net demand: even in the electricity following control strategy there is only a slight reduction in the mean compared to the "VRE only" case. By

introducing on-site cogeneration with the bigger gas turbine (1,600kW_{el} GT), there is a beneficial reduction in the mean that indicates that the fluctuations in the residual load are less rapid.

The viability assessment of on-site CHP and VRE integrated system for manufacturing industry could be expressed as a trade-off between its environmental benefits which are limited in time due to the progressively decarbonization of the grid and its beneficial effect on partially balancing the fluctuation introduced by the VRE system on the net demand. These two aspects have been investigated through two parameters: the normalized mean variability of the net demand $\bar{\sigma}_h^*$ and the carbon intensity of the electric load (considering fossil gas as fuel for the gas turbine). Both these parameters are normalized to the base case with no on-site cogeneration.

The equivalent carbon intensity of the electric load covered in part by the on-site cogeneration system and in part by the grid is normalized to the carbon intensity of the grid: three values of grid carbon intensity have been considered to simulate different decarbonization scenarios. The results are listed in Table 6.8.

In order to have a significant benefit on the net demand variability the bigger size of the gas turbine should be installed and run in the electricity following control strategy. While this configuration would bring significant environmental benefit when the carbon intensity of the grid is 0.3kg/kWh$_{el}$, with a progressively decarbonization of the grid the best configuration would be with the smaller gas turbine on-site but the environmental benefits would be extremely low; a lower carbon intensity for the electricity produced on-site would be achieved by using only the VRE system.

	No on-site	VRE only	800kW GT	1,600kW GT	
				EF	SF
$\bar{\sigma}_h^*$	1	4.3	4.1	2.8	5.4
Carbon intensity of the electric load assuming $CO_{2_{GridIntensity}}$					
0.3kg/kWh$_{el}$	1	0.76	0.62	0.51	0.58
0.2kg/kWh$_{el}$	1	0.76	0.7	0.68	0.74
0.1kg/kWh$_{el}$	1	0.76	0.95	1.19	1.19

TABLE 6.8: Comparison of the benefits of the different configurations of the on-site generation system.
Control strategies: EF = Electricity Following; SF = Steam Following.

6.3 Summary

The on-site cogeneration system (VRE, GT, HRSG and SB) is shown to be economically feasible for manufacturing facilities in the current analysed scenario ($PBT \backsimeq 6$ years) and it becomes even more profitable in future scenarios where higher VRE penetration would drive up electricity prices ($PBT \backsimeq 5$ years).

The environmental benefits of on-site cogeneration are limited in time as the grid is progressively decarbonized. In fact, if the on-site CHP system would start being operational in 2020, the total amount of CO_2 emissions avoided would be 3.5kton over 16kton of CO_2 emitted otherwise in the basecase with no on-site energy generation (22% emission reduction); however, as the carbon intensity of the grid progressively decreases, the share of emissions avoided compared to the basecase decreases as well, reaching overall a cumulative value of 2.5% emissions reduction. It has been shown that the minimum carbon intensity of the grid required to guarantee positive cumulative emissions saving would be higher than the forecast carbon intensity of the grid before 2040, limiting *de facto* the environmental benefits of on-site cogeneration to the next two decades. Manufacturing facilities are likely to exploit the on-site system purchased for its entire lifetime to generate more profit, despite the system may be not environmentally beneficial anymore. This may result in a misalignment between decarbonizing policies that aim to lower the environmental impact of energy production and consumption, and manufacturing facility economic strategies that aim to maximize profit.

There is a trade-off between reducing CO_2 emissions and decreasing the variability of the electric net demand. While in a decarbonized scenario (low carbon intensity of the grid) the environmental benefit would come from only VRE or the integrated system with the smaller gas turbine, a support to higher penetration of decentralized VRE systems in manufacturing industry would come from the bigger gas turbine run in the electricity following control strategy to absorb part of the intermittency of renewable sources availability.

In conclusion, the two main limitations of the on-site cogeneration system as the grid is progressively decarbonized have been identified to be the environmental benefits limited in time and the variability of the net demand, which is only slightly reduced through the flexible operation of the gas turbine.

For reducing the high variability of the residual electric load caused by the on-site cogeneration system the integration of a storage system is proposed and is investigated more in detail in Appendix B.

The use of biogas is proposed [111] to overcome the temporal limit of the environmental benefit of the system and a brief overview of the current state of the art of biogas production, its supply potential and cost is given in Appendix C.

Chapter 7

Conclusions and future work

7.1 Conclusions

The aim of this thesis is to investigate the feasibility of the Irish manufacturing industry assuming the role of energy prosumer (producer and consumer) in a progressively decarbonized energy system, by producing, on-site, part of the electric and thermal energy load in a more sustainable way. In order to do so, a new model has been developed and implemented in Matlab, that allows to simulate the techno-economic and environmental feasibility of on-site energy generation through an integrated renewable system and a Combined Heat and Power (CHP) system. The model is built as a robust and flexible tool that can be used for any facility worldwide by updating inputs such as geographical location, solar and wind availability and hourly energy demand. Real data from an existing manufacturing facility were used to provide realistic data as input to the feasibility analysis taking into consideration the constraints that characterize this type of end-user.

First, to evaluate which technologies are more suitable for on-site energy generation in this specific application, the energy demand for the different energy vectors used in the manufacturing facility (electricity, natural gas and water) was analysed, based both on internal monitoring and billing information (Chapter 4). The electric demand is almost constant throughout the year, with no significant diurnal, weekly or seasonal variations and therefore it is concluded that the electric consumption profile of a manufacturing site differs significantly from that of typical residential end-users. The average electric power required by the facility and currently provided through the national electric grid is 2,659kW, with a peak of 3,416kW, and the total annual electric energy demand is 23,296MWh. The thermal demand presents, instead, more relevant seasonal variations. The data from internal metering are intermittently available during the year: a statistical analysis was conducted to simulate a demand profile for the entire year based on the available data. The thermal energy is purchased in the form of natural gas: around 20% is used for space heating and other minor applications, and the remaining 80% is burned on-site in a vertical boiler to produce an average steam flow of 5,200kg/h at the saturated temperature of 196°C and 14 bar. The annual environmental impact of the energy load of the facility is estimated to be 16ktoe of

CO_2 emitted in the basecase with no on-site energy generation, considering the current carbon intensity of the grid. Having identified the energy requirements of the facility, different technologies for on-site energy generation were investigated.

Given the large land space that typically surrounds manufacturing facilities, the first option investigated to reduce the carbon emissions associated with the electric demand of the facility was a decentralized Variable Renewable Energy (VRE) system (Chapter 5). The two renewable sources considered were solar and wind: they are, in fact, less site specific and therefore more suitable for replicating the analysis to different facilities located elsewhere.

An integrated VRE system constituted of a solar PV and a wind system was modelled to simulate the renewable electricity potentially produced on-site. The hourly electricity generation was simulated based on historical meteorological data and techno-economic input parameters. The results show that solar energy presents a more predictable daily and seasonal trend while the wind system introduces a high variability in the net demand (which represents the residual load covered by the electric grid). Overall, the on-site VRE system is technically viable: it satisfies part of the electric load of the facility with only limited overproduction (less than 1% of the time during the year).

The economic feasibility was assessed based on the Pay Back Time (PBT) of the system, considering that existing manufacturing facilities are not likely to invest in projects with a PBT higher than 10 years and often as low as 5 years. The sensitivity of the results to different techno-economic parameters was assessed, to consider both current and likely future scenarios. The results show that while the wind system could be economically viable if small incentives are provided or if a reduction in the capital cost occurs, the PV system has a PBT not acceptable in any of the simulated conditions. For the integrated system of wind and solar PV, while a technical opportunity does exist, the economic feasibility is subject to all the following conditions:

- acceptance of a long Pay Back Time;
- substantial subsidy either as a direct subsidy or as an avoided penalty (e.g. carbon tax);
- technological improvements yielding a reduction in the capital cost.

Achieving all these conditions seems unlikely, and therefore it is concluded that on-site renewable generation is not economically feasible for Irish manufacturing facilities in isolation in the conditions evaluated. Nonetheless, producing part of the electric demand of the Irish manufacturing industry on-site from renewable sources may help reduce the carbon intensity of the national economy, which may be a reasonable policy goal.

A second option was explored to support the penetration of decentralized VRE generation in Irish manufacturing facilities. An integrated system of a gas turbine (GT) and a Heat Recovery Steam Generator (HRSG) was considered for Combined Heat and Power (CHP)

cogeneration. CHP is a commercially mature technology widely used in industrial applications and therefore it may successfully support the VRE system by reducing its PBT. The CHP system would work in parallel with the grid and the on-site VRE system for providing the energy required by the facility: while the VRE system is suitable for electricity generation only, the CHP system produces both electricity and also the high temperature and high flow rate steam required by the manufacturing facility in the production lines.

The technical, economic and environmental feasibility of the integrated system (gas turbine, heat recovery steam generator, and VRE system) were analysed in different scenarios (Chapter 6). The hourly electricity and steam production profiles of each technology on-site were simulated for the entire lifetime of the system: the on-site integrated cogeneration system results to be technically feasible since it successfully provides part of the electric and thermal load of the facility. The system is also economically viable with a PBT of approximately 6 years, which decreases to 5 years in future scenarios where higher VRE penetration would drive up the electricity price. The CHP system successfully decreases the PBT of the VRE system, making on-site energy cogeneration a viable option.

The installation of CHP systems in industrial sites has shown a reduction of energy-related carbon emissions compared to the separate purchase of grid electricity and on-site steam generation. However, it is not clear whether this environmental benefit will persist with the progressive decarbonization of the electric grid. It is important to ensure that if the manufacturing facility invests in a CHP system to support distributed VRE generation, the environmental benefits of the integrated system endure for its entire lifetime.

The analysis conducted on the environmental benefits of on-site cogeneration shows that they are temporally limited to the next two decades. If the on-site cogeneration system was to be commissioned in 2020 for a manufacturing facility in Ireland, the minimum carbon intensity of the grid required to guarantee positive cumulative CO_2 emissions savings would be higher than the planned carbon intensity of the grid before 2040; after that the integrated cogeneration system of CHP and VRE will produce more CO_2 emissions compared to purchasing the electricity from the decarbonized grid and using on-site natural gas only for steam generation.

Since manufacturing facilities are likely to exploit the on-site system purchased for its entire lifetime to generate more profit (despite the system's increased environmental impact), this may result in a misalignment between decarbonizing policies that aim to lower the environmental impact of energy production and consumption, and the manufacturing facility's economic strategy that aim to maximize profit.

A possible solution to the temporal limit of environmental benefits is the use of biogas in the CHP system, which is currently limited in Ireland but it is forecast to significantly increase in the next decades. However, the economic viability of biogas in this scenario appears, *prima facie* (see Appendix C), to be poor and so has not been investigated in depth here.

Another issue arising with the on-site VRE system is the high variability in the residual

load that is caused by the intermittency in renewable sources. It was investigated whether the introduction of a flexible technology such as a gas turbine has a positive impact on reducing the variability of the residual load that the grid has to cover, acting effectively as a balancing service provider. The gas turbine does not improve significantly the variability of the residual load. The effect of integrating a Battery Energy Storage System (BESS) on the net demand variability was investigated as well and is presented in Appendix B. The results show that for higher capacities of the battery bank the average variability of the residual load slightly decreases, however even with the biggest storage system investigated the manufacturing facility retains the role of net consumer. Therefore the reduction in the residual load variability would not benefit the manufacturing facility but rather the Transmission System Operator (TSO), who would have to incentivize the installation of a BESS.

The question posed at the beginning of the thesis was whether it is feasible for an Irish manufacturing facility to be an energy prosumer, considering the progressive decarbonization of the energy system.

It is concluded that it is technically and economically feasible for an Irish manufacturing facility to produce on-site part of the electric and thermal energy load through a VRE system integrated with a CHP system, however the environmental benefits of on-site cogeneration are limited to the next 20 years. The CHP system, with its flexible operation and low PBT, supports the penetration of distributed VRE making it economically feasible and partially reducing the variability of the residual electric load caused by the intermittency of renewables; nonetheless, it causes a higher consumption of natural gas that, as the grid decarbonizes, does not lead to positive carbon emissions savings. The use of biogas in the CHP system could overcome the temporal limit of the environmental benefits, making CHP a viable option for supporting distributed VRE in manufacturing sites. The economic cost of this option is currently limiting its application.

The manufacturing facility remains in all the analysed cases a net consumer, with a significantly variable residual load that the electric grid has to cover. Only a limited reduction in the net demand variability is achievable with a battery storage system, unless the on-site VRE system is oversized, which will require a higher expenditure and will depend on the facility's land availability.

7.2 Future work

The main objective of this thesis was to investigate the feasibility for the Irish manufacturing industry to assume the role of energy prosumer in a progressively decarbonized energy system, by producing electric and thermal energy on-site in a more sustainable way. More work could be done to further enrich and strengthen the conclusions of this analysis. A deeper investigation is suggested on the following points:

- A limitation of the thesis lies in the simplified approach used for estimating the carbon intensity of the Irish electric grid in the future. This is due to the limited information available on the decarbonization trend for the Irish electric grid. A more accurate simulation could be done with the assistance of specifically designed software.

- Due to the unavailability of additional data from other Irish manufacturing facilities, the simulations are based on real data from one facility only. It would be interesting to replicate the analysis conducted in this thesis to other manufacturing industries, producing different categories of products that requires both electric and thermal energy (e.g. food production), and located elsewhere. A preliminary analysis was conducted on an Italian manufacturing facility producing resins. The preliminary results show that the PV system, sized based on the energy requirements and land availability, is technically feasible and more economically viable due to a higher solar Global Tilted Irradiance, compared to the Irish case study, but still does not reach an acceptable PBT. The wind system, instead, shows worst economic performance compared to the Irish case study given the low average wind speed registered in the Italian region where the facility is located. This preliminary analysis shows the dependence of the on-site VRE feasibility on the geographical location of the facility.

- Another interesting analysis could be done on a cluster of manufacturing facilities located close to each other. A commonly owned distributed energy system could satisfy part of the aggregated energy load, managed effectively as a micro grid. The effects on the electric grid should be investigated.

- In Appendix B, it has been shown that one limitation to the benefits of the battery bank on-site is the limited energy overproduced by the VRE system, sized based on land availability, physical constraints and energy requirements. Larger space around the facility would allow the installation of a higher renewable capacity that could be better exploited by the battery system and that may have a positive impact on the variability of the residual load. More work could be done in investigating the sensitivity of the results to the available land footprint.

- More work could be done in finding a metric for assessing the variability of the residual demand that the electric grid has to cover. This will become more and more relevant as the penetration of distributed Variable Renewable Energy increases and with it the fluctuations occurring in the net demand of end-users.

Appendix A

State of the art of PV, wind and CHP technologies

A.1 Solar photovoltaic

In this section, the state of the art of different solar photovoltaic (PV) technologies both already available in the market and currently under development, and the actual and forecast costs of PV systems are presented.

Solar radiation can be converted in different form of energy based on the technology used. Photovoltaic cells are semiconductor devices that convert solar radiation in Direct Current (DC) electricity. Cells are grouped in modules, which are then combined to form strings, arrays and systems with a capacity range that goes from 1 Watt to 10^9 Watts. The current photovoltaic technologies can be classified in three groups: first, second and third-generation [112].

- The first-generation PV systems use very mature technologies that are already fully commercialized and include mono and multi-crystalline wafer-based Silicon technologies (c-Si).
- The second-generation consists of thin-film technology.
- The third-generation is based on technologies still under development or not fully commercialized, as concentrating PV (CPV) and organic PV cells.

Before going into detail about the differences between these various systems, a brief explanation on how a solar cell works is given.

Most of the photovoltaic cells are based on the same physical working principle. Two layers of a semiconductor material (e.g. Silicon) are used. One layer is doped with Phosphorous, which creates an extra electron in the Si atomic structure (N-type Si). The other layer is doped with Boron, which creates a hole in the Si atomic structure (P-type Si). These two layers, joined together in correspondence of the p-n junction, modify the conduction and valence bands of the original material, reducing the band gap. When photons (solar radiation) reach the surface of the solar cells and impact on the electrons, if the energy absorbed by the

electron is equal or higher that the band gap, the electron jumps from the valence band to the conduction band and flows from the N-type to the P-type material. The p-n junction, also called depletion region, does not let the electron back in the N-region, which is now positively charged. An electric circuit is connected to the solar cell to allow the electron to flow back in the N-type layer. The flow of electrons through the electric circuit produces DC current [113]. In Figure A.1, the structure of the silicon cell is shown.

Silicon, which is one of the most abundant element on earth's crust, is the semiconductor material used in the *first-generation* systems. Russell Ohl in 1941 observed for the first time that high purity Silicon produced a "well-defined barrier having a high degree of photovoltaic response", what nowadays is identified as p-n junction.

This technology was firstly commercialized by Hoffman Electronics and the first commercial application for the 9% efficient crystalline Si cells was on board of the 1958 NASA Vanguard I satellite [113]. Since then, a steady increase in cells efficiency lead this PV technology to be the most commercialized.

FIGURE A.1: Silicon cell structure

In 1970, the violet-cell was introduced: with an improved response to short wavelengths, it reached an efficiency of 15%. In 1974, the black-cell was designed: the front-surface reflectance of solar radiation was reduced with chemical etches on the cell's surface and the application of anti-reflection coatings. An efficiency of 17% was reached. In the following 20 years, the technology of silicon cells continued to improve with the Metal-Insulator-NP (MINP) junction (1985), followed by the Passivated Emitter Solar Cell (PESC), the Passivated Emitter and Rear Contacts (PERC) and ultimately Passivated Emitter, Rear Locally-diffused (PERL) cells, which reached 24.8% efficiency in mono-crystalline form [114]. The majority of mono-crystalline Si material is produced from polysilicon, available from the electronics industry as a waste, with the Czochralski method [115]. In alternative, the float zone [116] or the recently studied Magnetically grown Czochralski (Mcz) silicon [117] techniques are used. The two layers of Phosphorous-doped Si and Boron-doped Si have, respectively, a thickness of around 0.3 μm and 250 μm and the resulting band gap is 1.1 eV.

The crystalline silicon solar cells represents 90% of the current PV market [118].

The *second-generation* systems, thin-film solar cells, are less commercialized than the first one but their share is recently growing. Thin-film cells are made of a cheap substrate (glass, polymer or metal) that supports many successive thin solar cells layers (1-4 μm). The advantage is that they have a very lightweight and flexible structure so they represent a viable

option for building-integrated PV. They also need less semiconductor material to absorb the same amount of solar radiation therefore it may become a more economical alternative to the c-Si solar cells because of its lower capital cost, given by the low production and material costs. On the other end, the potential savings are limited by a lower efficiency.

Three types of thin-film cells can be identified [112]:

- Amorphous Silicon (a-Si and μc-Si);
- Cadmium-Telluride (CdTe);
- Copper-Indium-Selenide (CIS) and Copper-Indium-Gallium-Diselenide (CIGS).

Amorphous silicon are the most developed and known second-generation solar cells. On a large cheap substrate, the amorphous Si is deposited using continuous deposition techniques. They have efficiencies in the range of 4 to 8%. The main issue they present is the high deterioration of performance over time. A variation is the multi-junction thin-film silicon solar cell, which combines the amorphous silicon cell with additional layer of a-Si and μc-Si applied on the substrate. In this way, radiation from a broader region of wavelengths is absorbed.

The Cadmium-Telluride cell has low production cost and higher efficiency than amorphous Si. The best research-cell efficiency reached was 16.7% and no progresses occurred for a decade. In 2016, however, this plateau was surpassed by First Solar, which reached 22.1% efficiency in a cell made with commercial-scale manufacturing equipment and materials (Figure A.2). A potential risk related to this cell is the toxicity and the limited availability of the materials, since Cadmium is a by product of zinc mining and Telluride is a by-product of copper processing.

The CIS/CIGS solar cells have the advantages of a very high optical absorptivity and an impressive laboratory-efficiency of 20.8%. It is considered a promising thin-film technology.

Thin-film solar cells account for 10% of the current market [118].

The *third-generation* systems are still under study and are not ready for the market yet. Some technologies are beginning to be commercialized but there is a high uncertainty on how successful they will turn out to be. The different technologies included in this category are discussed below.

Concentrating PV systems consist of an optical device (e.g. mirrors and lenses) to concentrate the solar radiation in a small area, where a high-efficient multi-junction PV system is placed. The Concentration Factor (CF) is highly variable (2 to 1,000 suns). This technology is often coupled with a single or double-axis tracking system so the optical devices are always directed toward the sun and maximize the electricity produced. A cooling fluid is often needed because of the high temperature reached by the PV cells where the radiation is concentrated. As a positive aspect, less semiconductor material is required and high efficiencies are reached but the installation and the advanced technology, on the other hand, are more expensive.

Other emerging technologies are dye-sensitized cells [119], organic solar cells [120] and super lattice technologies [121] but they are still at a primary phase. Third-generation solar cells represent less than 1% of the solar market [118].

An overall map of the available technologies with the maximum efficiencies registered over time is presented in Figure A.2.

The solar PV industry is experiencing a steady growth. Market prices are drastically decreasing and the new-built capacity is overall increasing. Since 2003, the cumulative photovoltaic capacity grew on average at a rate of 49% per year (Figure A.3). In 2013, 37 GW of new capacity were installed, reaching a total PV capacity of over 130 GW. China experienced a considerable growth, installing 11 GW of PV (more than all European countries together). Japan and United States followed its trend and ranked respectively second and third with 7 and 4 GW.

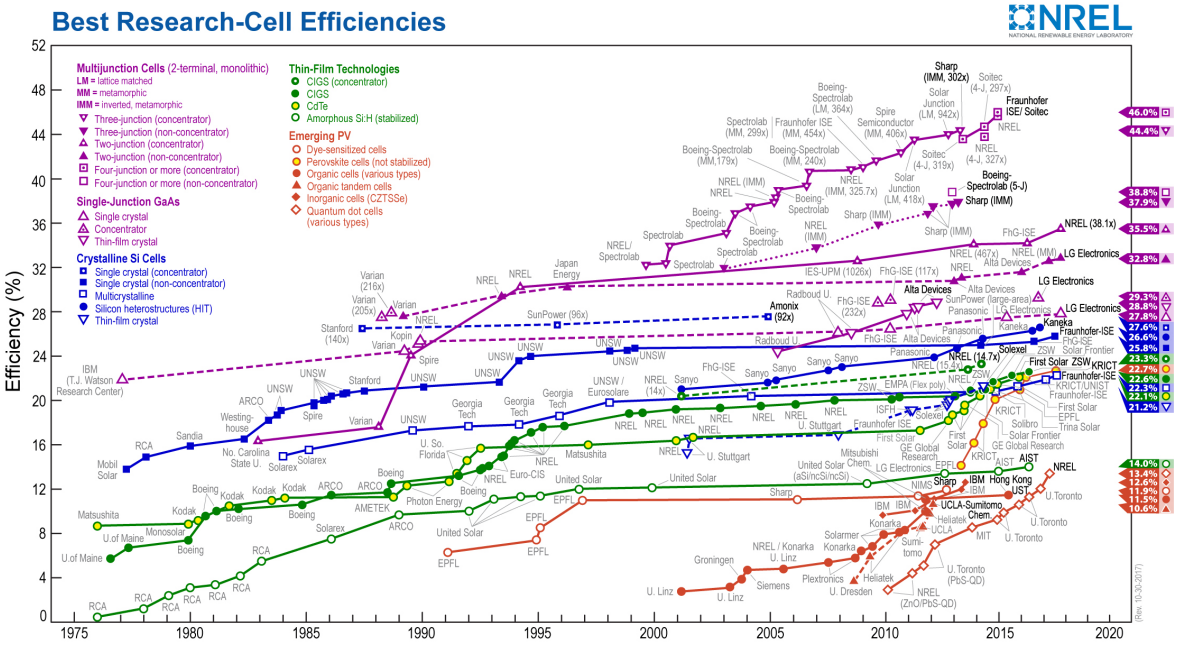

FIGURE A.2: Solar PV efficiency chart [122]

Friedman et al. [123] identify the different items of expenditure in a typical PV system and categorize them in:

- Hardware costs: module, inverter, cables and other equipments.
- Soft costs or non-hardware costs: profit and overhead, sales tax, permitting fee, interconnection cost, inspection cost, permitting preparation and submission, incentive application, electrical and mechanical installation labor, customer acquisition and system design.

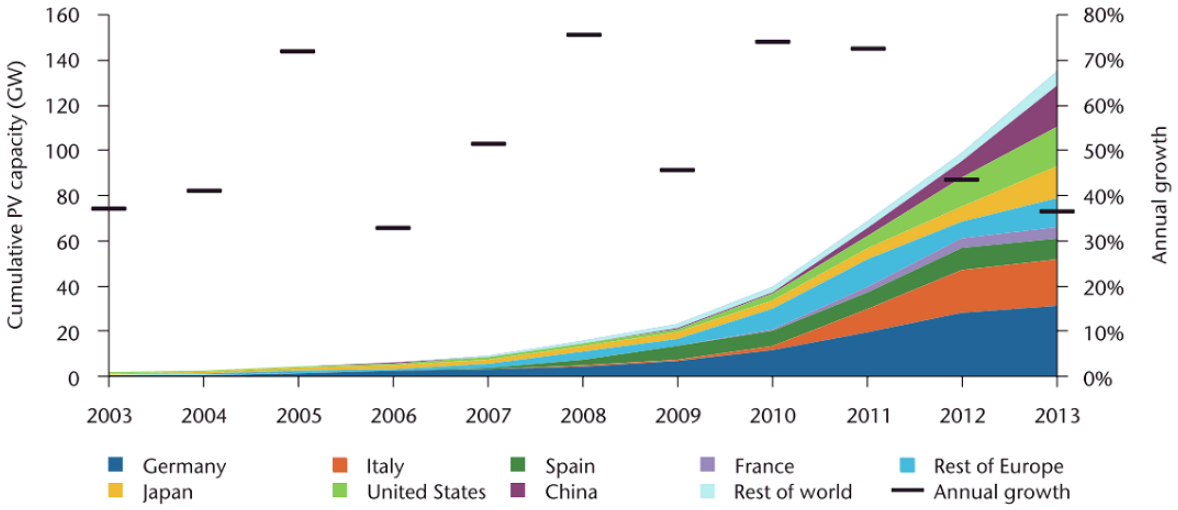

FIGURE A.3: Cumulative PV capacity and annual growth [118]

The cost of PV systems fell considerably in the last decade. As shown in Figure A.4, the cost for the production of modules is steadily decreasing due to the technical learning curve [118,124]. The cost for assembling modules to create a proper PV system, instead, registers a considerably slower decay. In order to correctly estimate the soft costs, it is required in the design phase of large PV systems to follow all the steps recommended by the International Finance Corporation IFC [125] which presents guidances for energy yield prediction, site selection, financial analysis, permits, licensing and environmental considerations. The National Renewable Energy Laboratory NREL has estimated that in 2018 soft costs for commercial application reached a peak, accounting for 56% of the total cost, while for residential and utility applications accounted respectively for 63% and 35% [126]. The decreasing trend in the price of PV panels is mainly caused by a reduction in hardware costs, as shown in Figure A.5.

Another important trend of the last decade is that the manufacturing process for modules is moving rapidly from OECD countries (Europe and United States) to non-OECD countries as China and Japan. In fact, in 2013, the cost and time for permits, incentive applications, interconnections and all the inspections were, on average, 0.01 USD/W and 0.14 h/kW in Japan, while they were respectively 0.10 USD/W and 1.21 h/kW in USA [123], making the PV production in Asia more competitive.

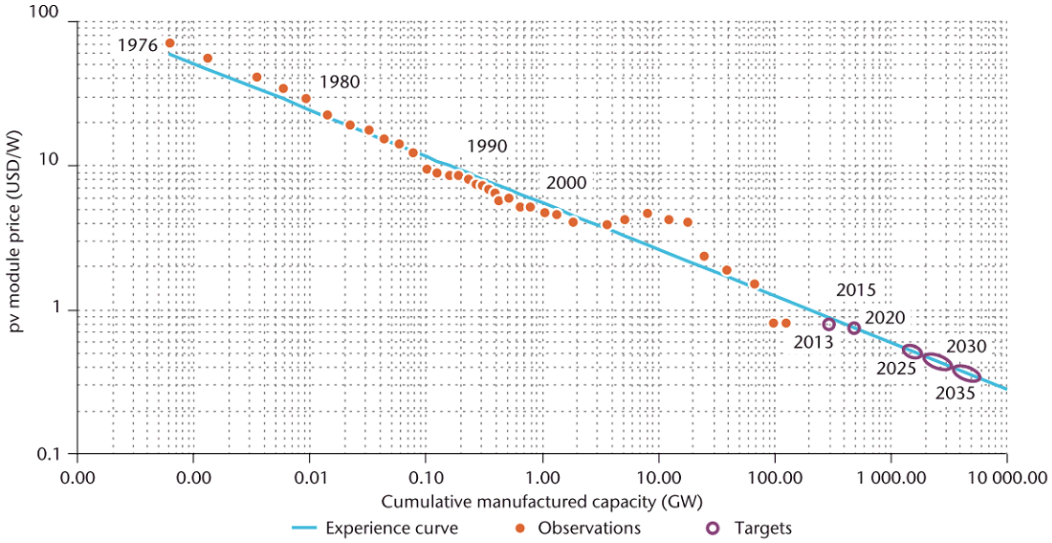

FIGURE A.4: Past module prices and projection to 2035 based on learning curve [118]

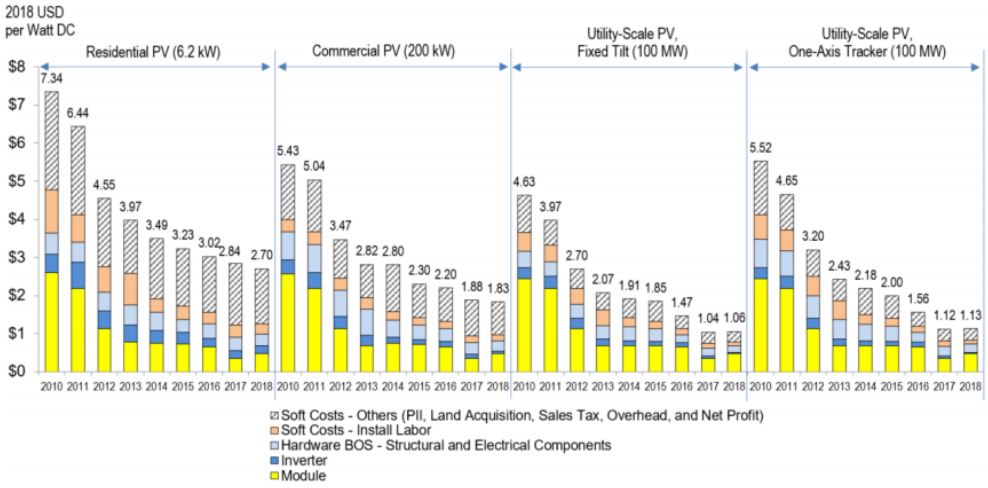

FIGURE A.5: Items of expenditure for residential, commercial and utility-scale PV systems [126]

A.2 Wind turbines

Another form of energy that derives from sun is wind energy. The earth's irradiance toward the atmosphere is not uniform, therefore, areas with different humidity and temperature are generated. In the cold areas (less radiation absorbed) the pressure of atmospheric gases is higher than the pressure in the warmer areas. Convective flows generate a macro-circulation: hot gases with a lower density go up in the atmosphere and attract cold air that flow on the earth's surface.

A mass of air that moves is defined as wind. Wind speed is influenced by the location. It is stronger on the top of high grounds and it slows down on irregular surfaces, like cities and

forests: the further from obstacles the closer to the free-stream speed. Wind speed changes in space but also in time, with a time scale of days, hours and minutes depending on the meteorological conditions.

Wind turbines produce electricity by converting wind kinetic energy in mechanical energy through blades rotation. Based on the construction technology used, they are classified as horizontal (HAWT) or vertical axis wind turbines (VAWT).

HAWTs have higher efficiency and low torque but also the gearbox and shaft at high altitudes, which introduce problems of noise and mechanical stress on the structure. Horizontal axis wind turbines with three blades represent almost 99% of the market. If the wind impacts first on the blades and then on the gearbox, the turbine is defined upwind; it is highly efficient because the shaft does not interfere with the wind, but they are not auto-aligned. If the gearbox is the first exposed to wind the turbine is called downwind and has the opposite advantages and disadvantages of an upwind turbine.

VAWTs have the gearbox on the ground, therefore less problem of noise and stress. They also have higher land exploitation, no preferential direction and low cut-in speed. Some disadvantages are the pulsating and low starting torque and the dynamic stability problems. They account for 1% of the market. They are classified in three categories: Savonius, Darrieus and Darrieus-Savonius [61].

The available energy increases as cubic function of wind speed, therefore it is important to choose an advantageous site with a high average speed. The wind blows more consistently and more smoothly at greater heights: this is the reason why wind industry tries to manufacture higher tower for wind turbines (Figure A.6).

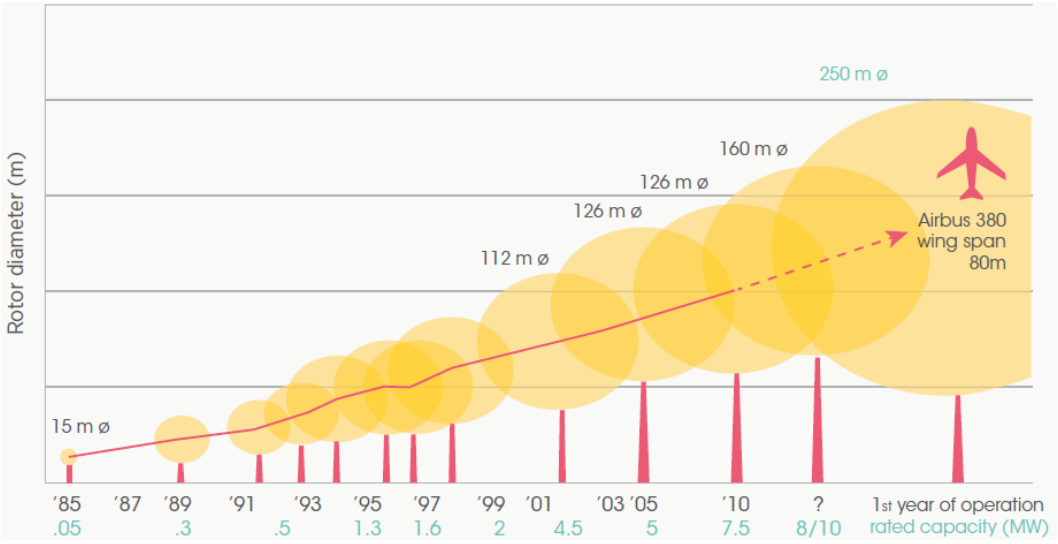

FIGURE A.6: Wind turbine diameter evolution since 1985 [127]

Wind plants can be build onshore or offshore. The capacity ranges from 0.5 to 9 MW per turbine. Wind turbines can be connected to the grid or used as stand alone systems coupled with a diesel generator.

A wind turbine is composed by different parts (Figure A.7):

- Blades: typically manufactured in fibreglass-reinforced polyester or epoxy resin. New materials as carbon fibre have recently been introduced.
- Nacelle: is the main structure of the turbine. A fibreglass structure contains the main turbine components.
- Rotor Hub: spins at a rate of 10 to 25 rounds per minute (rpm). The modern turbines have a pitch system to optimize the angle of the blades, guaranteeing a better control of rotor rpm and feathering the blades in high wind conditions to prevent damages.
- Gearbox: converts the low-speed/high-torque of the rotor in high speed/low-torque input to the generator.
- Generator: converts mechanical to electrical energy, providing three-phase alternating current.
- Controller: monitors and controls the turbine.
- Tower: the height of the tower highly depends on the site, on rotor diameter and wind speed average conditions. The higher the tower, the larger the diameter and the base.
- Transformer: is often contained in the tower. It converts the medium-voltage output from the generator to a high-voltage, based on the grid requirements.

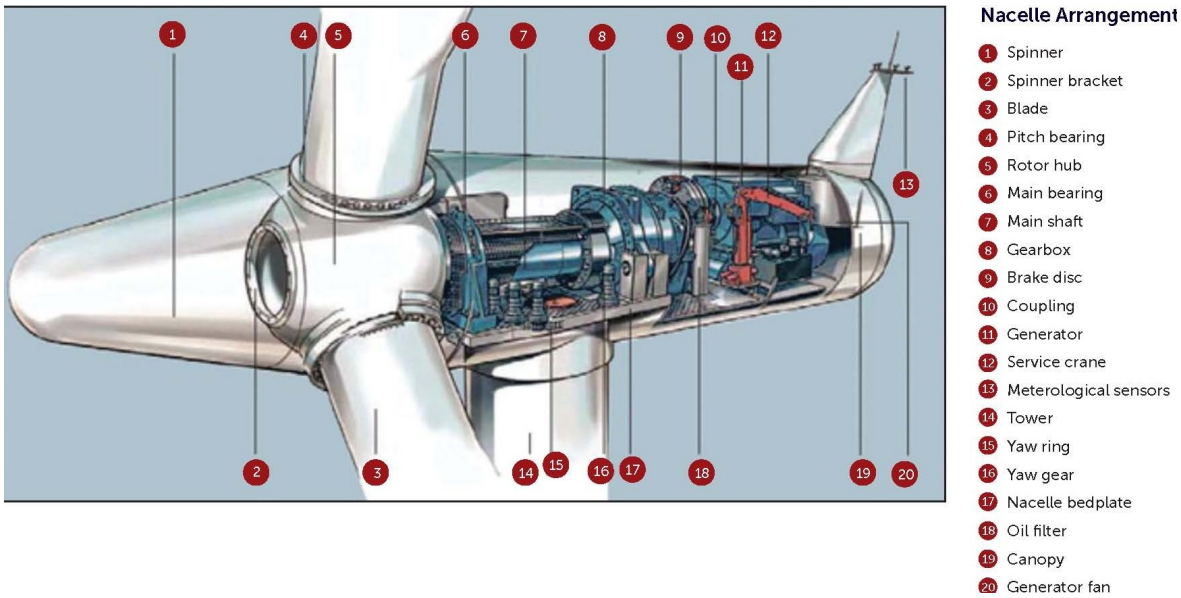

FIGURE A.7: Wind turbine components [128]

The blades, the tower and the gearbox are the most expensive components (Figure A.8). In a wind farm, the total capital cost for onshore systems is estimated to be 1,700-2,450USD/kW and the turbine cost represents 60-85% of it, while for offshore ones the total capital cost is on

average 3,350-5,000USD/kW and the wind turbine cost accounts for only 30-50%, given the high expenditures related to the grid connection and the construction of foundation, roads and infrastructures.

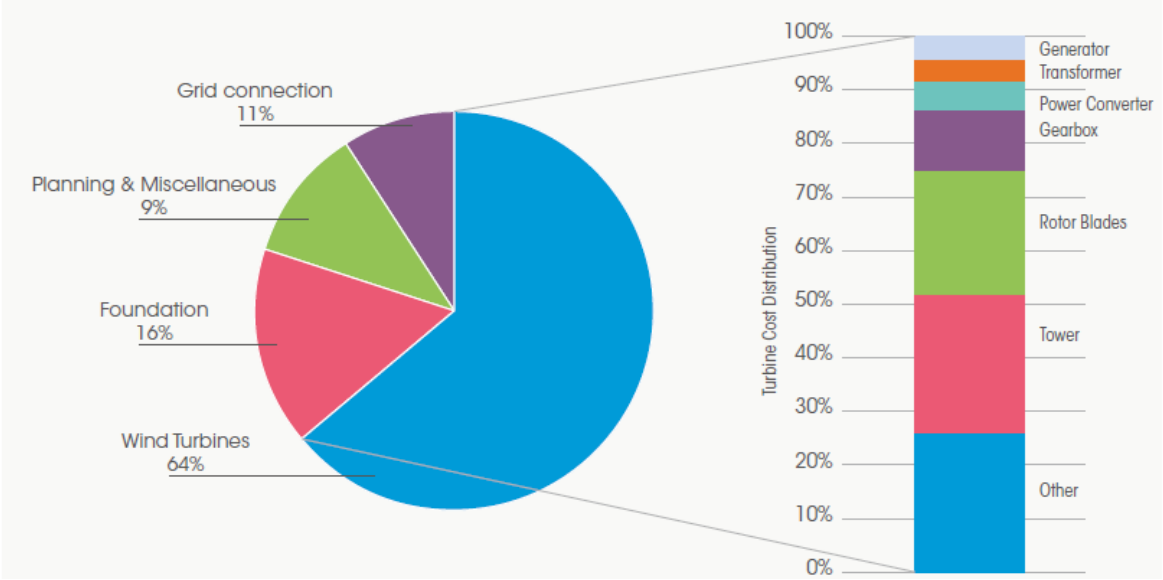

FIGURE A.8: Capital cost for a typical on-shore wind power system [127]

While the solar PV technologies saw a steady decrease in capital cost, wind turbines registered an opposite trend. Many reasons have been identified. The cost of commodities, steel and copper prices in particular, have rapidly increased over the last decades; the shift to offshore systems have also contributed to increase the average cost per new installed capacity in Europe, coupled with a more sophisticated design of the turbines. However, an important cost reduction may come from the learning curve of wind technology and from increased competition between different manufacturers, with an estimated 15% reduction by 2020 compared to 2011 level.

Operation and Maintenance (O&M) costs have declined substantially since 1980; current data are not widely available and can not be easily extrapolated from historical costs because of the drastic changes in wind technologies.

In 2015 more than 63GW of new wind capacity have been installed, mostly by non-OECD countries, reaching a total wind capacity of 433GW (Figure A.9). Wind is the leading source of new power generating capacity in Europe and USA and the second one in China and it is playing a major role in meeting the 2020 targets. The countries with the highest wind power capacity per inhabitant are Denmark, Sweden, Germany, Ireland and Spain. A detailed report about wind energy in every IEA country is presented in the IEA wind report [129].

The global penetration of wind reached a total share of around 4%. Technological developments and institutional policies are leading to higher penetration levels. However, it is difficult to predict exactly how the energy mix will look like in 2050 because of many possible unexpected events.

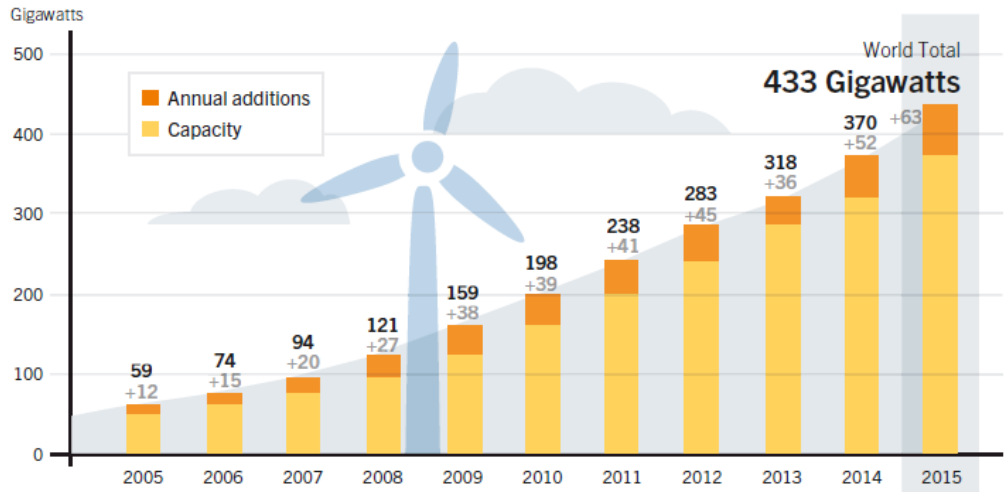

FIGURE A.9: Wind power global capacity and annual additions [130]

It is a good policy to propose and evaluate different scenarios. The World Wind Energy Association [131] estimates 40% to be a reasonable level of penetration for wind technology in 2050. It is linked to the forecast worldwide electricity demand, that is estimated to vary between 40×10^3TWh per year in the low scenario and 74×10^3TWh per year in the high scenario.

A.3 Cogeneration system: Gas turbine and Heat Recovery Steam Generator

A cogeneration system, also called Combined Heat and Power (CHP), uses a fuel as input to produce both electric and thermal energy. In a CHP system a fuel, for example natural gas, is used to generate electricity and the low grade waste heat from this conversion process is utilized as heating source. The energy generated is close to the location where it is needed, reducing transmission and distribution losses [136]. In IEA countries in 2015, for 2,056Mtoe of primary energy flowing in power plants 1,095Mtoe (64%) resulted in power losses, which include rejected heat [137]: using CHP systems, that simultaneously co-generate useful heat and power from a single fuel or energy source, could significantly improve the thermal efficiency and reduce conversion losses.

While there are many studies in the literature [9–11] on how the power and heating sector could interact to provide the flexibility needed with higher VRE penetration, they are mainly focus on heat pumps, suitable only for low temperature and low flow rate steam requirements. Kosmadakis [13] discusses the limited range of alternative solutions available at the moment for decarbonizing the heating consumption of industrial facilities with high temperature and high flow rate steam requirements. For this application, CHP has been proved to be a viable option and therefore has been considered in this thesis for on-site energy generation in manufacturing facilities. The almost flat electricity and heat demand profile of manufacturing

facilities represents an ideal case for the production of heat and electricity combined instead of purchasing electricity from the grid and generating heat through a traditional boiler. In fact, while the thermal efficiency of electricity generation for a centralized combined cycle gas turbine (CCGT) would be higher, requiring less fuel to produce the same electricity, the overall carbon intensity of the process is lower in a CHP system since the waste heat is reused for a useful purpose, reducing the total amount of CO_2 emitted for the same thermal and electric energy produced [138]. A CHP system has also the benefit of producing both electricity that can be used immediately, partially avoiding interactions with the grid, and heat that can be used locally, avoiding the necessity for distribution [100].

A CHP system is composed of two technologies, one for electricity generation and the other for heat recovery. The first sub-system has one input, fuel or energy source, and two outputs, electricity and waste heat. The latter is the input of the second sub-system which uses waste heat as a fuel source for producing useful thermal energy. The integration of these two sub-systems converts up to 80% of the fuel source into useful energy, reducing the energy-related CO_2 emissions (Figure A.10). The official definitions of CHP and cogeneration efficiency are given by the European Union Directive [139] and a complete training guide on combined heat and power systems is presented by the European Commission [140].

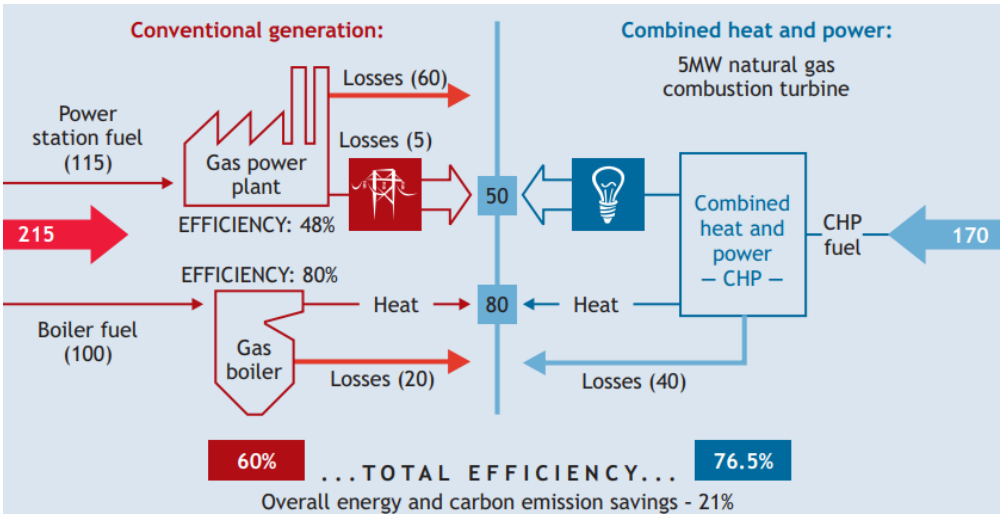

FIGURE A.10: Efficiency gains of a Combined Heat and Power system [141]

CHP does not need economic incentives to be a viable choice for power generation, however, targeted policies are still needed to address barriers that prevent it from reaching its full worldwide potential [136], as: economic and market issues (securing fair price for electricity produced by CHP systems and exported to the grid); regulatory issues (interconnection procedures); and social/political issues (lack of public awareness of CHP benefits).

CHP applications range from residential (micro-cogeneration) to industrial systems (1-500MW) up to District Heating and Cooling DHC (distribution of heat generated in a centralized location for residential and commercial heating requirements). Its main advantages are the reduction in emissions compared to two separate plants and less power losses in the

transmission and distribution network. It is also a viable option for re-powering old inefficient plants [142].

In Ireland, the total installed capacity of CHP in 2018 reached 354MW$_{el}$, 93.5% fuelled by natural gas, with a total of 438 units. Most units are installed in the service sector (hotels account for the majority), while the highest share of installed capacity is registered in the industrial sector (Table A.1).

	Units		Operational Capacity	
	No.	[%]	[MW$_e$]	[%]
Services	**262**	**83.2**	**39**	**12.3**
Hotel	67	25.6	8.7	22.4
Leisure	46	17.6	3.6	9.2
District Heating	34	13	0.2	0.5
Industry	**53**	**16.8**	**280**	**87.7**
Food	26	49.1	76.7	27.4
Manufacturing	6	11.3	10.6	3.8
Pharmaceutical	14	26.4	24.7	8.8

TABLE A.1: Number of cogeneration units and operational capacity per sector in Ireland [143]

The overall efficiency of CHP installations has increased from 76% in 2001 up to 83% in 2018. By using combined heat and power generation instead of separate electricity and heat production, the emission of 438kton of CO_2 has been avoided in 2018 (Figure A.11). This technology is proven to be mature, reliable and also economically compatible with the requirement of the manufacturing industry (PBT strictly less than 10 years). The Association for Decentralized Energy published a report [144] describing the installation of a CHP plant in the manufacturing facility of Bausch + Lomb in Ireland. The plant supplies 72% of the electric and 91% of the thermal load of the facility which operates 24/7/365. It led to an annual operational cost saving of 1M€ and an annual CO_2 saving of 6.75kton. The estimated PBT is 3.4 years. Another successful example of CHP in the manufacturing industry is reported by Boston Scientific [145], which uses high-efficiency CHP power plants in its manufacturing sites located in Clonmel, Cork and Galway, Ireland.

There are many technologies that can be used as CHP systems. The most common solution, widely used in the industrial sector, is to couple a thermal power plant for electricity production to a Heat Recovery Steam Generator (HRSG) for wasted heat recovery and steam production. In a thermal power plant, the chemical energy contained in the primary energy sources such as fossil fuels is converted in thermal and then mechanical energy by a traditional power plant and finally in electrical energy through a generator. A detailed study of different power generation technologies, the underlying thermodynamic principles and their application is presented by Kiameh [146] and a detailed comparison of the combined-cycle plant with different thermal power stations on the basis of different parameters is described by Kehlhofer [147].

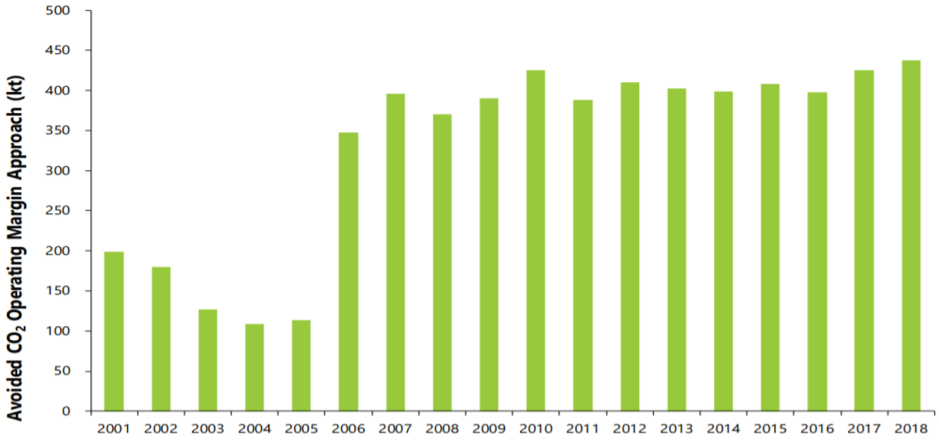

FIGURE A.11: CO_2 avoided with cogeneration systems [143]

The selected power generation technology for CHP is a gas turbine, which has the highest flexibility and the lowest maintenance and capital cost of any major prime mover [148]. While the electricity demand of the facility would suggest a cogeneration system based on a gas engine (typically used for electric power generation lower than 4MW), its application is more suitable for low pressure and low flow rate steam requirements. The manufacturing facility analysed requires high flow rates of steam at high temperature, therefore a gas turbine has been considered. Although the most common application for industrial gas turbine is for electric power generation higher than 4MW, this does not represent a technical limitation. There is, in fact, a niche market for smaller gas turbines that provide high temperature and high flow rate steam.

The gas turbine technology saw a large growth in the last 20 years. New coating materials, new cooling scheme for the turbine's first stage, a higher Pressure Ratio (PR) in the compressor and the implemented European strategies [149] have led to an increase in thermal efficiency up to 45%.

A gas turbine system is based on the Brayton cycle and is mainly composed of a compressor, a combustor and a gas turbine. A generic 3D representation and an operational scheme of a gas turbine system for industrial applications are shown in Figure A.12 and A.13.

The air, at ambient temperature and pressure, flows first into the *compressor*, which is a device that pressurizes the working fluid.

The function of the *combustion chamber* is to increase the temperature of the working fluid through the chemical energy contained in the fossil fuel that is burned. A small percentage of air flows in the combustor (10%) while most of it bypasses the combustor and is used for cooling and mixing purposes. The resulting combustion products are mixed with cooler air to achieve a suitable turbine inlet temperature. This mixture is called exhaust or flue gases. The air that enters in the combustor flows in three main regions (Figure A.14): the *primary zone*, where the combustion takes place, the *dilution zone* and the *annular space* between the liner and the casing. More details about this component are presented by Boyce [148] and Lozza [152].

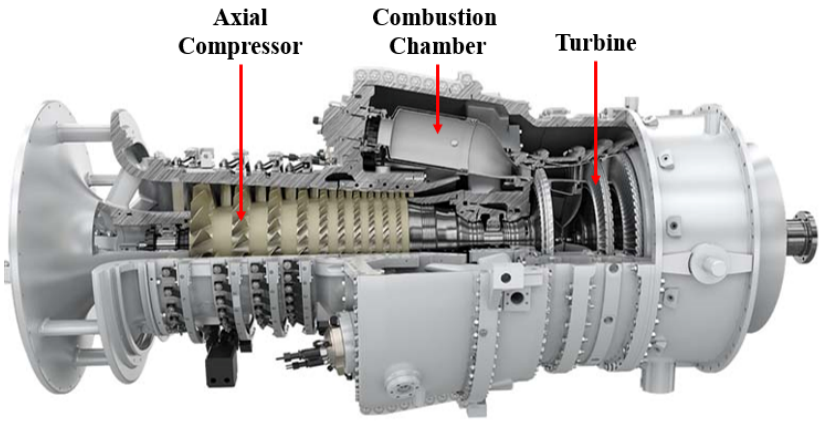

FIGURE A.12: Gas turbine system [150]. Copyright www.siemens.com/press for the gas turbine image used for graphical purpose only

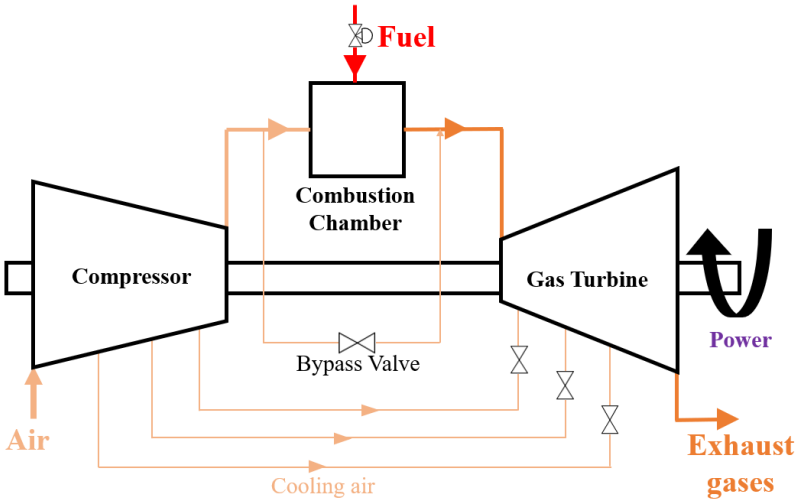

FIGURE A.13: Gas turbine operational scheme

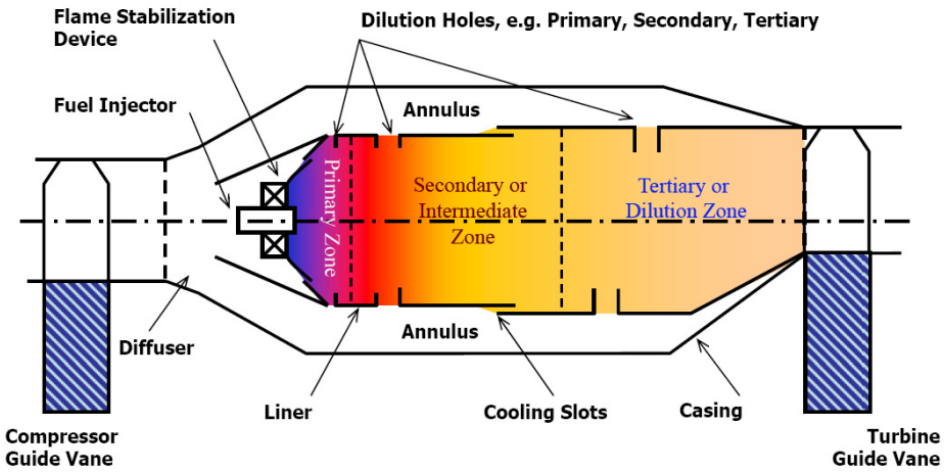

FIGURE A.14: Layout of a typical combustion chamber [153]

When the exhaust gases leave the combustion chamber, they enter into the *turbine*. Gas turbine systems use axial-flow turbines in 95% of all the applications; the other technology available, less common, is the radial-inflow turbine.

In this component, the mechanical power is obtained by the exhaust pressure drop.

The energy content of the exhaust gases going out from the turbine is still high since their temperature is around 500°C. The objective of a Heat Recovery Steam Generator (HRSG) is to convert this thermal energy content in useful energy. A HRSG is basically a heat exchanger that produces steam from water by using the thermal energy of exhaust gases. Then the steam can be either used as it is if needed in the facility, like in the case of this study, or sent in a steam turbine to produce more electrical power. The Heat Recovery Steam Generator is composed by an economizer (ECO), an evaporator associated with a drum boiler (EVA) and, depending on the application, also by a superheater (SH). A generic scheme of the heat exchanger and of the overall plant is displayed in Figure A.15.

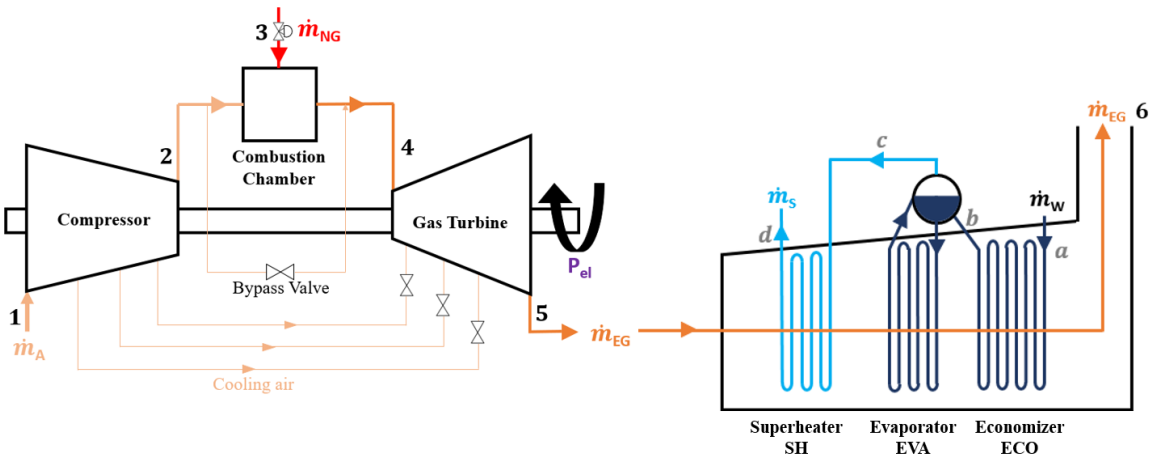

FIGURE A.15: Gas turbine system followed by a Heat Recovery Steam Generator

The economizer preheats the feed water that then goes in the drum. It is located at the end of the HRSG, where the flue gases have lower temperature. The evaporator receives saturated water from the economizer and produces saturated steam in the drum. The drum is, in fact, the connection point between these three main heat exchangers; it acts both as storage tank to balance the water and steam flows and as separator for the steam-water mixture. If the required steam temperature is higher than the saturated temperature, the saturated steam flows in the superheater. This heat exchanger is located at the beginning of the HRSG since it needs to exchange heat with the exhaust gases at their highest temperatures.

For small applications, one water-steam cycle is enough but for bigger systems it may be required to use more cycles at different pressure levels. A HRSG can be designed based on natural circulation or forced circulation [154], depending on the needed layout (vertical or horizontal).

The overall cogeneration system can be design to be driven by the thermal or the electric energy demand. Based on the chosen driver, a control strategy can be implemented. A detailed review and explanation of process control and optimization is presented by Liptak [155] and Aurora et al. [156]. If the energy demand profile is almost constant over time, the gas turbine and HRSG work at constant load. If, instead, the energy vectors' demand varies significantly over time, the control system regulates the load. While the regulation occurs instantaneously, the output of the system changes with a certain inertia until it reaches the new steady state. In this situation, the gas turbine is very flexible and reacts to a load change with a transient period of the order of minutes; the HRSG, instead, is the bottleneck of the system because of its thermal inertia. When the net energy demand is highly variable, the number of transient operations of the cogeneration system may increase, therefore a dynamic simulation of the system may be required to estimate the electricity and thermal energy produced over time. After a detailed analysis of different dynamic simulation methods [157–163] and a statistical study of the variation in the demand profiles of electricity and steam, it is concluded that for the present investigation a static approach is sufficient, since the time-step considered to be significant for demand's variation is one hour, which is enough time for the system to reach a new steady state after a transient operation.

Appendix B

On-site energy storage

B.1 Energy Storage System

The on-site energy system discussed in Chapter 6 has shown a significant reduction of the demand for grid electricity but it also causes high fluctuations in the net demand, substituting an almost constant electric load (Figure B.1-a) with a highly variable one (Figure B.1-b). As shown in Table 6.7, the flexible operation of the 1,600kW$_{el}$ gas turbine in electricity following control strategy gives the highest reduction of the average net demand variability but the positive effects are limited compared to the base case with no on-site energy generation.

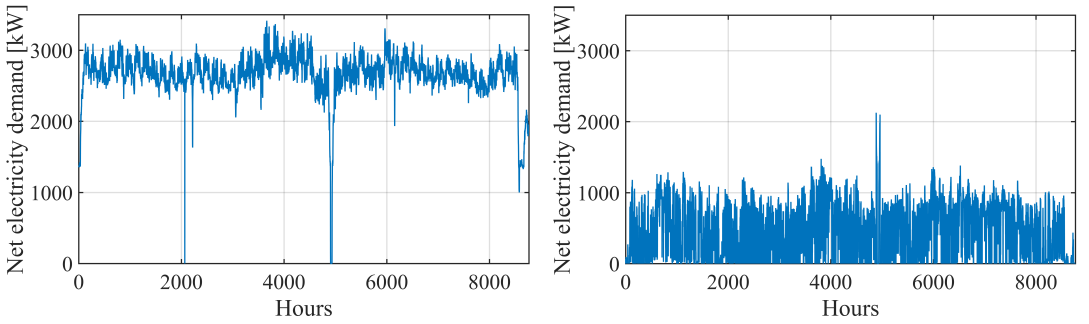

(a) No on-site generation

(b) With on-site generation: PV, wind and 1,600kW$_{el}$ gas turbine in electricity following control strategy

FIGURE B.1: Net demand for grid electricity without and with the on-site generation system

For the electric grid a sudden change from a constant and easily predictable demand profile to a highly variable one may represent a complication in the management of the grid balance, especially if a growing number of manufacturing facilities located in close geographical areas would adopt on-site generation systems.

The potential benefit of installing an on-site storage system to reduce the high variability of the residual electric load that the grid has to cover has been evaluated.

B.1.1 Available technologies

With the increasing penetration of Variable Renewable Energy (VRE) in the electric grid, managing the high variability and intermittency of renewable sources has become extremely important. Energy Storage Systems (ESSs) are considered an effective tool to strengthen the grid flexibility, supporting the penetration of more variable renewable power.

Storage systems in the past decades were used to decouple energy production from the supply typically over the day: by having a large-scale electricity storage, utility generation plants could be dimensioned on the average demand rather than the peak and operate at full capacity (close to the most efficient operational point) leaving to the storage system the final balance of the electricity demand and supply curve [164]. Recent development and advances in ESS have made energy storage technologies a viable solution to compensate the high variability and the supply intermittency introduced in the electric grid by VRE and enhance the flexibility of the electric system. As the penetration of VRE increases, the need for flexible capacity and for decoupling electricity generation and supply will grow to guarantee the balance of the grid and reduce energy curtailment.

ESSs can be classified by different criteria. Chen et al. [164] categorize ESSs based on their function and based on the form of energy stored.

A simplified classification based on functionality is:

- Storage technologies for power quality and reliability. They are primarily intended for high power ratings and include capacitors/supercapacitors, Superconducting Magnetic Energy Storage (SMES), flywheels and batteries.
- Storage technologies for energy management. They include Pumped Hydroelectric Storage (PHS), Compressed Air Energy Storage System (CAES), Thermal Energy Storage (TES), fuel cells and batteries.

Another classification can be made based on the form in which energy is stored:

- Electrical energy storage: capacitors and supercapacitors (electrostatic energy); SMES (magnetic energy).
- Mechanical energy storage: flywheels (kinetic energy); PHS and CAES [1] (potential energy).
- Chemical energy storage: conventional batteries (such as lead-acid and lithium ion); fuel cells (chemical energy); solar hydrogen, solar ammonia dissociation–recombination and solar methane dissociation–recombination storage (thermochemical energy).
- Thermal energy storage: aquiferous cold energy storage, cryogenic energy storage (low temperature energy); sensible heat systems such as steam or hot water accumulators, latent heat systems such as phase change materials (high temperature energy).

[1] It is specified that CAES could also be classified as a thermal energy storage system given the relevant thermal component involved (Adiabatic-CAES)

Zhao et al. [165] summarize for the main ESS technologies various important parameters such as capital cost, ramp rate, efficiency, response time, life and cycle time. A brief description of the characteristics and applications of the most used ESS technologies is presented.

- Pumped Hydro Storage (PHS). PHS exploits the potential energy content of a large body of water at a relatively high elevation. The water is pumped from a lower to a upper reservoir during off-peak hours. When electricity is needed, the water is discharged and its potential energy is converted first in kinetic and then in electric energy through hydro turbines connected to generators. PHS is a well established technology with high technical maturity: it has a power rating range from 100 to 5,000MW, a typical discharge time of the order of hours to days and a response time of the order of minutes; the round-trip efficiency can reach 80% and the lifetime is very long, higher than 50 years (or more than 15,000 cycles). The main disadvantaged of PHS are the geographical restrictions, low energy density (large footprint), high initial investment costs and long construction period. PHS is the largest and most mature energy storage technology, accounting for 99% of the globally installed power rating with over 150GW [166].

- Compressed Air Energy Storage (CAES). CAES stores energy in the form of compressed air. When excess electricity is available electrical motors drive air compressors and store compressed air in underground systems or systems of vessels and pipes. When electricity is needed, the compressed air is mixed with natural gas and burned, then the exhaust gases flow is expanded in a gas turbine to generate electricity. The power rating range is from 5 to 300MW with a typical discharge time of the order of hours to days, a response time of the order of minutes and a lifetime of 25 years (or 10,000 cycles). The round-trip efficiency is variable (41%-75%) and depends on how the compressed air is stored and then used, for example Adiabatic Compressed Air Energy Storage A-CAES can reach high efficiency of 70%. CAES is a technology in use since the 19th century and the installed power rating is currently 0.6GW, however many projects are under development globally for installing new CAES plants [166].

- Flywheel Energy Storage (FES). FES allows the storage of rotational energy in an accelerated rotor, and when needed is discharged by the flywheel that drives the machine as a generator. The power rating range is from 0 to 0.25MW with a typical discharge time of the order of seconds to hours and a response time of the order of seconds; the efficiency is very high (80%-90%) and the lifetime is excellent, around 15-20 years or up to 1 million cycles. This technology is mainly applied as a power quality device for its excellent cycle stability, long life with full charge-discharge cycles, little maintenance cost and high efficiency. The main drawbacks are the high self-discharge losses and low energy density. First generation flywheels have been in use since 1970; today more advanced systems are under implementations with new materials that allow higher energy densities and superconductive bearings for reducing friction losses.

- Battery Energy Storage System (BESS). BESS stores electricity in the form of chemical energy. Every cell that composes a battery is made of an electrolyte together with anode and cathode. When a potential is applied to both the electrodes, an internal chemical reaction occurs which charges the battery. When energy is needed the reaction is reversed. There are many different types of batteries, such as Lead acid (LA), Nickel Cadmium (NiCd), Nickel Metal Hydride (NiMH), Lithium-ion (Li-ion) and Sodium Sulphur (NaS) batteries. They have very rapid response time (less than a second) and can track load changes, which makes them particularly suitable for system stability. They have low self-discharge loss and high efficiency. BESS is a modular technology (high power and energy density), with a lifetime strongly dependent on the number of cycles and cycle depth. Certain batteries contain toxic materials (such as Lithium and Cadmium) that represent a problem for final disposal [167].

  LA batteries are the most widely used batteries, commercially available since 1890. They are suitable for both mobile and stationary applications for emergency power supply, stand-alone systems, fluctuations mitigation of output power in presence of VRE systems. They have a good cost-performance ratio, a relatively low energy density, a high round-trip efficiency (up to 90%). However, the usable capacity decreases when high power is discharged.

  Li-ion batteries are the most used storage technology for mobile and portable applications. They have a very high round-trip efficiency (98%), high energy density and a wide discharge time range (from second to weeks), which make them a very flexible and universal technology. They have a relatively long lifetime and low self-discharge rate. However, they have the highest capital cost.

- Superconducting Magnetic Energy Storage (SMES). SMES consists of a superconductive coil where DC current circulates, creating a magnetic field where the required energy is stored. This technology is characterized by a short response time ($<$ sec) and it is suitable for load levelling and power stabilization. The main drawback is the sensitivity of the superconductive coil to changes in temperature, which requires a refrigeration system and a large amount of power to keep the coil at low temperatures. SMES are nowadays present in the market only in small applications.

- Super-Capacitor (SC). SCs are composed by two solid conductors with an electrolyte solution in between. SC batteries have large power density which makes them suitable for power quality (fast response) applications, they are characterized by fast charging and discharging due to low inner resistance, high reliability and a long lifetime. They are environmentally friendly (easily recycled) and highly efficient (90%) with a discharge time ranging from seconds to hours. The main drawbacks are the low energy density, the low voltage of individual cells (higher voltages require serial connections) and high self-discharge rate compared to electrochemical batteries.

A through analysis on Electrical Energy Storage is presented by the International Electrotechnical Commission IEC [168], and a review is presented by Aneke and Wang [169], and by Guney and Tepe [170]. An overview of the different power ratings and discharge time for different ESSs is displayed in Figure B.2 and their maturity status is shown in Figure B.3.

There are many studies in the literature that either investigate the potential and need for storage technologies with the progressive increase of VRE or analyse Energy Storage Systems used by medium/large industrial consumers in presence of a VRE systems. However they are either studies conducted on an aggregate level [171–177] or focused on the overall optimization of integrated energy systems [178–183]. The aim of the analysis conducted here is not to optimize the on-site generation system but to investigate if any significant reduction in the net demand variability can be achieved by installing a storage system.

It has been shown that there are many technologies available for energy storage, each with different advantages and disadvantages. The technology investigated for this application is Li-ion battery storage, which is the most used storage technology for mobile and portable applications. It is a modular technology with a discharge time ranging from seconds to weeks, an efficiency of the order of 95% and a low self discharge rate per day. Its lifetime is highly dependent on the number of cycles and on the cycle depth and typically ranges between 1,000 and 10,000 cycles [168, 170].

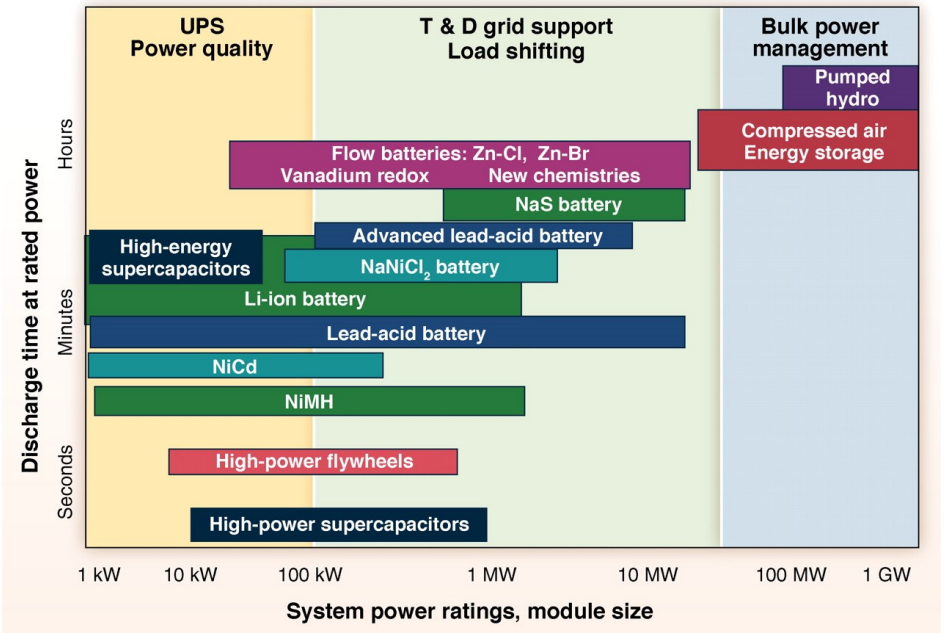

FIGURE B.2: Power ratings and discharge time for different storage technologies [184]. UPS: uninterruptable power supply; T&D: Transmission and Distribution

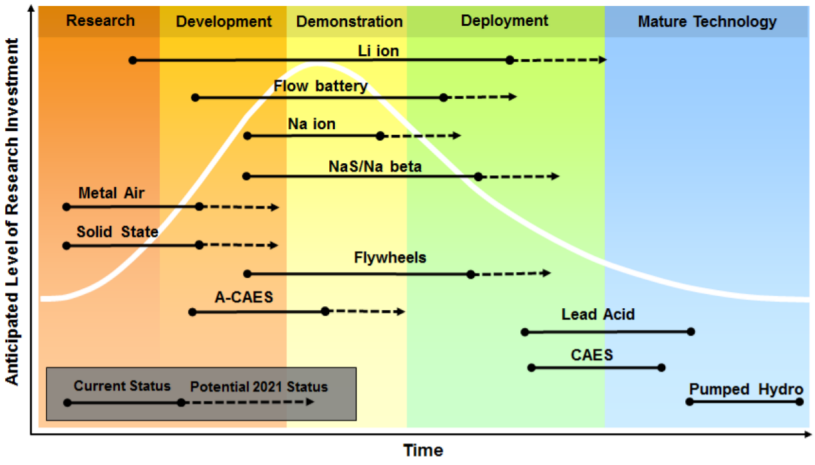

FIGURE B.3: Maturity status of different storage technologies [184]

B.2 Effects of battery storage on the variability of the residual load for the electric grid

The analysis conducted considers the on-site cogeneration system composed of the PV and wind system, the 1,600kW$_{el}$ gas turbine, the Heat Recovery Steam Generator and the secondary boiler. The gas turbine is run in the electricity following control strategy since it is the configuration that showed the highest reduction of net demand variability (Table 6.7 and 6.8). While the on-site energy cogeneration system has been simulated through the implemented Matlab model described in Chapter 5 and 6 of this thesis, the lifetime simulation of the battery system performances has been conducted with the tool SAM (System Advisory Model) [88], which provides complete and accurate models for simulating battery storage systems. Different sizes have been investigated. The bank capacity ranges from 1,000kWh to 10,000kWh, with a corresponding battery bank power between 200kW and 1,000kW. The depth of discharge, the number of cycles performed and the progressive capacity degradation of the different battery banks are simulated; if the resulting lifetime of the storage system is shorter than 25 years a replacement is scheduled when the battery is not able to provide more than 80% of its original capacity. The main parameters are briefly summarized in Table B.1. All the other parameters are set automatically by the SAM software [185].

A parametric simulation has been run for all the different battery bank sizes. As explained in section 6.2.4 of this thesis, the variability of the net demand is assessed by calculating the standard deviation of the net electric load provided by the grid over a five-hour window spanning two hours before and after every hour of the year (eq. 6.9) [110]. The indicator used for evaluating comparatively the benefits of different battery bank sizes is the mean of the net demand variability normalized to a base case $\bar{\sigma}_h^*$ (eq. 6.12). The benefits of introducing a battery bank are evaluated in comparison to a base case, which is defined in this analysis as the on-site cogeneration system with the best performance for variability reduction (PV, wind, 1,600kW$_{el}$ GT in electricity following control strategy and no ESS).

Parameters	
Battery type	Lithium Ion
Bank capacity [kWh]	1,000 - 10,000
Bank power [kW]	200 - 2,000
Dispatch model	Peak shaving
Minimum state of charge	15%
Maximum state of charge	95%
Price for electricity [€/kWh]	0.096

TABLE B.1: Main parameters of the battery systems simulated in SAM

The comparison of the normalized mean $\bar{\sigma}_h^*$ is displayed in Figure B.4 for the different battery bank sizes. Higher values of $\bar{\sigma}_h^*$ indicate that the net electric demand that the grid has to supply has more rapid and higher fluctuations; lower values indicate a net electric demand that, on average, changes less rapidly during the year. With bigger battery banks a smaller variability $\bar{\sigma}_h^*$ is registered.

This indicator is presented in the form of normalized values to compare the different analysed cases and draw qualitative conclusions rather than creating a metric for quantifying the variability of the net electric load. A deeper discussion on the chosen time window and on the indicator to evaluate the variability is presented in Appendix B.2.1.

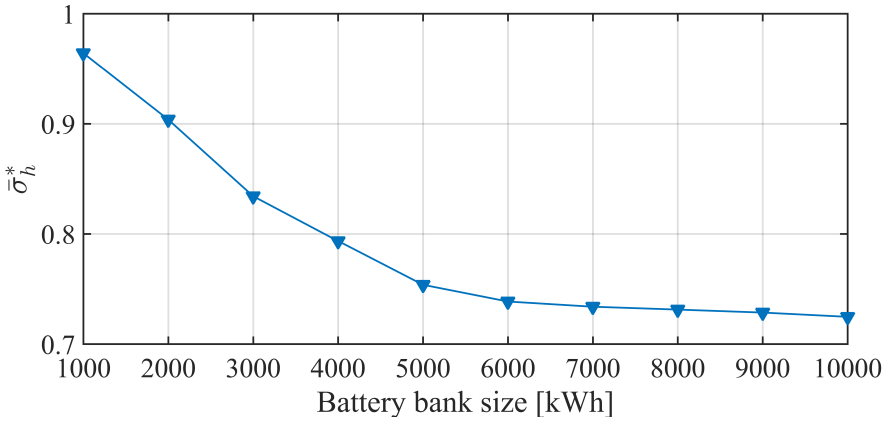

FIGURE B.4: $\bar{\sigma}_h^*$ normalized to the base case (PV, wind, 1,600kW$_{el}$ GT in electricity following control strategy, no ESS) for the different battery bank sizes

It is interesting to analyse, alongside $\bar{\sigma}_h^*$, the Cumulative Distribution Function CDF of the variability ${\sigma_h}^*$, normalized to a reference value $\sigma_{h_{ref}}$ (eq. B.1), for different battery bank sizes and for the base case (Figure B.5).

The normalized variability ${\sigma_h}^*$ is defined as:

$$ {\sigma_h}^* = \frac{\sigma_h}{\sigma_{h_{ref}}} \tag{B.1} $$

where $\sigma_{h_{ref}}$ is a reference value of maximum variability σ_h that is never exceeded with any of the battery bank sizes.

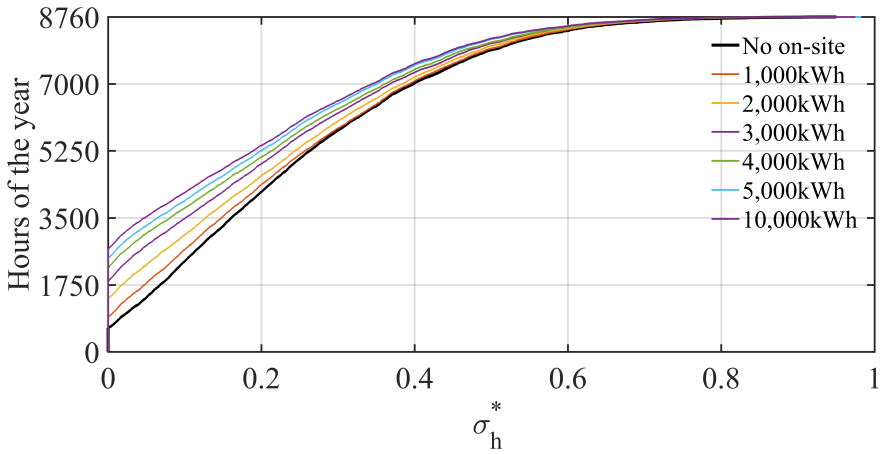

FIGURE B.5: Cumulative Distribution Function (CDF) of ${\sigma_h}^*$ for the different battery bank sizes

Overall, by increasing the battery bank size a null variability of the net demand is registered more often during the year (${\sigma_h}^* = 0$) and a reduction in the mean and maximum variability of the net load occurs; however, high peaks in the variability are still registered even with the biggest battery bank. The mean of the net demand variability $\bar{\sigma}^*_h$ steadily decreases with the battery bank size but no significant reduction is seen after the 5,000kWh battery bank. This is confirmed by the analysis of ${\sigma_h}^*$, where only a small difference is registered in the CDF of the 5,000kWh and 10,000kWh battery banks. Hence, the additional cost of options bigger than 5,000kWh would not be justified, as shown by the progressive increase of the Pay Back Time (PBT) of the battery system, due to higher investment costs and limited additional savings (Table B.2).

Bank size [kWh] – power [kW]	$\bar{\sigma}^*_h$	PBT of battery system [years]
Base case	1	-
1,000 – 200	0.96	1.3
2,000 – 400	0.9	2.4
3,000 – 600	0.83	3.4
4,000 – 800	0.79	4.4
5,000 – 1,000	0.75	5.3
10,000 – 2,000	0.72	10.3

TABLE B.2: Mean of the net demand variability $\bar{\sigma}^*_h$ normalized to the base case (PV, wind, 1,600kW$_{el}$ GT in electricity following control strategy, no ESS) and PBT for the different bank sizes

A trade-off is seen between the PBT and the reduction in the net demand variability, which influence the choice of the size of the on-site battery system.

Since the battery bank with 5,000kWh capacity and 1,000kW power has shown good performances in terms of reduction of the mean variability of the net demand and has a PBT acceptable for a manufacturing facility, a more detailed analysis is presented.

The battery bank with a power of 1,000kW and a capacity of 5,000kWh shows a reduction

in the normalized mean variability of 25% compared to the on-site cogeneration system with no ESS (Table B.2). It has been investigated whether better results may be achieved with different control strategies.

It is possible to change the control logic of the battery bank, from day-ahead peak shaving to a target of maximum power from the grid. No improvement is seen by switching control logic: the normalized mean variability of the net demand $\bar{\sigma}_h^*$ is higher (0.88) and the reduction in the variability compared to the base case is limited to 12%.

Another option would be to impose that the battery bank charge only from the overproduction of the on-site generation system. This option yields worst results: $\bar{\sigma}_h^*$ increases to 0.95 with a reduction compared to the base case of only 5%. The manufacturing facility, in fact, registers overproduction for only a limited number of hours during the year (20% of the year with an average electricity overproduced of 148kWh per hour). In order to make this option viable, the gas turbine should run at full load at all times to maximize the overproduction of electricity that can be used to charge the battery bank. This solution is not sustainable given the amount of extra steam that would be produced and that would go to waste.

To limit steam overproduction, the gas turbine could be run in steam following control strategy. This option presents a very high variability of the net electric demand, increasing $\bar{\sigma}_h^*$ to 1.3, compared to 0.75 of the electricity following case.

It has been shown that introducing on-site generation causes the electricity demand typical of manufacturing facilities, almost constant during the year and therefore predictable for the grid, to become highly volatile. The introduction of a flexible technology such as a gas turbine for on-site cogeneration slightly improves the variability of the net demand, but to reach a considerable reduction the system should be significantly oversized: this would entail higher investment costs and a lower thermal efficiency of the gas turbine working more often at partial loads (below the maximum efficiency load). The inclusion of a battery system contributes to a further reduction of the variability but also in this case significant fluctuations occur during the year.

Even with the biggest battery system, the facility retains the role of net consumer, therefore the manufacturing facility does not benefit from installing an on-site battery storage system. A reduction in the variability of the manufacturing facility's electric load would benefit the electric grid, which could incentivize the manufacturing facility to adopt on-site battery storage or find alternative solutions to manage the increasing variability of the load.

B.2.1 Sensitivity analysis on the time window chosen

As mentioned in section 6.2.4 and section B.2, there is not a wide literature on how to quantify or even define the variability of a residual electric load: different approaches may be used.

In this thesis the variability has been quantified by calculating the standard deviation σ_h of the net demand over a five-hour window spanning two hours before and two hours after every hour h of the year (equation 6.9). This method is proposed by Palmateer [110].

The window standard deviation σ_h (and so its normalized mean $\bar{\sigma}_h^*$) depends on the time window chosen. Palmateer [110] suggests to chose a 5-hour window and this is the approach followed in this thesis. However, a sensitivity analysis has been conducted to investigate whether the qualitative conclusions drawn from the analysis previously presented change with this parameter. For different sample windows, the mean variability for the smallest (1,000kWh-200kW) and biggest (10,000kWh-5,000kW) battery bank considered in this analysis has been calculated and has been normalized to the mean variability of the considered base case (VRE, 1,600kW$_{el}$ GT in electricity following and no ESS) which also varies with the sample window chosen. The results are shown in Figure B.6.

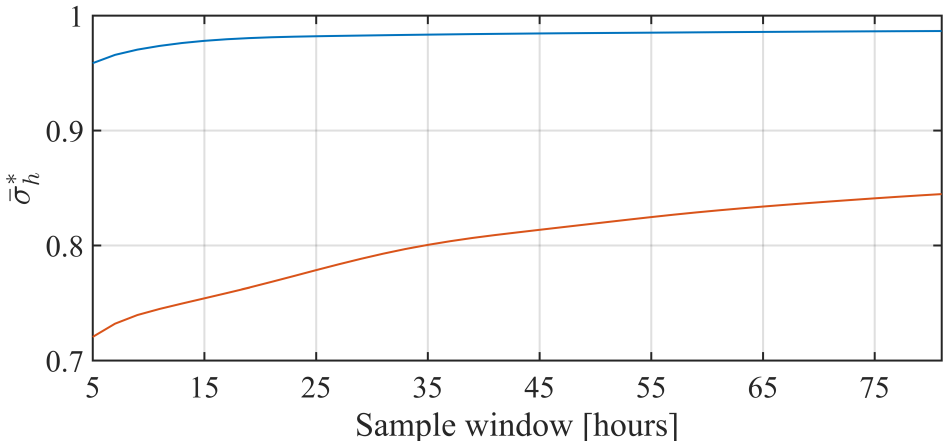

FIGURE B.6: Normalized mean variability $\bar{\sigma}_h^*$ for different sample windows
— Small battery bank — Big battery bank

The smaller battery bank has a lower $\bar{\sigma}_h^*$ compared to the base case, however the reduction in the variability is very small and it decreases with larger time window. More benefits in terms of variability reduction are given by the bigger battery bank, as previously discussed. However, the reduction in the variability compared to the base case is progressively lower as the time window increases.

It is concluded that the normalized mean variability $\bar{\sigma}_h^*$ is a useful tool to draw qualitative conclusions on the relative benefit of introducing on-site battery storage. It should be used, however, only as a qualitative comparative tool and an extremely cautious approach is suggested in comparing in absolute terms numerical values for this variable. This investigation, in fact, has not been conducted to identify a metric for the variability *per se* but to compare qualitatively the benefits of different configurations.

Appendix C

Use of biogas in the on-site cogeneration system

In Ireland, biogas currently represents only 1.9% of the renewable contribution to the Total Final energy Consumption TFC (0.08% of TFC) and is mostly used for generating renewable thermal energy through Combined Heat and Power (CHP) technologies: in 2018, 5% of the CHP units installed used biogas for a total installed capacity of 9.5MW [16]. While biogas is not extensively used in Ireland a the moment due to stringent purification requirements before its usage, it is recognised by the Sustainable Energy Authority of Ireland (SEAI) to have an important role in the pathway to achieve the 2030 and 2050 targets [111]. In fact, while the actual global production of biogas and biomethane is 35Mtoe, the sustainable potential is estimated by the International Energy Agency (IEA) to be 730Mtoe and its full utilization could cover around 20% of today's worldwide gas demand [186]. Biogas is steadily growing in IEA scenarios since it could allow a reduction in emissions in hard-to-abate sectors such as heavy industry and transport, and limit the cost of decarbonizing the heating sector by taking advantage of the existing gas infrastructures [187]. The cost of biogas is higher compared to natural gas, however the gap is estimated to narrow in the future, as the required technologies to produce it will become more commercially mature and carbon pricing, or other forms of disincentives for fossil fuels, will make natural gas less competitive.

Biogas can be produced in different ways. The most common is through anaerobic digestion plants: a digester vessel is used, which contains micro-organisms that break down the organic matter contained in the feedstock to produce biogas, which is typically 60% methane (CH_4) and 40% carbon dioxide (CO_2) by volume. This rate changes depending on the type of feedstock and includes also small quantities of other gases. Feedstock ranges from food wastes to animal slurries to energy crops specifically grown for the purpose. Different technologies use anaerobic digestion to produce biogas:

- Biodigesters: the organic material is diluted in water and is broken down by micro-organisms that form naturally. The reaction occurs in airtight systems such as containers and tanks. Biogas is then clean from contaminants and moisture before usage.

- Landfill gas recovery systems: decomposition of municipal solid waste at landfill sites in anaerobic conditions produces biogas that can be captured using pipes or extraction wells and conveyed to a central collection point with a compressor.
- Wastewater treatment plants: they can be equipped with a recovery system for the organic matter, solids and nutrients from sewage sludge. This matter can be used as feedstock to produce biogas in an anaerobic digester.

Biomethane is instead a near-pure source of methane. It can be produced from biogas, by cleaning it in additional upgrading processes for CO_2 removal, or through thermal gasification of solid biomass followed by methanation. The 90% of global biomethane production that comes from biogas is upgraded using different properties of various gas contained within the biogas to separate CH_4. A detailed report on the available technologies for upgrading biogas is presented by the Swedish Gas Technology Centre SGC [188] and a detailed economic assessment is conducted by Khan et al. [189]. The remaining 10% is produced by breaking down biomass at high temperature and pressure in a low-oxygen environment into a mixture of gases, called syngas (mainly carbon monoxide, hydrogen and methane). The feedstock used for gasification processes is typically wood chips, pellets or solid waste derived fuels; they are more expensive compared to the feedstock for anaerobic digestions, which could in certain cases be acquired even at a negative cost. In the methanation process the syngas (acid and corrosive components removed) is sent through a catalyst that promotes the reaction between hydrogen and carbon monoxide to produce methane.

While biogas has a Lower Heating Value (LHV) ranging between 16 and 28MJ/m^3, biomethane has an average LHV of 36MJ/m^3 and can be used as a direct substitute of natural gas without changes in transmission and distribution infrastructure [186].

Considering the case of a manufacturing facility as analysed in this thesis, it would not be a feasible option to have a plant for on-site biogas production since it would require additional investments, space and resources. The most likely scenario is to consider that the temporal limitation of the on-site CHP environmental benefit could be overcome by using biogas or biomethane coming from the natural gas grid, i.e. produced by centralized plants and then distributed to final users. As shown by Khan et al. [189], purified biogas can be injected into the gas grid if the gas streams are of equal quality [1]. Biogas could then be used in an on-site CHP system: internal combustion engines and gas turbines have been proven in fact to successfully generate electricity and heat using biogas [190]. It is highly recommended, however, that water vapour is condensed to avoid condensation in gas lines and it is required that the level of hydrogen sulphide (H_2S) is below 300ppm (obtained through desulphurisation) to avoid corrosion of boiler and gas engine [191].

[1] Additional information about Irish regulation and guidelines are provided by SEAI [111].

If there is an opportunity for biogas in electricity and heat generation that would help reducing fossil fuels consumption, why its usage is still limited to less than 5% of its sustainable potential [2]?

One reason is related to the definition of biogas as renewable source. There is a lot of discussion about whether biogas should be considered sustainable. The IEA [186] suggests that biogas should be considered a sustainable source only if the feedstock used to produce it can be processed with existing technologies, if it is not competing with food for agricultural land and does not have any other adverse sustainability impacts such as reducing biodiversity. It is necessary to ensure that these conditions are met in order to consider biogas a sustainable choice.

Another limitation to the use of biogas lies in the cost [186]. It is estimated that today more that 700Mtoe of biomethane could be produced sustainably (20% of the global natural gas demand) at a cost displayed in Figure C.1.

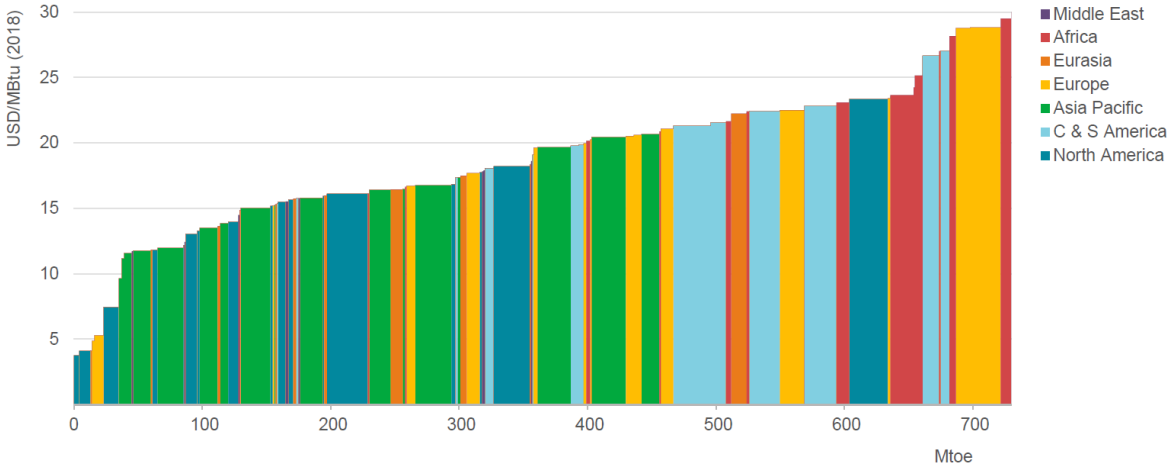

FIGURE C.1: Cost curve of potential global biomethane supply by region in 2018 [186]

The average cost of producing biomethane through biogas updating is around 19USD/MBtu, including both the production cost (which is the most relevant part) and the upgrading cost [3] [186].

Biomethane and natural gas costs vary significantly by region, as shown in Figure C.2, where the cost of producing the least expensive biomethane is compared to the natural gas price. While the gap between biomethane and natural gas prices is significant in advanced economies, this may not apply to developing regions such as in parts of Asia, where natural gas is imported and therefore relatively expensive, and where biogas feedstock is available at a very low cost.

[2] Sustainable potential of biogas is intended as defined by the IEA [186].
[3] Grid connection costs are not included and represent a potential additional cost.

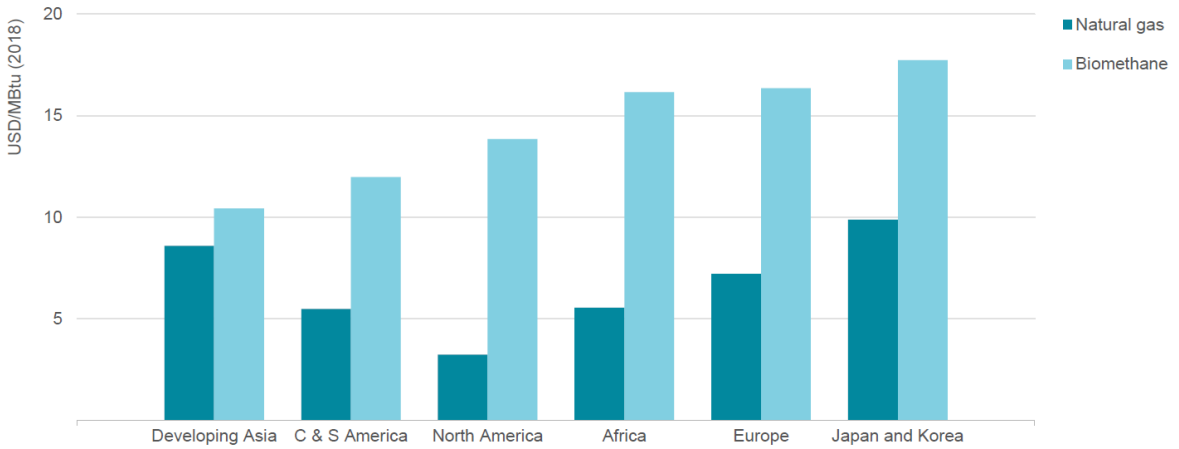

FIGURE C.2: Cost of using the least expensive biomethane to meet 10% of gas demand and natural gas prices in 2018 [186].
C&S America = Central and South America; Developing Asia = People's Republic of China, India, the Association of Southeast Asian Nations and other developing economies in Asia Pacific.

Looking at Ireland in particular, the SEAI [111] has estimated the Levelized Cost of Energy ($LCOE$) for biomethane produced from anaerobic digestion plants for different discount rates and compared it to the wholesale price of natural gas (calculated on the same $LCOE$ basis). Assuming a 8% discount rate, the cost of biomethane produced in new anaerobic digestion plant is between 0.9 and 7.0 c€/kWh greater than the wholesale price of natural gas (which is equal to 3c€/kWh). At a higher discount rate of 12%, the gap rises to 1.6 to 9.6 c€/kWh. A better economic opportunity exists for existing anaerobic digestion plants at sewage treatment plants, where the only extra cost would be the cost of upgrading and injecting the biomethane. In this case, the cost of the biomethane would be lower than natural gas. The process of gasification to produce syngas instead has a higher $LCOE$.

It has been shown that an opportunity for overcoming the temporal limitation of the environmental benefits of on-site energy cogeneration lies in the use of biogas supplied through the natural gas grid. The environmental benefits of biogas are proven under the condition that biogas is produced sustainably as previously explained. The higher cost of biogas compared to natural gas is slowing down the transition to this renewable fuel, however the price gap is likely to narrow in the future through economy of scale of larger facilities: overall the average cost of globally producing biomethane by 2040 is estimated to decrease by 25% [186].

Bibliography

[1] IPCC, "Special report: Global warming of 1.5°C," tech. rep., 2018.

[2] IEA, "CO_2 emissions from fuel combustion. Database documentation," tech. rep., 2018.

[3] IEA, "Data and Statistics." Available at `https://www.iea.org/data-and-statistics/?country=WORLD&fuel=CO2%20emissions&indicator=CO2%20emissions%20by%20sector`. Accessed on 05/01/2020.

[4] IEA, "Key world energy statistics," tech. rep., 2018.

[5] IPCC, "AR5 Climate Change 2014: Mitigation of Climate Change," tech. rep., 2014.

[6] A. Thornton, S. Kim, and S. Kara, "Sizing a hybrid renewable energy system to reduce energy costs at various levels of robustness for an industrial site," *Procedia CIRP*, vol. 69, pp. 371–376, 2018.

[7] E. Schmid, B. Knopf, and A. Pechan, "Putting an energy system transformation into practice: The case of the German Energiewende," *Energy Research & Social Science*, vol. 11, pp. 263–275, 2016.

[8] M. Schriever and D. Halstrup, "Exploring the adoption in transitioning markets: Empirical findings and implications on energy storage solutions-acceptance in the German manufacturing industry," *Energy Policy*, vol. 120, pp. 460–468, 2018.

[9] J. Kirkerud, T. Bolkesjø, and E. Trømborg, "Power-to-heat as a flexibility measure for integration of renewable energy," *Energy*, vol. 128, pp. 776–784, 2017.

[10] Industrial Technologies Program, "Industrial heat pumps for steam and fuel savings," tech. rep., 2003.

[11] T. Tveit, "Application of an industrial heat pump for steam generation using district heating as a heat source," *12th IEA Heat Pump Conference*, 2017.

[12] A. Vijay and A. Hawkes, "The techno-economics of small-scale residential heating in low carbon futures," *Energies*, vol. 10, pp. 1–23, 2017.

[13] G. Kosmadakis, "Estimating the potential of industrial (high-temperature) heat pumps for exploiting waste heat in EU industries," *Applied Thermal Engineering*, vol. 156, pp. 287–298, 2019.

[14] J. Tarrant, "Recent industrial development in Ireland," *Geography*, vol. 52, pp. 403–408, 1967.

[15] International Monetary Fund. Available at `https://www.imf.org/external/pubs/ft/weo/2019/02/weodata/weorept.aspx?pr.x=64&pr.y=11&sy=2016&ey=2021&scsm=1&ssd=1&sort=country&ds=.&br=1&c=178&s=NGDP_RPCH%2CNGDPD%2CPPPGDP%2CNGDPDPC%2CPPPPC%2CPCPIPCH&grp=0&a=`.

[16] SEAI, "Energy in Ireland 2019," tech. rep., 2019.

[17] European Union, "Emission Trading Scheme." Available at `https://ec.europa.eu/clima/policies/ets_en`.

[18] European Commission, "Report on the functioning of the European carbon market," tech. rep., 20019.

[19] Irish Statute Book, "S.I. No. 490/2012 - European Communities (Greenhouse Gas Emissions Trading) Regulations 2012.." Available at `http://www.irishstatutebook.ie/eli/2012/si/490/made/en/print`.

[20] M. Ahman and L. Nilsson, *Decarbonising industry in EU-Climate, trade and industrial policy strategies*. 2015.

[21] Sustainable Energy Authority Ireland, "Large Industry Energy Network." Available at `https://www.seai.ie/business-and-public-sector/large-business/lien/`.

[22] European Commission, "Regulation (EU) 2018/842 of the European Parliament and of the Council of 30 May 2018 on binding annual greenhouse gas emission reductions by Member States from 2021 to 2030," tech. rep., 2018.

[23] European Commission, "The European Green Deal," tech. rep., 2019.

[24] European Commission, "Directive 2009/28/EC," tech. rep., 2009.

[25] M. Di Silvestre, S. Favuzza, E. Riva Sanseverino, and G. Zizzo, "How decarbonization, digitalization and decentralization are changing key power infrastructures," *Renewable and Sustainable Energy Reviews*, vol. 93, pp. 483–498, 2018.

[26] A. Bublitz, D. Keles, F. Zimmermann, C. Fraunholz, and W. Fichtner, "A survey on electricity market design: Insights from theory and real-world implementations of capacity remuneration mechanisms," *Energy Economics*, vol. 80, pp. 1059–1078, 2019.

[27] United States Department of Energy, "Integrating renewable generation into grid operations: four international experiences," tech. rep., 2016.

[28] IEA, "Harnessing variable renewables: A guide to the balancing challenge," tech. rep., 2011.

[29] A. Brouwer, M. van den Broek, A. Seebregts, and A. Faaij, "Operational flexibility and economics of power plants in future low-carbon power systems," *Applied Energy*, vol. 156, pp. 107–128, 2015.

[30] J. Hu, R. Harmsen, W. Crijns-Graus, E. Worrell, and M. van den Broek, "Identifying barriers to large-scale integration of variable renewable electricity into the electricity market: A literature review of market design," *Renewable and Sustainable Energy Reviews*, vol. 81, pp. 2181–2195, 2018.

[31] ERGEG, "Revised ERGEG guidelines of good practice for electricity balancing markets integration (GGP-EBMI)," tech. rep., 2009.

[32] ENTSO-E, "ENTSO-E network code on electricity balancing," tech. rep., 2014.

[33] R. Scharff, *Design of electricity markets for efficient balancing of wind power*. PhD thesis, KTH Royal Institute of Technology, Stockholm, Sweden, 2015. Doctoral Thesis.

[34] L. Hirth and I. Ziegenhagen, "Balancing power and variable renewables: Three links," *Renewable and Sustainable Energy Reviews*, vol. 50, pp. 1035–1051, 2015.

[35] L. Hirth, F. Ueckerdt, and O. Edenhofer, "Integration costs revisited: An economic framework for wind and solar variability," *Renewable Energy*, vol. 74, pp. 925–939, 2015.

[36] J. de Jong, F. Genoese, and C. Egenhofer, "CEPS Task Force Report: Reforming the market design of EU electricity markets addressing the challenges of a low-carbon power sector," tech. rep., 2015.

[37] C. Monyei, B. Sovacool, M. Brown, K. Jenkins, S. Viriri, and Y. Li, "Justice, poverty, and electricity decarbonization," *The Electricity Journal*, vol. 32, pp. 47–51, 2019.

[38] M. Castaneda, M. Jimenez, S. Zapata, C. Franco, and I. Dyner, "Myths and facts of the utility death spiral," *Energy Policy*, vol. 110, pp. 105–116, 2017.

[39] F. Ueckerdt, R. Brecha, and G. Luderer, "Analyzing major challenges of wind and solar variability in power systems," *Renewable Energy*, vol. 81, pp. 1–10, 2015.

[40] F. Wiese and M. Baldini, "Conceptual model of the industry sector in an energy system model: A case study for Denmark," *Journal of Cleaner Production*, vol. 203, pp. 427–443, 2018.

[41] CER, "Review of typical domestic consumption - Values for electricity and gas customers," tech. rep., 2017.

[42] V. Smil, *Power Density. A Key to Understanding Energy Sources and Uses*. 2015.

[43] A. Sgobba and C. Meskell, "On-site renewable electricity production and self consumption for manufacturing industry in Ireland: Sensitivity to techno-economic conditions," *Journal of Cleaner Production*, vol. 207C, pp. 894–907, 2019.

[44] S. Wang, S. Wang, and D. Wang, "Combined probability density model for medium term load forecasting based on quantile regression and kernel density estimation," *Energy Procedia*, vol. 158, pp. 6446–6451, 2019.

[45] Y. He and H. Li, "Probability density forecasting of wind power using quantile regression neural network and kernel density estimation," *Energy Conversion and Management*, vol. 164, pp. 374–384, 2018.

[46] J. Jeon and J. Taylor, "Short-term density forecasting of wave energy using ARMA-GARCH models and kernel density estimation," *International Journal of Forecasting*, vol. 32, pp. 991–1004, 2016.

[47] B. Liu and R. Jordan, "The interrelationship and characteristic distribution of direct, diffuse, and total solar radiation," *Solar Energy*, vol. 4, pp. 1–9, 1960.

[48] J. Orgill and K. Hollands, "Correlation equation for hourly diffuse radiation on a horizontal surface," *Solar Energy*, vol. 19, pp. 357–359, 1977.

[49] D. Erbs, S. Klein, and J. Duffie, "Estimation of the diffuse radiation fraction for hourly, daily and monthly-average global radiation," *Solar Energy*, vol. 28, pp. 293–302, 1982.

[50] D. Reindl, W. Beckman, and J. Duffie, "Diffuse fraction correlations," *Solar Energy*, vol. 45, pp. 1–7, 1990.

[51] C. Demain, M. Journée, and C. Bertrand, "Evaluation of different models to estimate the global solar radiation on inclined surfaces," *Renewable Energy*, vol. 50, pp. 710–721, 2013.

[52] J. Bugler, "The determination of hourly insolation on an inclined plane using a diffuse irradiance model based on hourly measured global horizontal insolation," *Solar Energy*, vol. 19, pp. 477–491, 1977.

[53] R. Perez, R. Seals, P. Ineichen, R. Stewart, and D. Menicucci, "A new simplified version of the Perez diffuse irradiance model for tilted surfaces," *Solar Energy*, vol. 39, pp. 221–231, 1987.

[54] C. Gueymard, "From global horizontal to global tilted irradiance: How accurate are solar energy engineering predictions in practice?," *Solar Conference, San Diego, CA, American Solar Energy Society*, 2008.

[55] C. Gueymard, "An anisotropic solar irradiance model for tilted surfaces and its comparison with selected engineering algorithms," *Solar Energy*, vol. 38, pp. 367–386, 1987.

[56] T. Klucher, "Evaluation of models to predict insolation on tilted surfaces," *Solar Energy*, vol. 23, pp. 111–114, 1979.

[57] E. Evseev and A. Kudish, "The assessment of different models to predict the global solar radiation on a surface tilted to the south," *Solar Energy*, vol. 83, pp. 377–388, 2009.

[58] R. Pallabazzer, "Evaluation of wind-generator potentiality," *Solar Energy*, vol. 55, pp. 49–59, 1995.

[59] V. Okulov and J. Sørensen, "An ideal wind turbine with a finite number of blades," *Doklady Physics*, vol. 53, pp. 337–342, 2008.

[60] V. Okulov and J. Sørensen, "Refined Betz limit for rotors with a finite number of blades," *Wind Energy*, vol. 11, pp. 415–426, 2008.

[61] ABB, "Quaderni di applicazione tecnica N.13. Impianti eolici," tech. rep., 2011.

[62] G. Ngala, B. Alkali, and M. Aji, "Viability of wind energy as a power generation source in Maiduguri, Borno state, Nigeria," *Renewable Energy*, vol. 32, pp. 2242–2246, 2007.

[63] C. Ozay and M. Celiktas, "Statistical analysis of wind speed using two-parameter Weibull distribution in Alaçatı region," *Energy Conversion and Management*, vol. 121, pp. 49–54, 2016.

[64] T. Aukitino, M. Khan, and M. Ahmed, "Wind energy resource assessment for Kiribati with a comparison of different methods of determining Weibull parameters," *Energy Conversion and Management*, vol. 151, pp. 641–660, 2017.

[65] B. Karthikeya, P. Negi, and N. Srikanth, "Wind resource assessment for urban renewable energy application in Singapore," *Renewable Energy*, vol. 87, pp. 403–414, 2016.

[66] O. Ohunakin, "Wind resource evaluation in six selected high altitude locations in Nigeria," *Renewable Energy*, vol. 36, pp. 3273–3281, 2011.

[67] N. Nawri, G. Petersen, H. Bjornsson, A. Hahmann, K. Jonasson, C. Hasager, and N. Clausen, "The wind energy potential of Iceland," *Renewable Energy*, vol. 69, pp. 290–299, 2014.

[68] Y. Kantar, I. Usta, I. Arik, and I. Yenilmez, "Wind speed analysis using the Extended Generalized Lindley Distribution," *Renewable Energy*, vol. 118, pp. 1024–1030, 2018.

[69] K. Philippopoulos, D. Deligiorgi, and G. Karvounis, "Wind speed distribution modeling in the greater area of Chania, Greece," *International Journal of Green Energy*, vol. 9, pp. 174–193, 2012.

[70] J. Zhou, E. Erdem, G. Li, and J. Shi, "Comprehensive evaluation of wind speed distribution models: A case study for North Dakota sites," *Energy Conversion and Management*, vol. 51, pp. 1449–1458, 2010.

[71] S. Akpinar and E. Akpinar, "Estimation of wind energy potential using finite mixture distribution models," *Energy Conversion and Management*, vol. 50, pp. 877–884, 2009.

[72] S. Akdag, H. Bagiorgas, and G. Mihalakakou, "Use of two-component Weibull mixtures in the analysis of wind speed in the Eastern Mediterranean," *Applied Energy*, vol. 87, pp. 2566–2573, 2010.

[73] J. Shin, T. Ourda, and T. Lee, "Heterogeneous mixture distributions for modeling wind speed application to the UAE," *Renewable Energy*, vol. 35, pp. 40–52, 2016.

[74] P. Ramirez and J. Carta, "The use of wind probability distributions derived from the maximum entropy principle in the analysis of wind energy. A case study," *Energy Conversion and Management*, vol. 47, pp. 2564–2577, 2006.

[75] Y. Kantar and I. Usta, "Analysis of wind speed distributions: wind distribution function derived from minimum cross entropy principles as better alternative to Weibull function," *Energy Conversion and Management*, vol. 49, pp. 962–973, 2008.

[76] H. Holttinen, M. O'Malley, D. Flynn, M. Milligan, and J. Smith, "Recommended practices for wind integration studies," tech. rep., 2013.

[77] IWEA, "Best practise guidelines for the Irish wind energy industry," tech. rep., 2012.

[78] "HOMER ENERGY PRO Software." Available at `https://www.homerenergy.com/homer-pro.html`.

[79] Department of Housing, Planning and Local Government, "Wind Energy Development: Planning Guidelines." Available at `http://www.housing.gov.ie/sites/default/files/migrated-files/en/Publications/DevelopmentandHousing/Planning/FileDownLoad%2C1633%2Cen.pdf`. Accessed on 11/01/2018.

[80] World Bank Group, "Environmental, Health, and Safety Guidelines for Wind Energy." Available at `http://www.ifc.org/wps/wcm/connect/2c410700497a7933b04cf1ef20a40540/FINAL_Aug+2015_Wind+Energy_EHS+Guideline.pdf?MOD=AJPERES`. Accessed on 11/01/2018.

[81] NASA, "Surface meteorology and solar energy." Available at `https://eosweb.larc.nasa.gov/sse/`. Accessed on 12/12/2016.

[82] Met eireann. Available at `http://www.met.ie/climate-request/`. Accessed on 15/12/2016.

[83] D. Myers, "Solar radiation: Practical modeling for renewable energy applications," tech. rep., 2013.

[84] University of Minnesota, "Appendix D: Solar radiation." Available at `http://www.me.umn.edu/courses/me4131/LabManual/AppDSolarRadiation.pdf`. Accessed on 12/12/2016.

[85] M. Basunia, H. Yoshio, and T. Abe, "Simulation of solar radiation incident on horizontal and inclined surfaces," *The Journal of Engineering Research TJER*, vol. 9, pp. 27–35, 2012.

[86] ITACA, "Solar Geometry Calculator." Available at `https://www.esrl.noaa.gov/gmd/grad/antuv/SolarCalc.jsp`. Accessed on 12/12/2016.

[87] ITACA, "Solar Astronomy." Available at `http://www.itacanet.org/the-sun-as-a-source-of-energy/part-1-solar-astronomy/`. Accessed on 11/01/2018.

[88] System Advisor Model. Available at `https://https://sam.nrel.gov/`. Accessed on 12/12/2016.

[89] PVWatts Calculator. Available at `http://pvwatts.nrel.gov/`. Accessed on 12/12/2016.

[90] L. Ryan, J. Dillon, S. La Monaca, J. Byrne, and M. O'Malley, "Assessing the system and investor value of utility-scale solar PV," *Renewable and Sustainable Energy Reviews*, vol. 64, pp. 506–517, 2016.

[91] S. La Monaca and L. Ryan, "Solar PV where the sun doesn't shine: Estimating the economic impacts of support schemes for residential PV with detailed net demand profiling," *Energy Policy*, vol. 108, pp. 731–741, 2017.

[92] L. Ayompe, A. Duffy, S. McCormack, and M. Conlon, "Projected costs of a grid-connected domestic PV system under different scenarios in Ireland, using measured data from a trial installation," *Energy Policy*, vol. 38, pp. 3731–3743, 2010.

[93] Enercon E-44 model. Available at `https://en.wind-turbine-models.com/turbines/531-enercon-e-44`. Accessed on 15/01/2018.

[94] NASA MERRA-2, "Modern-era retrospective analysis for research and applications, version 2."

[95] I. Staffell and R. Green, "How does wind farm performance decline with age?," *Renewable Energy*, vol. 66, pp. 775–786, 2014.

[96] T. Kealy, M. Barrett, and D. Kearney, "How profitable are wind turbine projects? An empirical analysis of a 3.5 MW wind farm in Ireland," *International Journal on Recent Technologies in Mechanical and Electrical Engineering*, vol. 2, pp. 58–63, 2015.

[97] IRENA, "The power to change: Solar and wind cost reduction potential to 2025," tech. rep., 2016.

[98] European Commission, "EU energy trends to 2030," tech. rep., 2009.

[99] J. Blazquez, R. Fuentes-Bracamontes, C. Bollino, and N. Nezamuddin, "The renewable energy policy paradox," *Renewable and Sustainable Energy Reviews*, vol. 82, pp. 1–5, 2018.

[100] G. Pepermans, J. Driesen, D. Haeseldonckx, R. Belmans, and W. D'haeseleer, "Distributed generation: definition, benefits and issues," *Energy Policy*, vol. 33, pp. 787–798, 2005.

[101] Kawasaki. `http://global.kawasaki.com/en/energy/equipment/gas_turbines/cogeneration.html`, 2018. (Accessed September 2018).

[102] Energy and Environmental Economics, "Capital cost review of power generation technologies," tech. rep., 2014.

[103] G. D. P. da Silva, "Utilisation of the System Advisor Model to estimate electricity generation by grid-connected photovoltaic projects in all regions of Brazil," *International Journal of Software Engineering and its Applications*, vol. 11, pp. 1–12, 2017.

[104] Poyry, "Low carbon generation options for the all-island market. A report to EirGrid.," tech. rep., 2010.

[105] J. Vandewalle, K. Bruninx, and W. D'haeseleer, "Effects of large-scale power to gas conversion on the power, gas and carbon sectors and their interactions," *Energy Conversion and Management*, vol. 94, pp. 28–39, 2015.

[106] J. Glynn, M. Gargiulo, A. Chiodi, P. Deane, F. Rogan, and B. Ó Gallachóir, "Zero carbon energy system pathways for Ireland consistent with the Paris Agreement," *Climate Policy*, vol. 19, pp. 30–42, 2019.

[107] A. Chiodi, M. Gargiulo, F. Rogan, J. Deane, D. Lavigne, U. Rout, and B. Ó Gallachóir, "Modelling the impacts of challenging 2050 European climate mitigation targets on Ireland's energy system," *Energy Policy*, vol. 53, pp. 169–189, 2013.

[108] SEAI, "Ireland's energy projections - Progress to targets, challenges and impacts," tech. rep., 2017.

[109] A. Lamont, "Assessing the long-term system value of intermittent electric generation technologies," *Energy Economics*, vol. 30, pp. 1208–1231, 2008.

[110] R. Dorsey-Palmateer, "Effects of wind power intermittency on generation and emissions," *The Electricity Journal*, vol. 32, pp. 25–30, 2019.

[111] SEAI, "Assessment of cost and benefits of biogas and biomethane in Ireland," tech. rep., 2017.

[112] IRENA, "Renewable energy technologies: Cost anaysis series. Solar Photovoltaics," tech. rep., 2014.

[113] M. Archer and M. Green, *Clean Electricity from Photovoltaics*. 2015.

[114] X. Wang and Z. Wang, *High-Efficiency Solar Cells*. 2014.

[115] L. Arnberg, M. Di Sabatino, and E. Ovrelid, "State-of-the-art growth of silicon for PV applications," *Journal of Crystal Growth*, vol. 360, pp. 56–60, 2012.

[116] W. Zulehner, "Status and future of silicon crystal growth," *Material Science and Engineering: B*, vol. 4, pp. 1–10, 1989.

[117] F. Shimura, "Single-crystal silicon: Growth and properties," in *Springer Handbook of Electronic and Photonic Materials* (Springer, ed.), pp. 255–269, Boston, MA: Springer, 2006.

[118] IEA, "Technology roadmap: Solar photovoltaic energy," tech. rep., 2014.

[119] M. Gratzel, "Dye-sensitized solar cells," *Journal of Photochemistry and Photobiology C: Photochemistry Reviews*, vol. 4, pp. 145–153, 2003.

[120] N. Yeh and P. Yeh, "Organic solar cells: Their developments and potentials," *Renewable and Sustainable Energy Reviews*, vol. 21, pp. 421–431, 2013.

[121] A. Nozik, "Superlattice photoelectrodes for photoelectrochemical cells. Patent publication number us4634641 a.," tech. rep., 1987.

[122] NREL, "Efficiency chart." Available at `https://www.nrel.gov/pv/assets/images/efficiency-chart.png`. Accessed on 19/12/2017.

[123] B. Friedman, R. Margolis, and J. Seel, "Comparing photovoltaic (PV) costs and deployment driver in the Japanese and U.S. residential and commercial market," tech. rep., 2016.

[124] F. Kersten, R. Doll, A. Kux, D. Huljic, M. Gong, C. Breyer, J. Müller, and P. Wawer, "Pv learning curves: Past and future drivers of cost reduction," 2011.

[125] IFC, "Utility-scale solar photovoltaic power plants," tech. rep., 2015.

[126] NREL, "U.S. solar photovoltaic system cost benchmark: Q1 2018," tech. rep., 2018.

[127] SEAI, "Renewable energy technologies: Cost analiysis series. Wind power," tech. rep., 2012.

[128] Windpower Engineering & Development, "Regulations for wind turbine." Available at http://www.windpowerengineering.com/towers-construction/turbine-lab-on-an-80-m-tower/. Accessed on 18/12/2017.

[129] IEA Wind, "2015 Annual Report," tech. rep., 2015.

[130] REN21, "Renewables 2016. Global status report," tech. rep., 2016.

[131] WWEA, "Wind energy 2050. On the shape of near 100% RE grid. A WWEA technical commitee report on grid integration," tech. rep., 2015.

[132] C. Bataille, M. Ahman, K. Neuhoff, L. Nilsson, M. Fischedick, S. Lechtenböhmer, B. Solano-Rodriquez, A. Denis-Ryan, S. Stiebert, H. Waisman, O. Sartor, and S. Rahbar, "A review of technology and policy deep decarbonization pathway options for making energy-intensive industry production consistent with the Paris Agreement," *Journal of Cleaner Production*, vol. 187, pp. 960–973, 2018.

[133] M. Ruth and B. Kroposki, "Energy Systems Integration: An evolving energy paradigm," *The Electricity Journal*, vol. 27, pp. 36–47, 2014.

[134] M. Geidl and G. Andersson, "Optimal power dispatch and conversion in systems with multiple energy carriers," *Proceedings of the 15th power systems computation conference (PSCC)*, 2005.

[135] M. Mohammadi, Y. Noorollahi, B. Mohammadi-ivatloo, M. Hosseinzadeh, H. Yousefi, and S. Khorasani, "Optimal management of energy hubs and smart energy hubs: A review," *Renewable and Sustainable Energy Reviews*, vol. 89, pp. 33–50, 2018.

[136] IEA, "Cogeneration and district energy," tech. rep., 2009.

[137] IEA, "Sankey diagram." Available at https://www.iea.org/Sankey/#?c=IEATotal&s=Balance. Accessed on 06/12/2017.

[138] E. Tzimas, R. Moss, and P. Ntagia, "2011 Technology Map of the European Strategic Energy Technology Plan (SET-Plan)," tech. rep., 2011.

[139] EU, "Directive 2004/8/EC of the European Parliament and of the Council of 11 February 2004 on the promotion of cogeneration based on a useful heat demand in the internal energy market and amending Directive 92/42/EEC," tech. rep., 2004.

[140] European Commission, "Training guide on Combined Heat & Power systems," tech. rep., 2001.

[141] IEA, "Combined heat and power: Evaluating the benefits of greater global investment," tech. rep., 2008.

[142] G. Heyen and B. Kalitventzeffab, "A comparison of advanced thermal cycles suitable for upgrading existing powerplant," *Applied Thermal Engineering*, vol. 19, pp. 227–237, 1999.

[143] SEAI, "Combined heat and power in Ireland," tech. rep., 2019.

[144] Association for Decentralized Energy, "CHP in Baush + Lomb manufacturing plant," tech. rep., 2016.

[145] Boston Scientific, "Boston Scientific CHP," tech. rep., 2017.

[146] P. Kiameh, *Power generation handbook: Selection, applications, operation, maintenance*. McGraw-Hill, 2002.

[147] R. Kehlhofer, *Combined-Cycle Gas and Steam Power Plant*. PennWell, 1997.

[148] M. Boyce, *Gas Turbine Engineering Handbook*. Gulf Professional Publishing, 2001.

[149] P. Pilavachi, "Power generation with gas turbine systems and combined heat and power," *Applied Thermal Engineering*, vol. 20, pp. 1421–1429, 2000.

[150] Siemens, "Industrial gas turbine." Available at `https://www.siemens.com/global/en/home/products/energy/power-generation/gas-turbines`. Accessed on 02/01/2018.

[151] F. Righetti, "Control and optimization of the start-up of a combined cycle power plant," 2010.

[152] G. Lozza, *Turbine a gas e cicli combinati*. Esculapio, 2016.

[153] M. Khosravy El Hossaini, *Review of The New Combustion Technologies in Modern Gas Turbines*. Ernesto Benini, 2013.

[154] H. Nessler, R. Preiss, and P. Eisenkolb, "Development in HRSG technology," *The* 7_{th} *Annual Industrial & Power Gas Turbine O&M Conference*, 2001.

[155] B. Liptak, *Process control and optimization. Volume II*. CRC Press, 2006.

[156] C. Aurora, M. Diehl, P. Kuehl, L. Magni, and R. Scattolini, "Non-linear model predictive control of combined cycle power plants," *IFAC Proceedings Volumes*, pp. 127–132, 2005.

[157] H. Asgari, M. Venturini, X. Chen, and R. Sainudiin, "Modeling and simulation of the transient behavior of an industrial power plant gas turbine," *Journal of Engineering for Gas Turbines and Power*, vol. 136, 2014.

[158] D. Bouskela, G. Lebreton, C. Cedex, and B. El Hefni, "Dynamic modelling of a combined cycle power plant with ThermoSysPro," *Modelica 2011 conference proceedings*, 2011.

[159] A. Tica, "Design, optimization and validation of start-up sequences of energy production systems," 2012.

[160] F. Casella and F. Pretolani, "Fast start-up of a combined-cycle power plant: a simulation study with Modelica," 6^{th} *Modelica Conference*, 2006.

[161] P. Parini, "Object oriented modeling and dynamic optimization of energy systems with application to combined cycle power plant start-up," 2015.

[162] B. El Hefni and D. Bouskela, "Modeling and simulation of complex ThermoSysPro model with OpenModelica - Dynamic modeling of a combined cycle power plant," 12^{th} *International Modelica Conference*, 2017.

[163] I. Rossi, A. Sorce, and A. Traverso, "Gas turbine combined cycle start-up and stress evaluation: A simplified dynamic approach," *Applied Energy*, pp. 880–890, 2017.

[164] H. Chen, T. Cong, W. Yanf, C. Tan, Y. Li, and Y. Ding, "Progress in electrical energy storage system: A critical review," *Progress in Natural Science*, vol. 19, pp. 291–312, 2009.

[165] H. Zhao, Q. Wu, S. Hu, H. Xu, and C. Rasmussen, "Review of energy storage system for wind power integration support," *Applied Energy*, vol. 137, pp. 545–553, 2015.

[166] International Renewable Energy Agency IRENA, "Electricity storage and renewables: Costs and markets to 2030," tech. rep., 2018.

[167] A. Dehghani-Sanij, E. Tharumalingam, M. Dusseault, and R. Fraser, "Study of energy storage systems and environmental challenges of batteries," *Renewable and Sustainable Energy Reviews*, vol. 104, pp. 192–208, 2019.

[168] International Electrotechnical Commission, "Electrical Energy Storage. White Paper," tech. rep., 2019.

[169] M. Aneke and M. Wang, "Energy storage technologies and real life applications-A state of the art review," *Applied Energy*, vol. 179, pp. 350–377, 2016.

[170] M. Guney and Y. Tepe, "Classification and assessment of energy storage systems," *Renewable and Sustainable Energy Reviews*, vol. 75, pp. 1187–1197, 2017.

[171] F. Cebulla, J. Haas, J. Eichman, W. Nowak, and P. Mancarella, "How much electrical energy storage do we need? A synthesis for the U.S., Europe, and Germany," *Journal of Cleaner Production*, vol. 181, pp. 449–459, 2018.

[172] T. Ayodele and A. Ogunjuyigbe, "Mitigation of wind power intermittency: Storage technology approach," *Renewable and Sustainable Energy Reviews*, vol. 44, pp. 447–456, 2015.

[173] A. Solomon, M. Child, U. Caldera, and C. Breyer, "How much energy storage is needed to incorporate very large intermittent renewables?," *Energy Procedia*, vol. 135, pp. 283–293, 2017.

[174] J. Després, S. Mima, A. Kitous, P. Criqui, N. Hadjsaid, and I. Noirot, "Storage as a fleiblity option in power systems with high shares of variable renewable energy sources: a POLES-based analysis," *Energy Economics*, vol. 64, pp. 638–650, 2017.

[175] W. Yang and J. Yang, "Evaluating fast power response of variable speed pumped storage plant to balance wind power variations," *Energy Procedia*, vol. 158, pp. 6341–6345, 2019.

[176] G. Salgi and H. Lund, "System behaviour of compressed-air energy-storage in Denmark with a high penetration of renewable energy sources," *Applied Energy*, vol. 85, pp. 182–189, 2008.

[177] H. de Boer and D. van Vuuren, "Representation of variable renewable energy sources in TIMER, an aggregated energy system simulation model," *Energy Economics*, vol. 64, pp. 600–611, 2017.

[178] X. Wang, C. Yang, M. Huang, and Z. Ma, "Multi-objective optimization of a gas turbine-based CCHP combined with solar and compressed air energy storage system," *Energy Conversion and Management*, vol. 164, pp. 93–101, 2018.

[179] T. Kneiske and M. Braun, "Flexibility potentials of a combined use of heat storages and batteries in PV-CHP hybrid systems," *Energy Procedia*, vol. 135, pp. 482–495, 2017.

[180] J. Cervantes and F. Choobineh, "Optimal sizing of a nonutility-scale solar power system and its battery storage," *Applied Energy*, vol. 216, pp. 105–115, 2018.

[181] G. Xu, C. Shang, S. Fan, X. Zhang, and A. Cheng, "Sizing battery energy storage systems for industrial customers with photovoltaic power," *Energy Procedia*, vol. 158, pp. 4953–4958, 2019.

[182] W. Liu, N. Li, Z. Jiang, Z. Chen, S. Wang, J. Han, X. Zhang, and C. Liu, "Smart micro-grid systems with wind/PV/battery," *Energy Procedia*, vol. 152, pp. 1212–1217, 2018.

[183] A. Gimelli, F. Mottola, M. Mucillo, D. Proto, A. Amoresano, A. Andreotti, and G. Langella, "Optimal configuration of modular cogeneration plants integrated by a battery energy storage system providing peak shaving service," *Applied Energy*, vol. 242, pp. 974–993, 2019.

[184] Electric Power Research Institute EPRI, "Energy Storage Trends and Challenges." Available at `https://eea.epri.com/pdf/epri-energy-and-climate-change-research-seminar/2017/07d%20Energy%`

20Storage%20Trends%20and%20Challenges%20Haresh%20Kamath.pdf. Accessed on 31/03/2020.

[185] System Advisory Model SAM, "Technoeconomic modeling of battery energy storage in SAM," tech. rep., 2015.

[186] IEA, "Outlook for biogas and biomethane: prospect for organic growth," tech. rep., 2020.

[187] Imperial College London, "Analysis of alternative UK heat decarbonisation pathways," tech. rep., 2018.

[188] SGC, "Biogas upgrading-Review of commercial technologies," tech. rep., 2020.

[189] I. Khan, M. Othman, H. Hashim, T. Matsuura, A. Ismail, M. Rezaei-DashtArzhandi, and I. Azelee, "Biogas as a renewable energy fuel – A review of biogas upgrading, utilisation and storage," *Energy Conversion and Management*, vol. 150, pp. 277–294, 2017.

[190] Y. Jiang, S. Xiong, W. Shi, W. He, T. Zhang, X. Lin, Y. Gu, Y. LV, X. Qian, Z. Ye, and C. Wang, "Research of biogas as fuel for internal combustion engine," *Asia-Pacific Power and Energy Engineering Conference*, vol. 1, pp. 2–5, 2009.

[191] J. Holm-Nielsen, T. Al Seadi, and P. Oleskowicz-Popiel, "The future of anaerobic digestion and biogas utilization," *Bioresource Technology*, vol. 100, pp. 5478–5484, 2009.